Fatty acid metabolism driven mitochondrial bioenergetics promotes advanced developmental phenotypes in human induced pluripotent stem cell derived cardiomyocytes

Chrishan J.A. Ramachandra[1,a,b], Ashish Mehta[1,c], Philip Wong[a,b,d,e*], K.P. Myu Mai Ja[a], Regina Fritsche-Danielson[f], Ratan V. Bhat[g], Derek J. Hausenloy[a,b,h,i,j], Jean-Paul Kovalik[b] and Winston Shim[a,b,k*]

[a]National Heart Research Institute Singapore, National Heart Centre Singapore
[b]Cardiovascular & Metabolic Disorders Program, Duke-NUS Medical School, Singapore
[c]PSC and Phenotyping Laboratory, Victor Chang Cardiac Research Institute, Sydney, Australia
[d]Department of Cardiology, National Heart Centre Singapore
[e]School of Materials Science and Engineering, Nanyang Technological University, Singapore
[f]Cardiovascular and Metabolic Disease Innovative Medicines and Early Development Unit, AstraZeneca Research and Development, Gothenburg, Sweden
[g]Strategy and External Innovation Department, AstraZeneca, Gothenburg, Sweden
[h]The Hatter Cardiovascular Institute, University College London, United Kingdom
[i]Barts Heart Centre, St Barthlomew's Hospital, London, United Kingdom
[j]Yong Loo Lin School of Medicine, National University of Singapore
[k]Health and Social Sciences Cluster, Singapore Institute of Technology

[1]Both authors contributed equally

Running title: Cardiomyocyte metabolism and bioenergetics

*Corresponding authors:

Philip Wong
National Heart Centre Singapore, 5 Hospital Drive, Singapore 169609
Email: philip.wong.e.h@nhcs.com.sg; Phone: +65 6704 8964; Fax: +65 6844 9053

Winston Shim
National Heart Research Institute Singapore, 5 Hospital Drive, Singapore 169609
Email: winstonshim@gmail.com; Phone: +65 6704 2194; Fax: +65 6844 9053

Abstract

Background: Preferential utilization of fatty acids for ATP production represents an advanced metabolic phenotype in developing cardiomyocytes. We investigated whether this phenotype could be attained in human induced pluripotent stem cell derived cardiomyocytes (hiPSC-CMs) and assessed its influence on mitochondrial morphology, bioenergetics, respiratory capacity and ultra-structural architecture.

Methods and Results: Whole-cell proteome analysis of day 14 and day 30-CMs maintained in glucose media revealed a positive influence of extended culture on mitochondria-related processes that primed the day 30-CMs for fatty acid metabolism. Supplementing the day 30-CMs with palmitate/oleate (fatty acids) significantly enhanced mitochondrial remodeling, oxygen consumption rates and ATP production. Metabolomic analysis upon fatty acid supplementation revealed a β-oxidation fueled ATP elevation that coincided with presence of junctional complexes, intercalated discs, t-tubule-like structures and adult isoform of cardiac troponin T. In contrast, glucose-maintained day 30-CMs continued to harbor underdeveloped ultra-structural architecture and more subdued bioenergetics, constrained by suboptimal mitochondria development.

Conclusion: The advanced metabolic phenotype of preferential fatty acid utilization was attained in hiPSC-CMs, whereby fatty acid driven β-oxidation sustained cardiac bioenergetics and respiratory capacity resulting in ultra-structural and functional characteristics similar to those of developmentally advanced cardiomyocytes. Better understanding of mitochondrial bioenergetics and ultra-structural adaptation associated with fatty acid metabolism has important implications in the study of cardiac physiology that are associated with late-onset mitochondrial and metabolic adaptations.

Keywords: Mitochondria; Metabolism; Bioenergetics; Cardiomyocytes; T-tubules; Human induced pluripotent stem cells

Introduction

Cardiomyocytes harbor the largest number of mitochondria, among all cell types, generating greater than 95% of ATP consumed by the adult human heart. These ATPs are utilized for critical cellular functions including growth, contraction, calcium homeostasis, signaling and survival[1]. Adaptative changes to the mitochondrial bioenergetic machinery is crucial in meeting increased metabolic demands of developing cardiomyocytes. It is not surprising, therefore, that dysregulation in mitochondrial function leads to various cardiomyopathies and heart failure[2, 3]. Cardiomyocytes derived from human induced pluripotent stem cells (hiPSC-CMs) offer a valuable platform to study cellular pathophysiological processes[4, 5]. We have previously identified key signaling pathways governing formation of cardiomyocytes from hiPSCs[6, 7]. While mitochondrial biogenesis has been reported to be important for cardiomyocyte derivation[8], information regarding their involvement in metabolic remodeling and ultra-structural development post-cardiomyocyte formation remains relatively undefined.

Maintenance of mitochondrial morphology through fusion and fission events together with cytoplasmic motility are key in remodeling mitochondrial networks necessary for intra-cellular distribution of ATP in adult cardiomyocytes[9]. During these events, adaptive modification of mitochondrial morphology through interplay between fusion proteins such as optic atrophy 1 (OPA1) and mitofusins (MFN1, MFN2) as well as fission proteins like dynamin-related protein 1 (DRP1) and fission protein 1 (FIS1) is continuously observed to sustain energy flux associated with supply and demand of cellular activities. Fetal cardiomyocytes are populated with mostly fragmented mitochondrial networks[10] and rely majorly on glucose as their main energy substrate[11]. In contrast, as cardiomyocytes undergo terminal differentiation, and adapt to postnatal life, metabolic remodeling towards β-oxidation occurs with fatty acids becoming the dominant energy substrate. This metabolic shift results in increased mitochondrial bioenergetic capacity[1], a change which is necessary for maintaining the high levels of ATP.

In the current study, as evidence of *bona fide* metabolic remodeling, we show that by day 30 of differentiation, hiPSC-CMs adapt to metabolizing fatty acids as the primary energy substrate, resulting in increased mitochondrial bioenergetics and respiratory

capacity coinciding with ultra-structural organization of junctional complexes of fascia adherens, gap junctions and desmosomes supporting intercalated discs/t-tubule-like structures, consistent with developmentally advanced cardiomyocytes. Although glucose-maintained day 30-CMs showed improved mitochondrial functionality in comparison to day 14-CMs, their bioenergetics, respiratory capacity and ultra-structural architecture remain subdued when compared to those of the day 30-CMs supplemented with fatty acids. We conclude that attaining the advanced metabolic phenotype of preferential fatty acid utilization is crucial for sustaining cardiac bioenergetics required for augmenting ultra-structural architecture in hiPSC-CMs.

Methods

hiPSC maintenance and cardiac differentiation

Normal dermal fibroblast-derived hiPSC line (CL-1)[12] and BJ fibroblast-derived-mRNA reprogramed hiPSC line (CL-2)[13] were maintained and differentiated into cardiomyocytes using a previously described embryoid body (EB) based protocol[14].

Western blot and whole-cell proteome analysis

Western blots and whole-cell proteome analysis were performed as described previously[6, 15]. Antibodies used in the study are listed in Supplementary table 1. Peptides obtained from day 30-CMs were compared against day 14-CMs and those with a 20%-fold change (up-regulated and down-regulated) (nonparametric t-test; $p<0.05$) were analyzed using DAVID Bioinformatics Resources 6.8. The proteome assay was performed in triplicate and the principal component analysis (PCA) was performed using Clustvis[16].

Mitochondrial functional assays

Cardiac clusters were dissociated into single cells and stained with either JC-1 dye (10µg/mL; Thermo Fisher Scientific) or TMRM (0.25µM; Thermo Fisher Scientific) for 15 minutes at 37^{o}C. For mitochondrial complex inhibition studies, JC-1 stained cells were treated with rotenone, thenoyltrifluoroacetone and antimycin A (Sigma-Aldrich), respectively. Changes in JC-1 fluorescence intensity were measured using SpectraMax M3 (Molecular Devices, CA, USA). TMRM-stained cells were analyzed on BD FACSAria II (BD Biosciences, CA, USA). A total of 10,000 gated events were

evaluated for each time-point and data analysis was performed using FlowJo software. Hexokinase Colorimetric Assay Kit (Sigma-Aldrich), L-Carnitine Assay Kit (Sigma-Aldrich) and ATP Determination Kit (Thermo Fisher Scientific) were used in this study. Cardiac clusters were lysed in respective buffers and assayed as per manufacturer's instructions.

MitoTracker and Immunostaining

Cardiac clusters were dissociated into single cells and stained with MitoTracker (0.1μM; Thermo Fisher Scientific) for 15 min at 37ºC. For immunostaining, cells were fixed with 4% PFA, permeabilized with 0.3% Triton X-100, blocked with 5% BSA and stained with primary antibodies overnight (Supplementary table 1). Cells were washed, probed with respective fluorophore-conjugated secondary antibodies and counterstained with DAPI the following day. Stained cells were examined under Zeiss LSM710 NLO multi-photon confocal microscope (Carl Zeiss Microscopy GmbH, Jena, Germany). For sarcomere length measurements, cells were stained with sarcomeric α-actinin (Sigma-Aldrich) and the distance between sarcomeres was measured by drawing a perpendicular line across adjacent Z-discs using ImageJ. The profile of stained Z-discs was plotted and the distance between the maximum intensity of each neighboring Z-disc was tabulated as sarcomere length.

Mitochondrial respiration assay

Cardiac clusters were dissociated into single cells and seeded on a Seahorse 24-well XF Cell Culture Microplate (Agilent Technologies, CA, USA) at approximately 1 x 10^5 cells/well. Prior to initiation of the assay, cardiomyocyte maintenance media was replaced with XF Media (with/without fatty acids). During measurements of OCR, oligomycin (2.5 μM), FCCP (1 μM) and antimycin A/rotenone (2.5 μM) was injected into the system. Non-mitochondrial OCR values (average values post antimycin A/rotenone treatment) were deducted from basal and maximal OCR values. Basal OCR was the average values taken from the start of the experiment until addition of oligomycin. Maximal OCR was the average values taken from addition of FCCP until treatment with antimycin A/rotenone. Respiratory reserve capacity was the difference in values between maximal and basal OCR.

Cardiac troponin T isoform analysis

RNA from cardiac clusters was converted to cDNA using SuperScript III First-Strand Synthesis System (Thermo Fisher Scientific). Using Platinum PCR SuperMix (Thermo Fisher Scientific) and *TNNT2* primers listed in Supplementary table 2, cDNA templates were cycled as follows: 2 min at 94°C, followed by 35 cycles of 30s at 94°C, 30s at 60°C and 30s at 72°C. Electrophoresis of amplified products was performed on a 3% agarose gel, run at 100V for 50 min.

Statistical analysis

Data with normal Gaussian distribution were analyzed by standard parametric tests. Data with non-Gaussian distribution were analyzed by nonparametric t-test and Kruskal-Wallis test was applied for multi-group comparison followed by Dunn's post-hoc test. A p-value of <0.05 was considered statistically significant.

Results

Extended culture influences mitochondrial function and network expansion

We previously reported the use of an embryoid body (EB)-based cardiac differentiation protocol which yielded vigorously beating cardiac clusters by day 14 with high purity of hiPSC-CMs (approximately 95% NKX2-5^{+} cardiac committed cells with up to 85% positive for cTnT; Supplementary figure 1A)[12, 14]. To study subsequent bioenergetic, metabolic and developmental advancements, our day 14 hiPSC-CMs were further maintained as cardiac clusters until day 30 in standard glucose medium.

A whole-cell proteome profiling revealed 654 down-regulated and 844 up-regulated proteins (Supplementary table 3) when day 14-CMs were maintained until day 30. Among the most enriched biological processes (Supplementary table 4) and cellular compartments (Supplementary table 5), protein families located in the extracellular matrix, cytoplasm and nucleus which regulate cell adhesion, transcription and translation activities were down-regulated in the day 30-CMs, while families belonging to the mitochondria and sarcomere compartments which regulate energy production (including that of fatty acid β-oxidation) and contractile function, were up-regulated (Figure 1A and Supplementary figure 1B-C), signifying a major switch from basic cellular functions towards specific metabolic and bioenergetic development.

Upon further evaluation of the enriched proteins in mitochondrial-related processes, family members involved in the formation of complex I (NADH dehydrogenase) in the electron transport chain (ETC) were most abundantly represented in day 30-CMs as compared to day 14-CMs (Supplementary figure 1D). We postulated that day 30-CMs may have enhanced complex I activity in comparison to day 14-CMs. To validate this, using JC-1 dye as an indicator of mitochondrial membrane potential ($\Delta\Psi_m$), complex I, II and III were selectively inhibited with rotenone, thenoyltrifluoroacetone (TTFA) and antimycin A respectively (Figure 1B and Supplementary figure 1E), as reported previously[17]. While TTFA and antimycin A treatment expectedly decreased $\Delta\Psi_m$ in a time-dependent manner in both day 14- and day 30-CMs, rotenone treatment decreased $\Delta\Psi_m$ only in day 30-CMs (Figure 1B and Supplementary figure 1E), confirming dominant presence of enhanced complex I activity that is consistent with increasing importance of complex I, reported in developmentally advanced cardiomyocytes[17]. Similarly, flow cytometry analysis using tetramethylrhodamine methyl ester (TMRM)[18] for evaluation of $\Delta\Psi_m$ indicated the day 30-CMs to have an overall higher $\Delta\Psi_m$ as compared to day 14-CMs (Figure 1C). Increased complex I activity together with improved $\Delta\Psi_m$ in day 30-CMs indicated an augmented mitochondrial respiratory function which was confirmed by enhanced ATP production (Figure 1C).

In agreement with the proteome analysis which indicated up-regulated mitochondrial-related processes during the transition from day 14- to day 30-CMs, mitochondrial fusion proteins OPA1, MFN1 and MFN2 were up-regulated while the fission protein, FIS1, was down-regulated in comparison to day 14-CMs (Figure 1D and Supplementary figure 2A-B). Furthermore, pro-fission activity of DRP1 was similarly reduced in day 30-CMs as fission-inducing phosphorylation at Ser616 ($pDRP1^{S616}$) was decreased while phosphorylation at Ser637 ($pDRP1^{S637}$) that counteracted fission[19, 20] was increased (Figure 1D and Supplementary figure 2A-B). Consistent with evidence of pro-fusion events in day 30-CMs, imaging of cellular distribution of mitochondria using MitoTracker as well as staining against cytochrome c oxidase subunit IV (COXIV) revealed disparate mitochondrial morphologies between day 14- and day 30-CMs, with the former containing isolated mitochondria with fragmented foci, whereas the latter were populated with extensive interconnected filamentous networks (Figure 1E and Supplementary figure 2C).

Furthermore, analysis of mitochondrial morphology by transmission electron microscopy (TEM) confirmed day 30-CMs to have elongated, large-sized mitochondria in the sarcoplasm with denser intra-mitochondrial cristae matrix in comparison to day 14-CMs, which had mostly round-shaped mitochondria with sparse cristae, located around the perinuclear region (Figure 1F). Such morphological differences supported the observed differential expression of mitochondrial fusion and fission proteins in the day 14- and day 30-CMs (Figure 1D and Supplementary figure 2A-B). Collectively, these results support increased mitochondrial fusion events leading to mitochondrial network expansion in the day 30-CMs.

Fatty acid supplementation induces extensive mitochondrial remodeling in day 30-CMs

Fetal cardiomyocytes are known to derive ATP requirements primarily through glucose metabolism, while adult cardiomyocytes transit to mainly rely on fatty acid β-oxidation[1, 11]. To validate the metabolic adaptation towards augmented energy production, day 14- and day 30-CMs were subjected to hexokinase (catalyzes first step in glucose metabolism) and L-carnitine (essential for fatty acid transport into the mitochondria) assays to assess the levels of glucose and fatty acid metabolism respectively. The results indicated day 14-CMs to have high hexokinase, but low L-carnitine activity while an inverse profile was apparent for day 30-CMs (Figure 2A and Supplementary figure 3A). These results supported that day 30-CMs were undergoing metabolic remodeling, moving away from glucose as a fuel source and switching towards fatty acids as a primary energy substrate, a shift which is consistent with developmentally advanced cardiomyocytes.

To confirm the metabolic switch from glucose to fatty acids as the main energy substrate, day 30-CMs that were maintained in standard glucose media were specifically supplemented with palmitate and oleate, which is more physiological and less toxic than palmitate alone[21, 22]. Post-fatty acid (FA) supplementation, gene expression profiling indicated fatty acid supplemented day 30-CMs (day 30-CMs + FA) maintained a high expression level of markers involved in mitochondrial remodeling (e.g. *OPA1*), turnover (e.g. *BECN1*) and fatty acid β-oxidation (e.g. *CPT1B*) in comparison to glucose-maintained day 14- or day 30-CMs (Figure 2B).

Furthermore, immunostaining against COXIV as well as TEM analysis validated our gene expression profile by revealing highly abundant filamentous mitochondrial networks (Figure 2C and Supplementary figure 3B) and densely compacted mitochondrial bundles (Figure 2D) spanning an inter-sarcomeric distribution in the sarcoplasm of fatty acid supplemented day 30-CMs (Supplementary figure 3C) that differed drastically to those perinuclear localized mitochondria observed in day 14-CMs (Figure 1F). Moreover, TEM analysis of mitochondria morphology in fatty acid supplemented day 30-CMs demonstrated further increased mitochondria size, decreased circularity index and more defined cristae matrix in comparison to glucose-maintained day 30-CMs (Figure 2E). Collectively, these results supported that fatty acids fueled mitochondrial development, gearing the cardiomyocytes towards attaining an advanced metabolic phenotype.

Fatty acid supplemented day 30-CMs adaptively metabolize fatty acids as an energy substrate

To confirm gearing of metabolic competency towards fatty acid β-oxidation, we performed metabolomic analysis on glucose-maintained day 30-CMs and fatty acid supplemented day 30-CMs (maintained in palmitate/oleate supplemented glucose media). We profiled the acylcarnitines to identify species of fatty acids that have translocated into the mitochondrial matrix via the carnitine shuttle[23]. In comparison to glucose-maintained day 30-CMs, levels of short-chain acylcarnitines (e.g. C3, C5), which are derived from amino acid catabolism[23, 24] remained relatively unchanged, whereas levels of long-chain acylcarnitines (e.g. C16, C18:1) increased significantly (Figure 3A) in fatty acid supplemented day 30-CMs which supported metabolic fuel switching towards fatty acid driven β-oxidation[23, 25]. Consistent with actively functioning β-oxidation, increased α-ketoglutarate and fumerate levels together with a stable tricarboxylic acid (TCA) cycle intermediate pool (Figure 3B) indicated a well coupled bioenergetic machinery, as depletion of TCA cycle intermediates by excessive fatty acid β-oxidation rates has been implicated in metabolic dysfunction in diabetic rodent models[23, 25]. Consistently, fatty acid supplemented day 30-CMs showed increased levels of amino acids (Figure 3C) which have been reported to play a role in replenishing the TCA cycle intermediates through amino acid catabolism pathways[26].

The increased presence of long-chain acylcarnitines suggested that fatty acid supplemented day 30-CMs were likely to undergo augmented cellular respiration sustained by β-oxidation. Consistently, analysis of oxygen consumption rate (OCR) showed fatty acid supplemented day 30-CMs exhibited increased respiration rates whereby maximal OCR was approximately two-fold higher in comparison to glucose-maintained day 30-CMs (Figure 3D). The respiratory reserve capacity (which is indicative of extra amounts of ATP that can be produced during sudden increase in energy demands) was also increased by more than five-fold in fatty acid supplemented day 30-CMs, while a larger OCR to ECAR (extracellular acidification rate) ratio (Supplementary figure 4A) suggested that mitochondria-linked oxidative phosphorylation (rather than glycolysis) was highly active in these cardiomyocytes. This metabolic adaptation towards fatty acids resulted in a significant increase in ATP production in the fatty acid supplemented day 30-CMs as compared to glucose-maintained day 30-CMs (Figure 3E). However, supplementing day 14-CMs with fatty acids did not result in further increase in ATP levels or OCR (Supplementary figure 4B-D). Therefore, the increased bioenergetics in glucose-maintained day 30-CMs in comparison to day 14-CMs (Figure 1B-C), and their further enhancement in fatty acid supplemented day 30-CMs (Figure 3D-E) were likely hinged on adaptation of bioenergetic machinery associated with continuous remodeling of mitochondrial networks that accompanied the metabolic switch in energy substrate utilization. These results cumulatively supported that structurally elongated and pan-sarcoplasmic networked mitochondria in fatty acid supplemented day 30-CMs geared metabolic adaptation selectively towards β-oxidation that fueled the augmented ATP production.

Fatty acid supplementation augments ultra-structural architecture

Accompanying the metabolic adaptation of the mitochondria, fatty acid supplemented day 30-CMs developed extensively organized sarcomeres that uniformly populated throughout the sarcoplasm while glucose-maintained day 30-CMs still consisted of sarcoplasmic zones with sparse sarcomeres (Figure 4A). Furthermore, fatty acid supplemented day 30-CMs showed increased multi-nucleation (Figure 4A), which is consistent with increased bi-nucleation of up to 30% of developmentally advanced adult human cardiomyocytes observed previously[27] as well as underwent cellular hypertrophy (Figure 4A and Supplementary figure 5A).

Rod-like morphology was observed in approximately 14% of fatty acid supplemented day 30-CMs (n=137/981) which exhibited extensively organized sarcomeres that longitudinally traversed the sarcoplasm (Figure 4B). These rod-like fatty acid supplemented day 30-CMs displayed bi-nucleation at two distal poles and had a length/width aspect ratio ranging from 1:7 to 1:13. Immunostaining against sarcomeric thick (ventricular myosin light chain) and thin filaments (α-actinin) revealed potential existence of M-lines, suggestive of ultra-structural maturity in fatty acid supplemented day 30-CMs (Figure 4B). In comparison to glucose-maintained day 30-CMs, there was further increase in sarcomere lengths to approximately 1.9 µm (Figure 4B and Supplementary figure 5A and Supplementary table 6) that were similarly observed in long-term (120 days) cultured hiPSC-CMs[28].

Consistently, TEM indicated that fatty acid supplemented day 30-CMs were populated with abundant sarcomeres constituting regular registry of Z-disc, M-line, I-band and A-band (Figure 4C and Supplementary figure 5B). Intercalated disc (ICD)-associated junctional complexes including fascia adherens, desmosomes and gap junctions which coincided with late-stages of cardiomyocyte development[29] was observed (Figure 4C). Furthermore, t-tubule-like projections juxtaposed on top of ICD and Z-disc (Figure 4C) that are characteristic of developmentally advanced cardiomyocytes[30] was observed in the fatty acid supplemented day 30-CMs. The identity of those t-tubule-like projections were supported by Western blot analysis of key junctional markers known to be enriched in t-tubules[31-33]. Our Western blot analysis showed significantly augmented levels of L-type calcium channel, sodium-calcium exchanger (NCX1), caveolin-3, amphiphysin, junctophilin-2 and Tcap, confirming the presence of t-tubule-like structures in the fatty acid supplemented day 30-CMs (Figure 4D and Supplementary figure 5C). Consistent with these ultra-structural observations, fatty acid supplemented day 30-CMs displayed markedly improved calcium handling properties with faster peak and decay times in comparison to glucose-maintained day 30-CMs (Figure 4E) that were consistent with characteristics reported previously in hiPSC-CMs with established t-tubule network[34]

Fatty acid supplemented day 30-CMs express adult human cardiac troponin T isoform

Differential expression of cTnT isoforms was known to coincide with various developmental stages of human cardiomyocytes[35, 36] whereby a longer isoform 1 is expressed in human fetal cardiomyocytes while a shorter isoform 3 is expressed in adult cardiomyocytes. Since a 30-bp differentially spliced exon in the 5` coding region discriminates between the two isoforms[35], we evaluated the expression levels of cTnT isoforms in glucose-maintained day 14- and day 30-CMs as well as in fatty acid supplemented day 30-CMs. Our RT-PCR results indicated that while day 14-CMs predominantly expressed isoform 1, day 30-CMs expressed both isoform 1 and isoform 3 (Figure 4F). Importantly, fatty acid supplemented day 30-CMs mostly expressed isoform 3, indicative of a transition away from fetal cardiac physiology. The 30-bp spliced fragment was validated through Sanger sequencing (Supplementary figure 5D) and the isoform switching phenomena was further confirmed by Western blot analysis that similarly corroborated the dominant presence of the adult cTnT isoform post-attainment of the advanced metabolic phenotype (Figure 4G and Supplementary figure 5E-F).

Discussion

In this study, we demonstrate that mitochondria of hiPSC-CMs at day 30 post-differentiation developmentally attained a metabolic competency predominantly geared towards fatty acid metabolism. This was mainly due to adaptive morphological remodeling of networked mitochondria driven primarily by heightened fusion events and possibly also by augmented mitochondrial biogenesis as our gene expression panel revealed an increased expression level of markers for fusion (e.g. *OPA1, MFN1, MFN2*) as well as biogenesis (e.g. *TFAM*, *NRF1*) during the transition from day 14 to day 30. The extensive mitochondrial networks present in fatty acid supplemented day 30-CMs enabled active metabolization of fatty acids as a major energy substrate that significantly increased bioenergetics and promoted structural/functional changes that resemble those observed in developmentally advanced cardiomyocytes.

ATP in the mitochondria is produced via oxidative phosphorylation and its coupling to the transfer of electrons from complex I to V. Correct assembly of more than 40 sub-units is necessary for complex I functionality[37]. The incomplete expression of such complex I subunits in the day 14-CMs together with their reliance on glycolysis

coincided with its suboptimal contribution to $\Delta\Psi_m$ and lower ATP levels in comparison to day 30-CMs with the observed better complement of complex I assembly. Furthermore, our proteome profile indicated day 30-CMs expressed proteins encoding for the Q module (responsible for electron transfer)[38] of complex I (Supplementary table 7), which in turn would increase $\Delta\Psi_m$, resulting in elevated ATP production as observed in the current study. These data are in agreement with a previous study which showed enhanced complex I activity in developmentally advanced cardiomyocytes isolated from mouse heart [17].

The adult heart has a daily ATP turnover of approximately 20 times its own weight[1], and fatty acids represent the predominant energy substrate. The significant amount of energy produced through β-oxidation of fatty acids is essential for fueling the incessant contractile requirement and other energy demanding activities, which may not be met by glucose metabolism alone[39, 40]. In the current study, fatty acid supplementation resulted in a heightened bioenergetic capacity likely sustained via active β-oxidation as evidenced in the acylcarnitine metabolomic profile. No change in acetylcarnitine (C2) levels were observed between glucose-maintained day 30-CMs and fatty acid supplemented day 30-CMs, suggesting that increased reliance on β-oxidation did not result in excessive build-up of acetyl-CoA in the latter. The overall metabolomic data supported heightened respiration capacity in fatty acid supplemented day 30-CMs in comparison to glucose-maintained day 30-CMs, which was confirmed through our Seahorse metabolic flux data. Though the basal OCR was similar between glucose-maintained day 30-CMs and fatty acid supplemented day 30-CMs, the maximal OCR and respiratory reserve capacity was significantly higher in the latter, which indicated augmented mitochondrial functionality. This together with increased ATP output observed in the fatty acid supplemented day 30-CMs, was indicative of an active β-oxidation process that was systemically coupled to the TCA cycle and ETC machinery to sustain increased energy demands that was consistent with developmentally advanced cardiomyocytes[11]. The heightened bioenergetic capacity of fatty acid supplemented day 30-CMs likely fueled the observed hypertrophic growth, multi-nucleation, enhanced sarcomeric organization as well as continued development and maintenance of extensive inter-sarcomeric mitochondrial networks. However, fatty acid supplementation in our day 14-CMs did not induce any respiratory or bioenergetic changes, suggesting that mature

mitochondrial networks are needed to meaningfully metabolize fatty acids. This is consistent with the low levels of L-carnitine present in day 14-CMs which may be insufficient for transporting fatty acids into the mitochondria for ATP production[41]. Similarly, depleted carnitine levels have been reported in heart failure patients with reduced fatty acid utilization related energy deficiency[42].

Long-term culture of hiPSC-CMs of up to 365 days[28, 43] has been reported in an attempt to obtain terminally differentiated phenotypes. More recently, an engineered human myocardium has been shown to generate hiPSC-CMs with important structural and functional properties of maturing myocardium[44, 45]. Various parameters have been proposed as indicators of maturing cardiomyocytes[46-48], however it has yet to be determined if hiPSC-CMs can attain a developmentally advanced cardiac bioenergetic capability of actively metabolizing fatty acids as a primary energy source. In this study, we show that upon fatty acid supplementation, advanced ultra-structural architecture could be achieved in approximately 30 days in culture with no requirement for complex tissue engineered constructs[49], specific matrices[34] or exogenous small molecules[48]. Furthermore, proteome enrichment in intercalated disc/t-tubule structures and bioenergetic compartments in day 30-CMs and their ultra-structural observations by TEM post-fatty acid supplementation, together with drastically reduced cellular proliferation (Supplementary figure 5G) were consistent with developmentally advanced human cardiac organoids reported recently[49]. In addition, our observations of a developmental switch from fetal to a pre-dominant adult cTnT isoforms were consistent with previous report of developmentally advanced cardiac physiology[35, 36].

Conclusions

In summary, we demonstrate that by actively metabolizing fatty acids as the dominant energy substrate, hiPSC-CMs sustain extensive filamentous mitochondrial networks and augmented ATP levels which leads to developmentally advanced phenotypes. Although lack of direct comparison to human heart tissues limits precise postnatal staging of the developmental status of our fatty acid supplemented day 30-CMs, this study lays the foundation for better understanding of cardiac bioenergetics and ultra-structural adaptation in hiPSC-CMs that may form an impetus for study of cardiac physiology that are associated with late-onset mitochondrial and metabolic

adaptations.

Funding

This study was supported by the National Research Foundation Singapore (NRF-CRP-2008-02); National Medical Research Council (NMRC/BNIG/1074/2012, MOHIAFCAT2/0002/2014, NMRC/OFYIRG/0073/2018); Goh Foundation Gift (Singapore)/Duke-NUS Graduate Medical School (GCR/2013/008, GCR/2013/010, and GCR/2013/011); SingHealth Foundation (SHF/FG569P/2014 and SHF/FG630S/2014) and Biomedical Research Council Singapore (BMRC13/1/96/19/686A). WS received funding from AstraZeneca Inc for iPSC stem cell research. DJH is supported by the Duke-National University Singapore Medical School, the National Institute for Health Research University College London Hospitals Biomedical Research Centre, the Singapore Ministry of Health's National Medical Research Council under its Clinician Scientist-Senior Investigator scheme (NMRC/CSA-SI/0011/2017) and Collaborative Centre Grant scheme (NMRC/CGAug16C006), the Singapore Ministry of Education Academic Research Fund Tier 2 (MOE2016-T2-2-021), and the European COST (Cooperation in Science and Technology) Action EU-CARDIOPROTECTION CA16225.

Acknowledgements

The authors thank Anuja Chitre, Chong Hui Lua and Pritpal Singh from National Heart Centre Singapore for their assistance in maintenance of hiPSC cultures and cardiac differentiation. Poh Ling Koh from Duke-NUS, Singapore for her assistance in performing Seahorse study. Dr. Sunil S. Adav and Prof. Siu Kwan Sze from School of Biological Sciences, Nanyang Technological University, Singapore, for their support in mass spectroscopy analysis. The authors acknowledge the facilities, and the scientific and technical assistance of the Advanced Bioimaging Core at DUKE NUS Singapore Health Services. The SingHealth Flow Cytometry Core Platform and the Duke-NUS Metabolomics Core Facility.

Author contributions

C.R. and W.S., wrote the manuscript. C.R., A.M., P.W. and W.S., funded the study. C.R., A.M. and K.P.J performed experiments, acquired/analyzed data. D.J.H., advised mitochondria study. J.P.K., supervised metabolomics study. C.R., W.S.,

R.F.D. and R.B. conceptualized the study. All authors have read and approved the manuscript.

Conflict of interest

R.F.D and R.B. are AstraZeneca employees and shareholders in the company.

References

[1] Kolwicz SC, Jr., Purohit S, Tian R. Cardiac metabolism and its interactions with contraction, growth, and survival of cardiomyocytes. Circulation research. 2013;113:603-16.
[2] Rosca MG, Hoppel CL. Mitochondrial dysfunction in heart failure. Heart failure reviews. 2013;18:607-22.
[3] Goldenthal MJ. Mitochondrial involvement in myocyte death and heart failure. Heart failure reviews. 2016;21:137-55.
[4] Bellin M, Mummery CL. Inherited heart disease - what can we expect from the second decade of human iPS cell research? FEBS letters. 2016;590:2482-93.
[5] Rajamohan D, Matsa E, Kalra S, Crutchley J, Patel A, George V, et al. Current status of drug screening and disease modelling in human pluripotent stem cells. BioEssays : news and reviews in molecular, cellular and developmental biology. 2013;35:281-98.
[6] Ramachandra CJ, Mehta A, Wong P, Shim W. ErbB4 Activated p38gamma MAPK Isoform Mediates Early Cardiogenesis Through NKx2.5 in Human Pluripotent Stem Cells. Stem cells. 2016;34:288-98.
[7] Ramachandra CJ, Mehta A, Lua CH, Chitre A, Ja KP, Shim W. ErbB Receptor Tyrosine Kinase: A Molecular Switch Between Cardiac and Neuroectoderm Specification in Human Pluripotent Stem Cells. Stem cells. 2016;34:2461-70.
[8] St John JC, Ramalho-Santos J, Gray HL, Petrosko P, Rawe VY, Navara CS, et al. The expression of mitochondrial DNA transcription factors during early cardiomyocyte in vitro differentiation from human embryonic stem cells. Cloning and stem cells. 2005;7:141-53.
[9] Ong SB, Hausenloy DJ. Mitochondrial morphology and cardiovascular disease. Cardiovascular research. 2010;88:16-29.
[10] Porter GA, Jr., Hom J, Hoffman D, Quintanilla R, de Mesy Bentley K, Sheu SS. Bioenergetics, mitochondria, and cardiac myocyte differentiation. Progress in pediatric cardiology. 2011;31:75-81.
[11] Lopaschuk GD, Jaswal JS. Energy metabolic phenotype of the cardiomyocyte during development, differentiation, and postnatal maturation. Journal of cardiovascular pharmacology. 2010;56:130-40.
[12] Mehta A, Ramachandra CJA, Singh P, Chitre A, Lua CH, Mura M, et al. Identification of a targeted and testable antiarrhythmic therapy for long-QT syndrome type 2 using a patient-specific cellular model. European heart journal. 2017.
[13] Mehta A, Verma V, Nandihalli M, Ramachandra CJ, Sequiera GL, Sudibyo Y, et al. A systemic evaluation of cardiac differentiation from mRNA reprogrammed human induced pluripotent stem cells. PloS one. 2014;9:e103485.
[14] Mehta A, Ramachandra CJ, Sequiera GL, Sudibyo Y, Nandihalli M, Yong PJ, et al. Phasic modulation of Wnt signaling enhances cardiac differentiation in human pluripotent stem cells by recapitulating developmental ontogeny. Biochimica et biophysica acta. 2014;1843:2394-402.
[15] Mehta A, Ramachandra CJA, Chitre A, Singh P, Lua CH, Shim W. Acetylated Signal Transducer and Activator of Transcription 3 Functions as Molecular Adaptor Independent of Transcriptional Activity During Human Cardiogenesis. Stem cells. 2017;35:2129-37.
[16] Metsalu T, Vilo J. ClustVis: a web tool for visualizing clustering of multivariate data using Principal Component Analysis and heatmap. Nucleic acids research. 2015;43:W566-70.
[17] Hom JR, Quintanilla RA, Hoffman DL, de Mesy Bentley KL, Molkentin JD, Sheu

SS, et al. The permeability transition pore controls cardiac mitochondrial maturation and myocyte differentiation. Developmental cell. 2011;21:469-78.
[18] Dedkova EN, Blatter LA. Measuring mitochondrial function in intact cardiac myocytes. Journal of molecular and cellular cardiology. 2012;52:48-61.
[19] Taguchi N, Ishihara N, Jofuku A, Oka T, Mihara K. Mitotic phosphorylation of dynamin-related GTPase Drp1 participates in mitochondrial fission. The Journal of biological chemistry. 2007;282:11521-9.
[20] Chang CR, Blackstone C. Cyclic AMP-dependent protein kinase phosphorylation of Drp1 regulates its GTPase activity and mitochondrial morphology. The Journal of biological chemistry. 2007;282:21583-7.
[21] Listenberger LL, Han X, Lewis SE, Cases S, Farese RV, Jr., Ory DS, et al. Triglyceride accumulation protects against fatty acid-induced lipotoxicity. Proceedings of the National Academy of Sciences of the United States of America. 2003;100:3077-82.
[22] Listenberger LL, Ory DS, Schaffer JE. Palmitate-induced apoptosis can occur through a ceramide-independent pathway. The Journal of biological chemistry. 2001;276:14890-5.
[23] Schooneman MG, Vaz FM, Houten SM, Soeters MR. Acylcarnitines: reflecting or inflicting insulin resistance? Diabetes. 2013;62:1-8.
[24] Newgard CB. Interplay between lipids and branched-chain amino acids in development of insulin resistance. Cell metabolism. 2012;15:606-14.
[25] Koves TR, Ussher JR, Noland RC, Slentz D, Mosedale M, Ilkayeva O, et al. Mitochondrial overload and incomplete fatty acid oxidation contribute to skeletal muscle insulin resistance. Cell metabolism. 2008;7:45-56.
[26] Owen OE, Kalhan SC, Hanson RW. The key role of anaplerosis and cataplerosis for citric acid cycle function. The Journal of biological chemistry. 2002;277:30409-12.
[27] Mollova M, Bersell K, Walsh S, Savla J, Das LT, Park SY, et al. Cardiomyocyte proliferation contributes to heart growth in young humans. Proceedings of the National Academy of Sciences of the United States of America. 2013;110:1446-51.
[28] Lundy SD, Zhu WZ, Regnier M, Laflamme MA. Structural and functional maturation of cardiomyocytes derived from human pluripotent stem cells. Stem cells and development. 2013;22:1991-2002.
[29] Angst BD, Khan LU, Severs NJ, Whitely K, Rothery S, Thompson RP, et al. Dissociated spatial patterning of gap junctions and cell adhesion junctions during postnatal differentiation of ventricular myocardium. Circulation research. 1997;80:88-94.
[30] Chen B, Guo A, Zhang C, Chen R, Zhu Y, Hong J, et al. Critical roles of junctophilin-2 in T-tubule and excitation-contraction coupling maturation during postnatal development. Cardiovascular research. 2013;100:54-62.
[31] Zuppinger C, Gibbons G, Dutta-Passecker P, Segiser A, Most H, Suter TM. Characterization of cytoskeleton features and maturation status of cultured human iPSC-derived cardiomyocytes. European journal of histochemistry : EJH. 2017;61:2763.
[32] Hong TT, Smyth JW, Gao D, Chu KY, Vogan JM, Fong TS, et al. BIN1 localizes the L-type calcium channel to cardiac T-tubules. PLoS biology. 2010;8:e1000312.
[33] Reynolds JO, Chiang DY, Wang W, Beavers DL, Dixit SS, Skapura DG, et al. Junctophilin-2 is necessary for T-tubule maturation during mouse heart development. Cardiovascular research. 2013;100:44-53.
[34] Parikh SS, Blackwell DJ, Gomez-Hurtado N, Frisk M, Wang L, Kim K, et al.

Thyroid and Glucocorticoid Hormones Promote Functional T-Tubule Development in Human-Induced Pluripotent Stem Cell-Derived Cardiomyocytes. Circulation research. 2017;121:1323-30.
[35] Anderson PA, Greig A, Mark TM, Malouf NN, Oakeley AE, Ungerleider RM, et al. Molecular basis of human cardiac troponin T isoforms expressed in the developing, adult, and failing heart. Circulation research. 1995;76:681-6.
[36] Anderson PA, Malouf NN, Oakeley AE, Pagani ED, Allen PD. Troponin T isoform expression in humans. A comparison among normal and failing adult heart, fetal heart, and adult and fetal skeletal muscle. Circulation research. 1991;69:1226-33.
[37] Lazarou M, Thorburn DR, Ryan MT, McKenzie M. Assembly of mitochondrial complex I and defects in disease. Biochimica et biophysica acta. 2009;1793:78-88.
[38] Mimaki M, Wang X, McKenzie M, Thorburn DR, Ryan MT. Understanding mitochondrial complex I assembly in health and disease. Biochimica et biophysica acta. 2012;1817:851-62.
[39] Allard MF, Schonekess BO, Henning SL, English DR, Lopaschuk GD. Contribution of oxidative metabolism and glycolysis to ATP production in hypertrophied hearts. The American journal of physiology. 1994;267:H742-50.
[40] Doenst T, Nguyen TD, Abel ED. Cardiac metabolism in heart failure: implications beyond ATP production. Circulation research. 2013;113:709-24.
[41] Lopaschuk GD, Ussher JR, Folmes CD, Jaswal JS, Stanley WC. Myocardial fatty acid metabolism in health and disease. Physiological reviews. 2010;90:207-58.
[42] Wang ZY, Liu YY, Liu GH, Lu HB, Mao CY. l-Carnitine and heart disease. Life sciences. 2018;194:88-97.
[43] Kamakura T, Makiyama T, Sasaki K, Yoshida Y, Wuriyanghai Y, Chen J, et al. Ultrastructural maturation of human-induced pluripotent stem cell-derived cardiomyocytes in a long-term culture. Circulation journal : official journal of the Japanese Circulation Society. 2013;77:1307-14.
[44] Tiburcy M, Hudson JE, Balfanz P, Schlick S, Meyer T, Chang Liao ML, et al. Defined Engineered Human Myocardium With Advanced Maturation for Applications in Heart Failure Modeling and Repair. Circulation. 2017;135:1832-47.
[45] Ronaldson-Bouchard K, Ma SP, Yeager K, Chen T, Song L, Sirabella D, et al. Advanced maturation of human cardiac tissue grown from pluripotent stem cells. Nature. 2018;556:239-43.
[46] Denning C, Borgdorff V, Crutchley J, Firth KS, George V, Kalra S, et al. Cardiomyocytes from human pluripotent stem cells: From laboratory curiosity to industrial biomedical platform. Biochimica et biophysica acta. 2016;1863:1728-48.
[47] Ribeiro MC, Tertoolen LG, Guadix JA, Bellin M, Kosmidis G, D'Aniello C, et al. Functional maturation of human pluripotent stem cell derived cardiomyocytes in vitro--correlation between contraction force and electrophysiology. Biomaterials. 2015;51:138-50.
[48] Yang X, Rodriguez M, Pabon L, Fischer KA, Reinecke H, Regnier M, et al. Tri-iodo-l-thyronine promotes the maturation of human cardiomyocytes-derived from induced pluripotent stem cells. Journal of molecular and cellular cardiology. 2014;72:296-304.
[49] Mills RJ, Titmarsh DM, Koenig X, Parker BL, Ryall JG, Quaife-Ryan GA, et al. Functional screening in human cardiac organoids reveals a metabolic mechanism for cardiomyocyte cell cycle arrest. Proceedings of the National Academy of Sciences of the United States of America. 2017;114:E8372-E81.

Figure legends

Figure 1: Extended culture influences mitochondrial function and network expansion. (A) Horizontal bar graphs showing up-regulated and down-regulated biological processes in CL-1 derived day 30-CMs when compared against day 14-CMs. Note that protein families involved in energy production and contractile function are significantly up-regulated in day 30-CMs. (B) Mitochondrial functional assay (top) in CL-1 derived day 14- and day 30-CMs showing time-dependent decrease in mitochondrial membrane potential (MMP) pre- and post-rotenone, TTFA and antimycin A treatment. Note that rotenone (complex I inhibitor) decreases MMP only in day 30-CMs and has minimal effect on day 14-CMs. Red arrowheads indicate the addition of inhibitory compounds. Bar graphs (bottom) showing MMP in CL-1 derived day 14- and day 30-CMs pre- and post-compound treatment at 60-minute interval. Bar graphs presented as mean ± SD (n=3 independent experiments; Kruskal-Wallis test). *p<0.05; **p<0.01; ***p<0.001 significantly different from the respective untreated group. (C) Flow cytometry analysis (left) of CL-1 derived day 14- and day 30-CMs stained with TMRM. A total of 10,000 gated events were analyzed. Note the strong shift in fluorescence intensity in day 30-CMs as compared to day 14-CMs. Bar graphs (right) showing ATP concentrations in CL-1 derived day 14- and day 30-CMs. Bar graphs presented as mean ± SD (n=3 independent experiments; Kruskal-Wallis test). (D) Western blots (left) showing expression levels of OPA1, MFN1, MFN2, FIS1 as well as total and phosphorylated DRP1 ($pDRP1^{S616}$/$pDRP1^{S637}$) in CL-1 derived day 14- and day 30-CMs with bar graphs (right) showing densitometry data normalized to GAPDH. Bar graphs presented as mean ± SD (n=3 independent experiments; nonparametric t-test). *p<0.05 significantly different from day 14-CMs. (E) Pictographs of CL-1 derived day 14- and day 30-CMs stained against α-actinin (pseudo-colored white), MitoTracker (red) and COXIV (green), counterstained with DAPI (blue). Note the expansive filamentous mitochondrial networks in day 30-CMs as opposed to the isolated fragmented foci in day 14-CMs. Inset represents magnified region. Scale bar: 50 µm. (F) Transmission electron microscopy pictographs of CL-1 derived day 14- and day 30-CMs showing differences in mitochondrial morphology and intra-sarcoplasmic distribution. Note that in day 14-CMs, mitochondria are round, contain poorly developed cristae networks and show perinuclear distribution, whereas in day 30-CMs, mitochondria are elongated, contain dense cristae networks and show sarcoplasmic distribution. Abbreviations: M-

mitochondria; N- nucleus.

Figure 2: Fatty acid supplementation induces extensive mitochondrial remodeling in day 30-CMs. (A) Bar graphs showing hexokinase activity (left) and L-carnitine concentrations (right) in CL-1 derived day 14- and day 30-CMs. Bar graphs presented as mean ± SD (n=3 independent experiments; nonparametric t-test). (B) Heat-map showing expression profile of panel of genes involved in mitochondrial remodeling, turnover and metabolism in CL-1 and CL-2 derived day 14-CMs as well as in day 30-CMs pre- and post-fatty acid (FA) supplementation. Note that in FA supplemented day 30-CMs, genes involved in mitochondrial remodeling and turnover as well as fatty acid metabolism are up-regulated (green), while genes involved in glucose metabolism are down-regulated (red) in comparison to glucose-maintained day 14- and day 30-CMs. (C) Pictographs of CL-1 derived day 30-CMs pre- and post-FA supplementation stained against COXIV (green) and α-actinin (red), counterstained with DAPI (blue). Note the abundant filamentous mitochondrial networks in FA supplemented day 30-CMs. Inset represents magnified region. Scale bar: 50 µm. (D) Transmission electron microscopy (TEM) pictograph of CL-1 derived FA supplemented day 30-CMs containing densely compact mitochondrial bundles proximity to sarcomeres. Abbreviations: M- mitochondria; S- sarcomeres. (E) TEM pictographs (top) of mitochondrial morphology in CL-1 derived day 30-CMs pre- and post-FA supplementation. Note the elongated morphology, increase in mitochondria size and highly developed cristae networks in FA supplemented day 30-CMs. Abbreviations: M- mitochondria; S- sarcomeres. Scatter dot plots showing mitochondria size (bottom left) and circularity index (bottom middle) in CL-1 derived day 30-CMs pre- and post-FA supplementation. Scatter dot plots presented as median with interquartile range (n=140 mitochondria analyzed per group from n=3 independent experiments; parametric t-test). Stacked graph (bottom right) showing number of mitochondria in CL-1 derived day 30-CMs pre- and post-FA supplementation with sparse cristae (0-10) and dense cristae (>10) networks (n=100 mitochondria analyzed per group).

Figure 3: Fatty acid supplemented day 30-CMs adaptively metabolize fatty acids as an energy substrate. (A) Bar graphs showing acylcarnitine species present in CL-1 derived day 30-CMs pre- and post-FA supplementation. Bar graphs presented as

mean ± SD (n=3 independent experiments; nonparametric t-test). *p<0.05; ***p<0.001 significantly different from glucose-maintained day 30-CMs. (B) Bar graphs showing TCA cycle intermediates present in CL-1 derived day 30-CMs pre- and post-FA supplementation. Bar graphs presented as mean ± SD (n=3 independent experiments; nonparametric t-test). *p<0.05 significantly different from glucose-maintained day 30-CMs. (C) Bar graphs showing amino acids present in CL-1 derived day 30-CMs pre- and post-FA supplementation. Bar graphs presented as mean ± SD (n=3 independent experiments; nonparametric t-test). *p<0.05; ***p<0.001 significantly different from glucose-maintained day 30-CMs. (D) Seahorse assay (left) showing oxygen consumption rate (OCR) in CL-1 derived day 30-CMs pre- and post-FA supplementation with bar graphs (right) showing basal, maximal, non-mitochondrial OCR as well as respiratory reserve capacity. Bar graphs presented as mean ± SD (n=8 wells analyzed per group from n=3 independent experiments; nonparametric t-test). ***p<0.001 significantly different between comparison groups. Abbreviations: ns- not significant. (E) Bar graphs showing ATP concentrations in CL-1 and CL-2 derived day 30-CMs pre- and post-FA supplementation. Bar graphs presented as mean ± SD (n=3 independent experiments; nonparametric t-test). ***p<0.001 significantly different between comparison groups.

Figure 4: Fatty acid supplementation augments ultra-structural architecture. (A) Pictographs of CL-1 derived day 30-CMs pre- and post-FA supplementation stained against α-actinin (pseudo-colored white) and counterstained with DAPI (blue). The dotted area in red indicates cell boundaries, while the dotted area in yellow indicates sarcoplasmic zones containing regular registry of sarcomeres. Note the extensively organized sarcomeres which uniformly populate the sarcoplasm in FA supplemented day 30-CMs as opposed to the large sarcoplasmic zone having no sarcomeres in glucose-maintained day 30-CMs. Scale bar: 50 µm. Bar graphs showing percentage of cell area containing organized sarcomeric zones (bottom left) as well as percentage of multi-nucleated (bottom middle) CL-1 derived day 30-CMs pre- and post-FA supplementation. Bar graphs presented as mean ± SD (Sarcomeric organization (%): n=36 cells analyzed for day 30-CMs; n=25 cells analyzed for FA supplemented day 30-CMs from n=3 independent experiments; nonparametric t-test. Multi-nucleation (%): n=178 cells analyzed for day 30-CMs; n=134 cells analyzed for

FA supplemented day 30-CMs from n=3 independent experiments; nonparametric t-test). Scatter dot plots (bottom right) showing cell size of CL-1 derived day 30-CMs pre- and post-FA supplementation. Scatter dot plots presented as median with interquartile range (n=130 cells analyzed per group from n=3 independent experiments; parametric t-test). (B) Pictograph (top) of CL-1 derived FA supplemented day 30-CMs stained against sarcomeric thick (MLC2v; red) and thin filaments (α-actinin; green), counterstained with DAPI (blue). Scale bar: 50 µm. Boxed area (yellow) indicates magnified region (bottom left). Note the existence of probable M-lines (white arrowheads) in FA supplemented day 30-CMs. Scatter dot plots (bottom right) showing inter-sarcomeric distance in CL-1 derived day 30-CMs pre- and post-FA supplementation. Scatter dot plots presented as median with interquartile range (n=50 cells analyzed per group from n=3 independent experiments; parametric t-test). (C) Transmission electron microscopy pictographs of CL-1 derived FA supplemented day 30-CMs showing highly developed sarcomeres (top panel) containing Z-disc, M-line, I-band and A-band, highly developed junctional structures (middle panel) including fascia adherens (FA), desmosomes (D) and gap junctions (GJ) as well as t-tubule-like projections (bottom panel, red arrowheads) juxtaposed atop of intercalated disc (ICD). Note the highly structured mitochondrial networks in FA supplemented day 30-CMs. Abbreviations: M- mitochondria; S-sarcomeres. (D) Western blots (top) showing expression levels of known t-tubule associated proteins of L-type calcium channel, sodium-calcium exchanger (NCX1), caveolin-3, amphiphysin, junctophilin-2 and Tcap in CL-1 derived day 14-CMs as well as in day 30-CMs pre- and post-FA supplementation with densitometry data (bottom) normalized to GAPDH. Bar graphs presented as mean ± SD (n=3 independent experiments; Kruskal-Wallis test). *p<0.05; **p<0.01; ***p<0.001 significantly different between comparison groups. Abbreviations: ns- not significant. (E) Representative calcium trace (top) with bar graphs (bottom) showing amplitude, time to peak and decay time constant in CL-1 derived day 30-CMs pre- and post-FA supplementation. Bar graphs presented as mean ± SEM (n=10 cells analyzed per group; nonparametric t-test). *p<0.05; significantly different from glucose-maintained day 30-CMs. (F) Stacked graph (left) showing percentage of fetal/adult cardiac troponin T (*TNNT2*) isoforms expressed in CL-1 derived day 14-CMs as well as in day 30-CMs pre- and post-FA supplementation. Stacked graphs presented as mean ± SD (n=3 independent experiments; Kruskal-Wallis test). *p<0.001 significantly

different between comparison groups. DNA gel electrophoresis (bottom) showing discrimination of isoforms based on length of amplified product. Note that FA supplemented day 30-CMs predominantly express the shorter adult isoform. (G) Stacked graphs (top) showing percentage of fetal/adult cardiac troponin T isoforms expressed in CL-1 derived day 14-CMs as well as in day 30-CMs pre- and post-FA supplementation. Stacked graphs presented as mean ± SD (n=3 independent experiments; Kruskal-Wallis test). *$p<0.001$ significantly different between comparison groups. Western blots (bottom) showing discrimination of isoforms based on molecular weight. Note that FA supplemented day 30-CMs predominantly express the adult isoform.

Figure 1

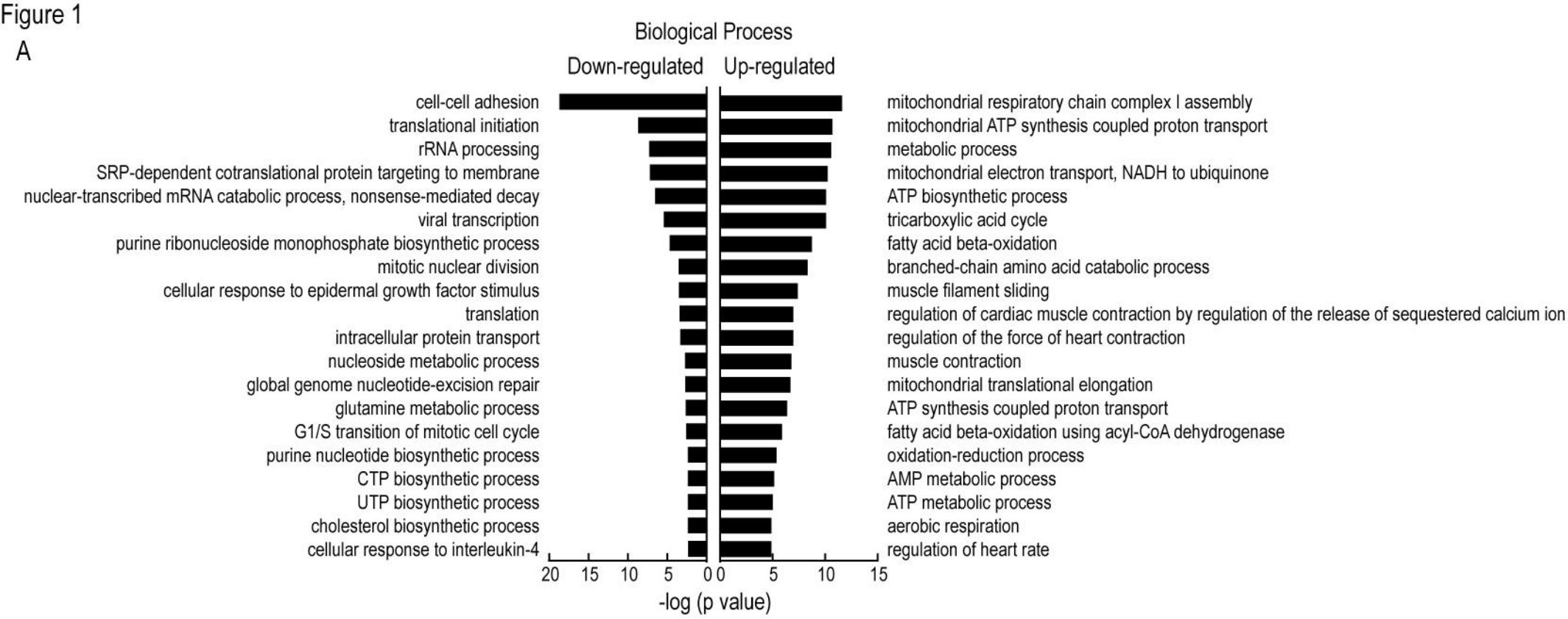
A
Biological Process
Down-regulated
Up-regulated
cell-cell adhesion
translational initiation
rRNA processing
SRP-dependent cotranslational protein targeting to membrane
nuclear-transcribed mRNA catabolic process, nonsense-mediated decay
viral transcription
purine ribonucleoside monophosphate biosynthetic process
mitotic nuclear division
cellular response to epidermal growth factor stimulus
translation
intracellular protein transport
nucleoside metabolic process
global genome nucleotide-excision repair
glutamine metabolic process
G1/S transition of mitotic cell cycle
purine nucleotide biosynthetic process
CTP biosynthetic process
UTP biosynthetic process
cholesterol biosynthetic process
cellular response to interleukin-4
mitochondrial respiratory chain complex I assembly
mitochondrial ATP synthesis coupled proton transport
metabolic process
mitochondrial electron transport, NADH to ubiquinone
ATP biosynthetic process
tricarboxylic acid cycle
fatty acid beta-oxidation
branched-chain amino acid catabolic process
muscle filament sliding
regulation of cardiac muscle contraction by regulation of the release of sequestered calcium ion
regulation of the force of heart contraction
muscle contraction
mitochondrial translational elongation
ATP synthesis coupled proton transport
fatty acid beta-oxidation using acyl-CoA dehydrogenase
oxidation-reduction process
AMP metabolic process
ATP metabolic process
aerobic respiration
regulation of heart rate
20 15 10 5 0
0 5 10 15
-log (p value)
B
Day 14
Day 30
MMP (ΔΨm)
Time (min)
Untreated
Rotenone
TTFA
Antimycin A
Day 14
Day 30
Untreated
Rotenone
TTFA
Antimycin A
C
Counts
TMRM
Isotype
Day 14
Day 30
ATP concentration (μM)
p=0.028
Day 14
Day 30
D
Day 14
Day 30
80-100 kDa
82 kDa
80 kDa
17 kDa
78-82 kDa
78-82 kDa
78-82 kDa
37 kDa
OPA1
MFN1
MFN2
FIS1
pDRP1S616
pDRP1S637
DRP1
GAPDH
Normalized arbitrary units
OPA1
MFN1
MFN2
FIS1
pDRP1S616
pDRP1S637
Day 14
Day 30
E
Day 14
Day 30
α-actinin/DAPI
MitoTracker/DAPI
COXIV/DAPI
MitoTracker/COXIV/DAPI
F
Day 14
Day 30
M
N
1 μm
1 μm

Figure 2

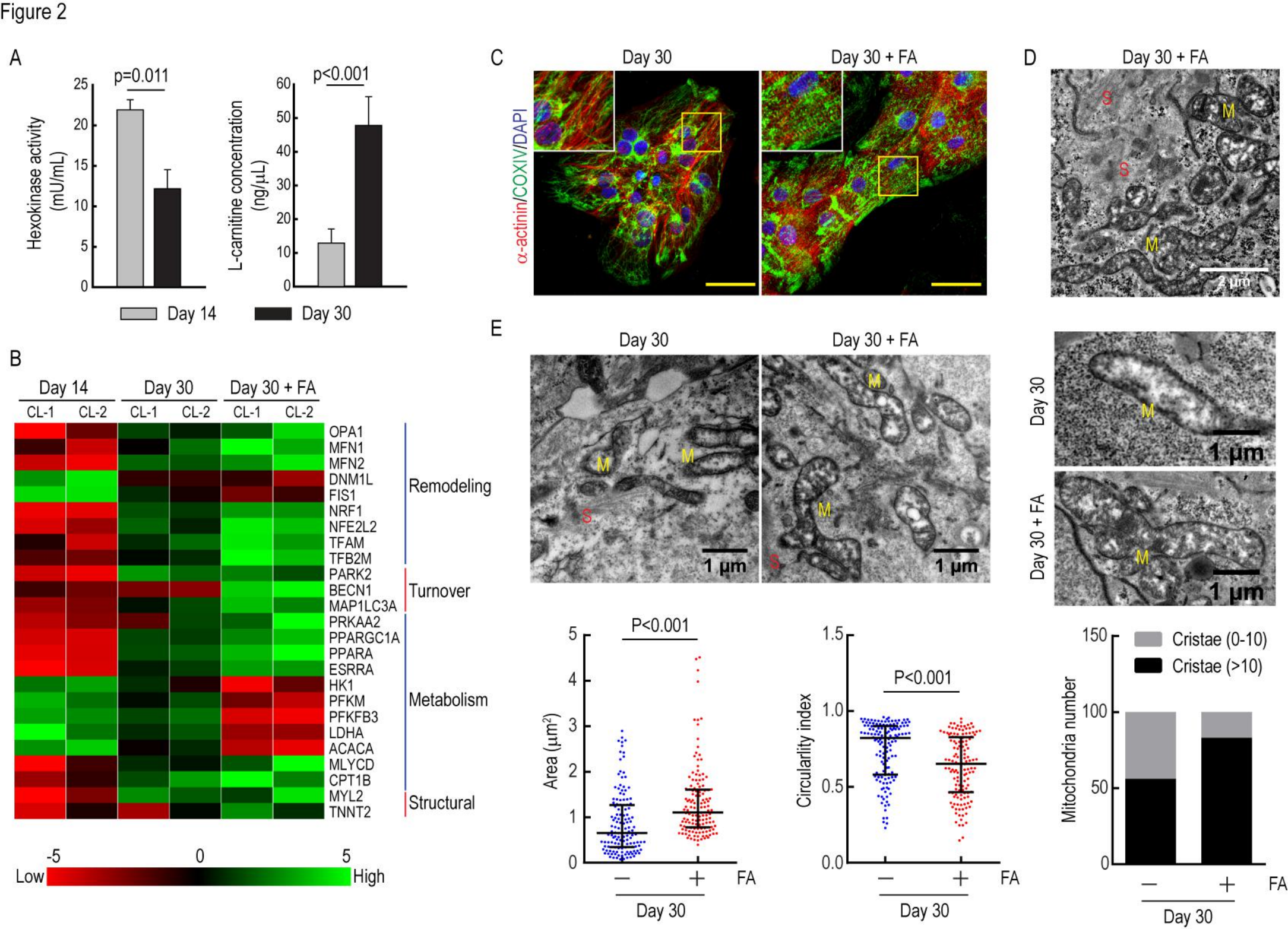
A
p=0.011
Hexokinase activity (mU/mL)
25
20
15
10
5
0
p<0.001
L-carnitine concentration (ng/μL)
60
50
40
30
20
10
0
Day 14
Day 30
B
Day 14
Day 30
Day 30 + FA
CL-1
CL-2
CL-1
CL-2
CL-1
CL-2
OPA1
MFN1
MFN2
DNM1L
FIS1
NRF1
NFE2L2
TFAM
TFB2M
PARK2
BECN1
MAP1LC3A
PRKAA2
PPARGC1A
PPARA
ESRRA
HK1
PFKM
PFKFB3
LDHA
ACACA
MLYCD
CPT1B
MYL2
TNNT2
Remodeling
Turnover
Metabolism
Structural
-5
0
5
Low
High
C
Day 30
Day 30 + FA
α-actinin/COXIV/DAPI
D
Day 30 + FA
S
M
S
M
2 μm
E
Day 30
Day 30 + FA
M
M
S
M
M
S
1 μm
1 μm
Day 30
Day 30 + FA
M
M
1 μm
1 μm
P<0.001
Area (μm²)
5
4
3
2
1
0
–
+
FA
Day 30
P<0.001
Circularity index
1.5
1.0
0.5
0.0
–
+
FA
Day 30
Mitochondria number
150
100
50
0
Cristae (0-10)
Cristae (>10)
–
+
FA
Day 30

Figure 3

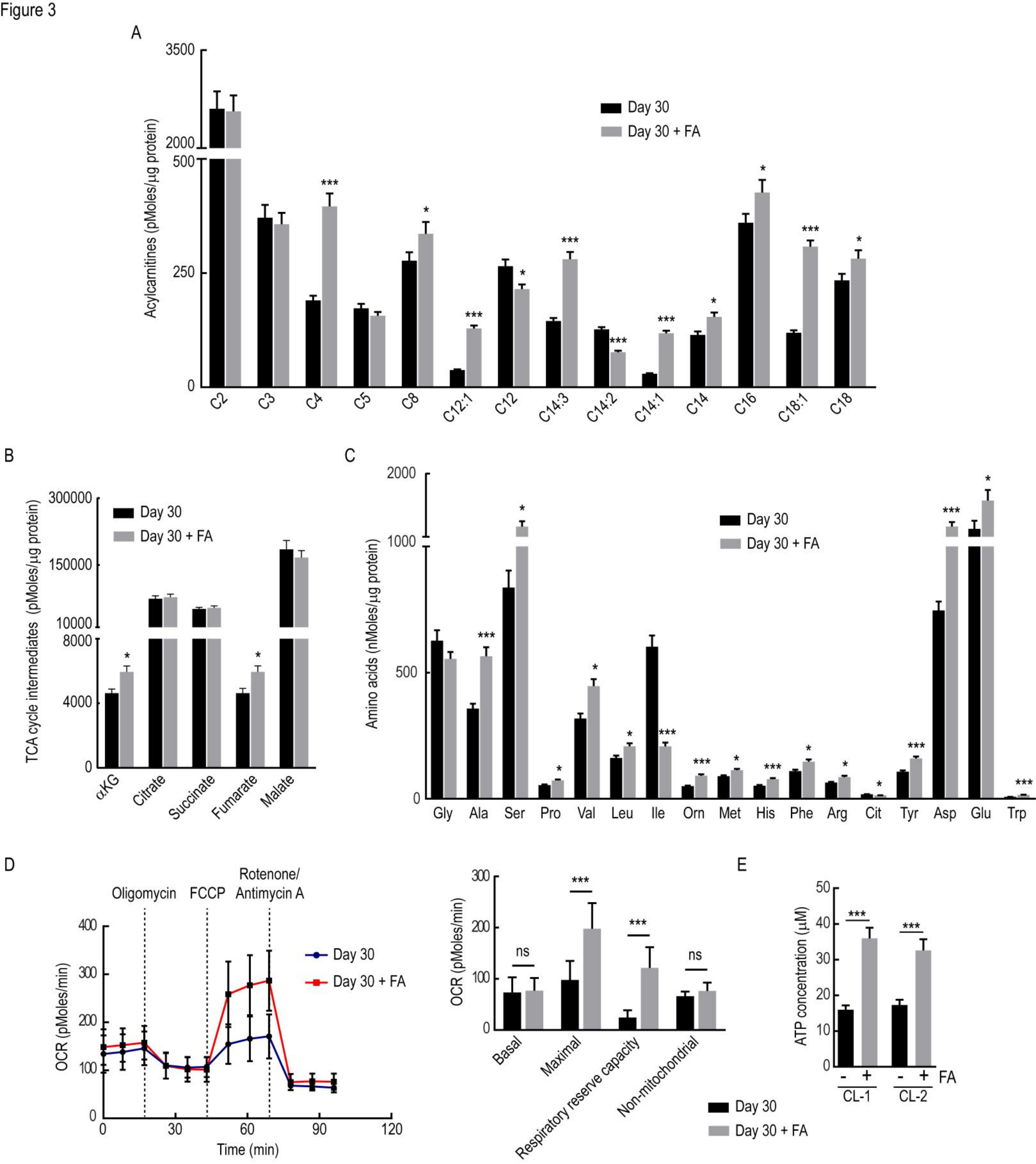
A
Acylcarnitines (pMoles/µg protein)
Day 30
Day 30 + FA
C2
C3
C4
C5
C8
C12:1
C12
C14:3
C14:2
C14:1
C14
C16
C18:1
C18
B
TCA cycle intermediates (pMoles/µg protein)
αKG
Citrate
Succinate
Fumarate
Malate
C
Amino acids (nMoles/µg protein)
Gly
Ala
Ser
Pro
Val
Leu
Ile
Orn
Met
His
Phe
Arg
Cit
Tyr
Asp
Glu
Trp
D
Oligomycin
FCCP
Rotenone/
Antimycin A
OCR (pMoles/min)
Time (min)
Basal
Maximal
Respiratory reserve capacity
Non-mitochondrial
ns
E
ATP concentration (µM)
CL-1
CL-2
FA

Figure 4

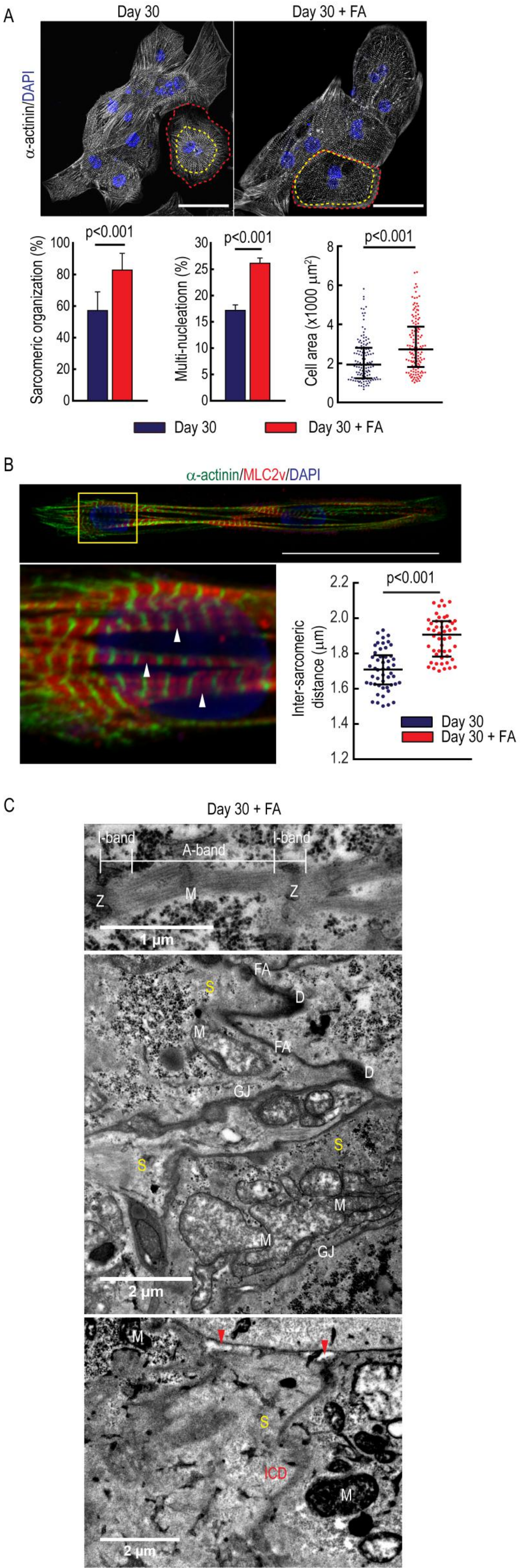
A
Day 30
Day 30 + FA
α-actinin/DAPI
Sarcomeric organization (%)
p<0.001
Multi-nucleationn (%)
p<0.001
Cell area (x1000 μm²)
p<0.001
Day 30
Day 30 + FA
B
α-actinin/MLC2v/DAPI
Inter-sarcomeric distance (μm)
p<0.001
Day 30
Day 30 + FA
C
Day 30 + FA
I-band
A-band
I-band
Z
M
Z
1 μm
FA
S
D
M
FA
D
GJ
S
S
M
M
GJ
2 μm
M
S
ICD
M
2 μm
D
Day 14
Day 30
Day 30 + FA
150 kDa
L-type Ca2+ channel
108 kDa
NCX1
21 kDa
Caveolin-3
76 kDa
Amphiphysin
74 kDa
Junctophilin-2
19 kDa
Tcap
37 kDa
GAPDH
Normalized arbitrary units
L-type Ca2+ channel
NCX1
Caveolin-3
Amphiphysin
Junctophilin-2
Tcap
ns
*
**
***
Day 14
Day 30
Day 30 + FA
E
Day 30
Day 30 + FA
F/F0
0.5s
Amplitude (F/F0)
Time to peak (s)
Decay time constant (s)
F
TNNT2 transcript levels (%)
Fetal
Adult
250 bp
Fetal
Adult
Day 14
Day 30
Day 30 + FA
G
cTnT protein levels (%)
Fetal
Adult
38 kDa
Fetal
Adult
Day 14
Day 30
Day 30 + FA

Supplementary Methods

hiPSC maintenance and cardiac differentiation

Normal dermal fibroblast-derived hiPSC line (CL-1)[1] and BJ fibroblast-derived-mRNA reprogramed hiPSC line (CL-2)[2] were maintained in mTeSR (Stemcell Technologies, Vancouver, Canada) under feeder-free conditions as previously reported[3]. Human iPSCs were differentiated into cardiomyocytes using a previously described embryoid body (EB) based protocol[4]. Briefly, the day prior to differentiation, hiPSCs were treated with 10μM ROCK inhibitor Y-27632 (Calbiochem, CA, USA). The following day, hiPSCs were dissociated into single cells using Accutase (Stemcell Technologies) and resuspended in mTeSR:DMEM/F12-B27 (1:1) medium supplemented with PVA (4mg/ml), ascorbic acid (284μM) and BMP-4 (770pM) to form 5,000 cell EBs in AggreWells (Stemcell Technologies). The following day, aggregated EBs were removed from the AggreWells and maintained (in suspension) in mTeSR:DMEM/F12-B27 (1:4) + PVA medium supplemented with ascorbic acid (284μM) and BMP-4 (1.5nM) and additional activin A (1.5nM), FGF2 (3.1nM) and SB203580 (5μM) for 72 hours, after which they were maintained in DMEM/F12-B27 + PVA medium supplemented with ascorbic acid (284μM), SB203580 (5μM), VEGF (1.5nM), cyclosporine A (2.5μM), IWP-4 (10μM), noggin (4.3nM), and A83-01 (1μM) for 48 hours. Finally, the EBs were maintained in the above DMEM/F12-B27 + PVA medium supplemented with ascorbic acid (284μM), SB203580 (5μM), VEGF (521pM), cyclosporine A (2.5μM), and IWP-4 (10μM) for 48 hours, after which they were plated on 0.1% gelatin-coated plates and maintained as cardiac clusters in DMEM (Thermo Fisher Scientific, MA, USA) supplemented with 2% FBS, non-essential amino acids and GlutaMAX (Thermo Fisher Scientific). For experiments involving fatty acids, a mixture of palmitate/oleate at a ratio of 1:1 were supplemented (100 μM) to the maintenance medium 72 hours prior to analysis. For certain assays (e.g. immunostaining, mitochondrial respiration assay) cardiac clusters were dissociated into single cell cardiomyocytes using Embryoid Body Dissociation Kit (Miltenyi Biotec, Bergisch Gladbach, Germany) and plated on 0.1% gelatin-coated plates. Growth factors were precured from R&D Systems (MN, USA), small molecules from Calbiochem and chemicals from Sigma-Aldrich (MO, USA).

Western blot and whole-cell proteome analysis

Western blots were performed as described previously[3]. Briefly, extracted proteins (25μg) from cardiac clusters were subjected to electrophoresis and transferred to nitrocellulose (NC) membranes using iBlot Dry Blotting System (Thermo Fisher Scientific). Nitrocellulose membranes were blocked and probed with primary antibodies overnight (Supplementary table 1). The following day, NC membranes were washed, probed with respective HRP-conjugated secondary antibodies and developed using Amersham ECL Western Blotting Analysis System (GE Healthcare Life Sciences, PA, USA). Images were captured using C-DiGit Blot Scanner (LI-COR, NE, USA). Densitometric analysis was performed using ImageJ. Whole-cell proteome analysis was performed as previously described[5]. Briefly, cardiac clusters and parental hiPSCs were lysed on ice for 1hr in buffer containing 7M Urea, 2M Thiourea, 4% CHAPS, Nuclease mix (GE Healthcare Life Sciences), Complete ULTRA Protease Inhibitor Cocktail and PhosSTOP phosphatase inhibitor (Sigma-Aldrich). Extracted proteins were quantified using 2D Quant Kit (GE Healthcare Life Sciences). Similar to Western blots, 200μg of protein were subjected to electrophoresis at 200V for 22 minutes using Bolt 4-12% Bis-Tris Plus Gels (Thermo Fisher Scientific). Once

complete, the gels were stained using SilverQuest™ Silver Staining Kit (Thermo Fisher Scientific). Each lain containing proteins was sliced separately and digested overnight at 37^0C using trypsin. The digested peptides were prepped for mass spectrometry and analyzed via Matrix-Assisted Desorption/Ionization Time-of-Flight (MALDI-TOF) as described previously[6]. Peptide fingerprints obtained were identified by Mascot (Matrix Science, London, UK). Peptides obtained from day 30-CMs were compared against day 14-CMs and those with a 20%-fold change (up-regulated and down-regulated) (nonparametric t-test; $p<0.05$) were analyzed using DAVID Bioinformatics Resources 6.8. The proteome assay was performed in triplicate and the principal component analysis (PCA) was performed using Clustvis[7].

Real-time PCR

Quantitative Real-time PCR (qRT-PCR) was performed as described previously[8]. Briefly, isolated RNA from cardiac clusters was converted to complementary DNA (cDNA) using SuperScript III First-Strand Synthesis System (Thermo Fisher Scientific). Using QuantiFast SYBR Green PCR Kit (Qiagen, Hilden, Germany) and RotorGene Q (Qiagen), cDNA templates were cycled as follows: 5 min at 95°C, followed by 40 cycles of 10s at 95°C and 30s at 60°C. Relative quantification was calculated according to $^{\Delta\Delta}$Ct method using GAPDH as endogenous control. Heat-maps were generated using Genesis. Primers used in the study are listed in Supplementary table 2.

Calcium analysis

Cardiac clusters were dissociated into single cells and stained with Fluo-4, AM (Thermo Fisher Scientific) for 15 minutes at 37^oC. Using C-Pace EP (IonOptix, MA, USA), cells were paced at 0.5 Hz and calcium transients were recorded using MetaMorph Imaging System (Molecular Devices). Calcium transients were analyzed using a previously described Excel based program[9].

Immunohistochemistry

Cardiac clusters were fixed with 4% PFA and embedded in paraffin. Four-micron sectioned were permeabilized with 0.1% Triton X-100 and treated with 3% hydrogen peroxide. Sections were blocked with 5% BSA and stained with primary antibody overnight (Supplementary table 1). The following day, sections were washed, probed with HRP-conjugated secondary antibodies and developed using Liquid DAB+ Substrate Chromogen System (Agilent Technologies, CA, USA). Sections were counterstained with DAPI and examined under Zeiss Axiovert 200M (Carl Zeiss Microscopy GmbH).

Supplementary Data

Supplementary figure 1

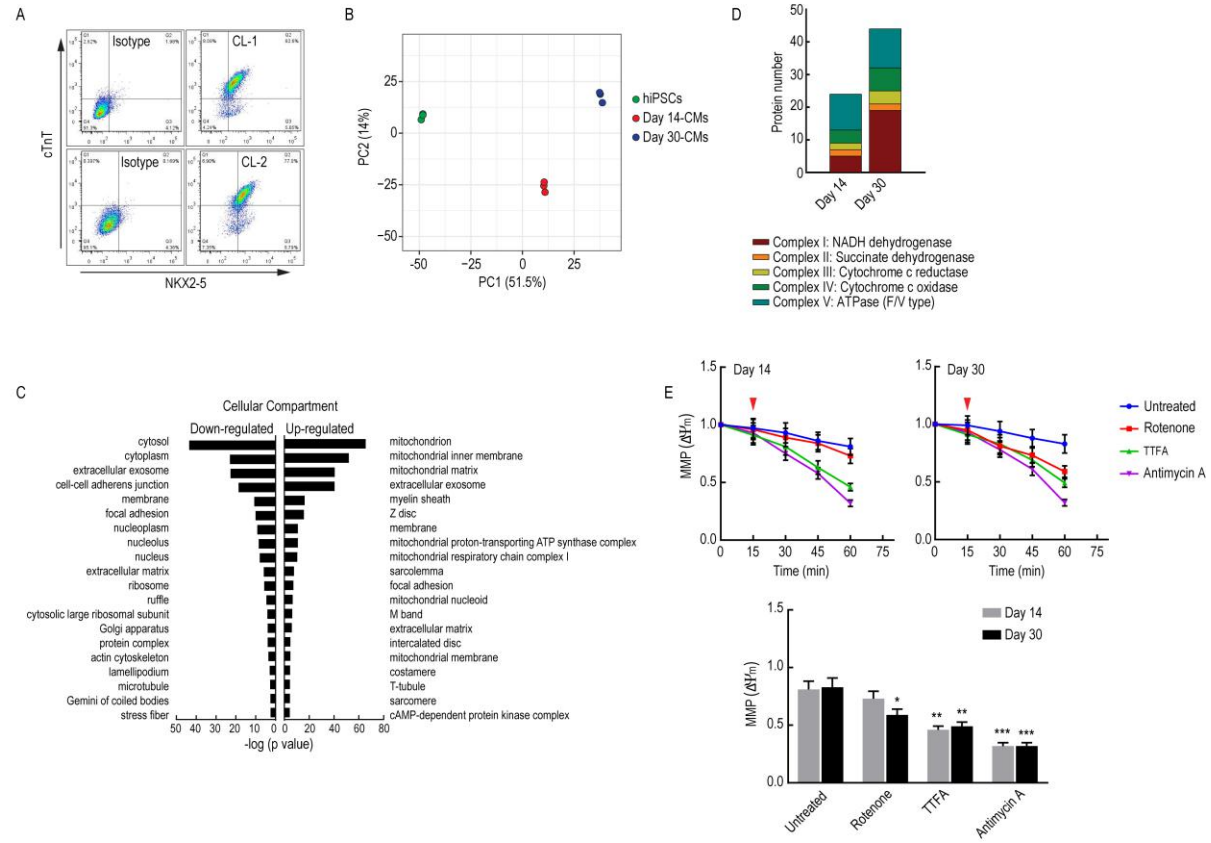

Supplementary figure 1: (A) Flow cytometry analysis of CL-1 and CL-2 derived day 14-CMs stained against NKX2-5 and cardiac troponin T (cTnT). A total of 10,000 gated events were analyzed. (B) PCA analysis of CL-1 hiPSC (green) and CL-1 derived day 14- (red) and day 30-CM (blue) proteome run in triplicate. Note the distinct clustering between different cell types. (C) Horizontal bar graphs showing up-regulated and down-regulated cellular compartments in CL-1 derived day 30-CMs when compared against day 14-CMs. Note that protein families located in the mitochondria and sarcomere compartments are significantly up-regulated in day 30-CMs. (D) Stacked graph showing abundance of proteins involved in electron transport chain complexes expressed in CL-1 derived day 14- and day 30-CMs. Note the abundant expression of complex I proteins in day 30-CMs. (E) Mitochondrial functional assay (top) in CL-2 derived day 14- and day 30-CMs showing time-dependent decrease in mitochondrial membrane potential (MMP) pre- and post-rotenone, TTFA and antimycin A treatment. Note that rotenone (complex I inhibitor) decreases MMP only in day 30-CMs and has minimal effect on day 14-CMs. Red arrowheads indicate the addition of inhibitory compounds. Bar graphs (bottom) showing MMP in CL-2 derived day 14- and day30-CMs pre- and post-compound treatment at 60-minute interval. Bar graphs presented as mean ± SD (n=3 independent experiments; Kruskal-Wallis test). *p<0.05; **p<0.01; ***p<0.001 significantly different from the respective untreated group.

Supplementary figure 2

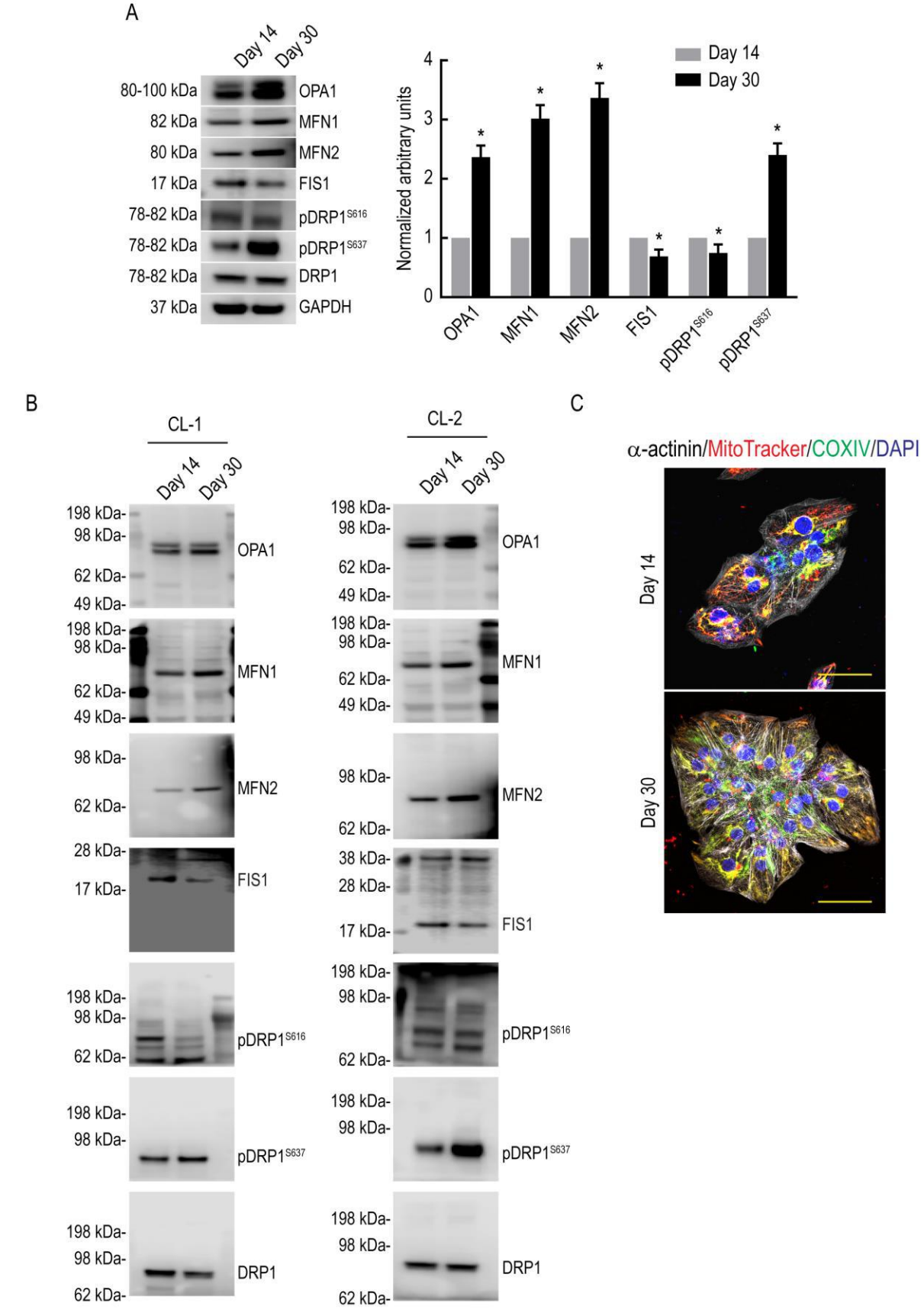

Supplementary figure 2: (A) Western blots (left) showing expression levels of OPA1, MFN1, MFN2, FIS1 as well as total and phosphorylated DRP1 (pDRP1^{S616}/pDRP1^{S637}) in CL-2 derived day 14- and day 30-CMs with bar graphs (right) showing densitometry data normalized to GAPDH. Bar graphs presented as mean ± SD (n=3 independent experiments; nonparametric t-test). *$p<0.05$ significantly different from day 14-CMs. (B) Uncropped Western blots showing expression levels of mitochondrial fusion and fission proteins in CL-1 and CL-2 derived day 14- and day 30-CMs. (C) Merged pictographs of CL-1 derived day 14- and day 30-CMs stained against α-actinin (pseudo-colored white), MitoTracker (red) and COXIV (green), counterstained with DAPI (blue). Note the expansive filamentous mitochondrial networks in day 30-CMs as opposed to the isolated fragmented foci in day 14-CMs. Scale bar: 50 µm.

Supplementary figure 3

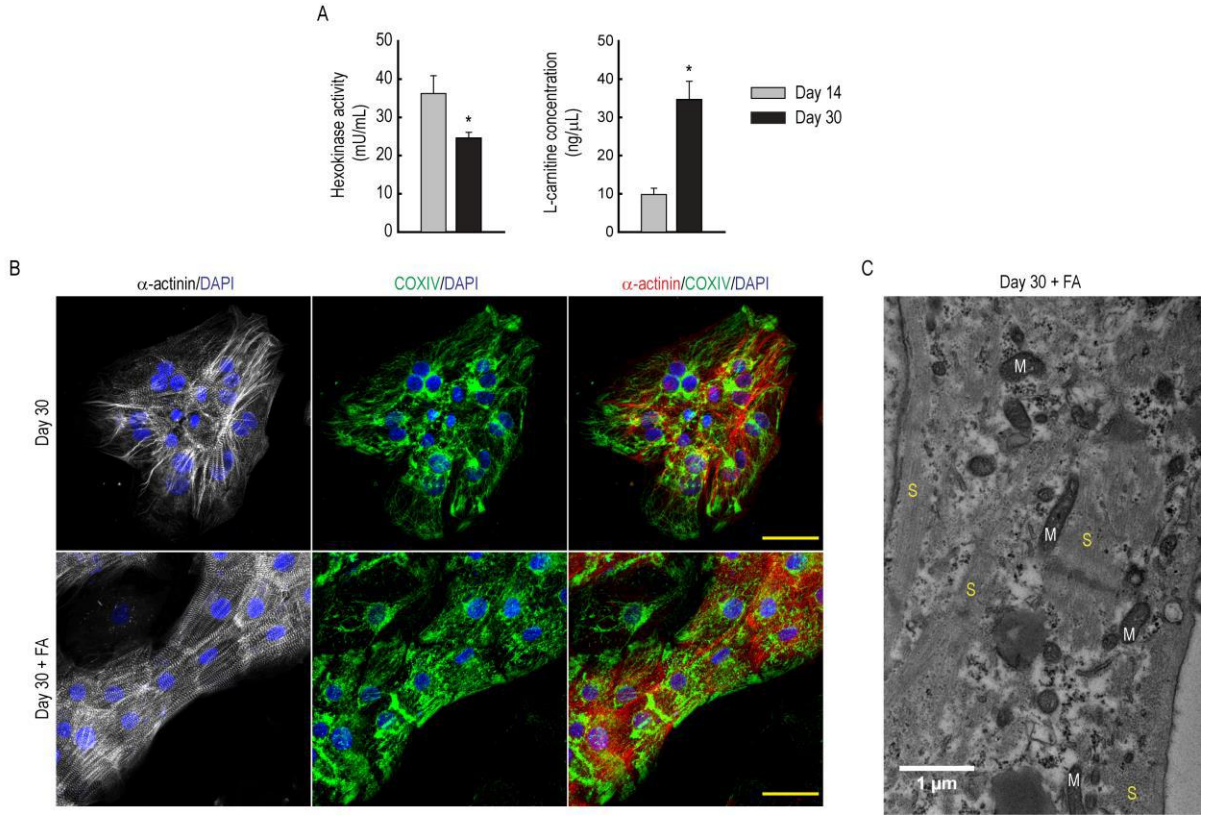

Supplementary figure 3: (A) Bar graphs showing hexokinase activity (left) and L-carnitine concentrations (right) in CL-2 derived day 14- and day 30-CMs. Bar graphs presented as mean ± SD (n=3 independent experiments; nonparametric t-test). *p<0.05 significantly different from day 14-CMs (B) Pictographs of CL-1 derived day 30-CMs pre- and post-FA supplementation stained against α-actinin (pseudo-colored white) and COXIV (green), counterstained with DAPI (blue). Note the abundant filamentous mitochondrial networks in FA supplemented day30-CMs. Scale bar: 50 µm. (C) Transmission electron microscopy pictograph of CL-1 derived FA supplemented day 30-CMs showing inter-sarcomeric distribution of mitochondria. Abbreviations: M- mitochondria; S- sarcomeres.

Supplementary figure 4

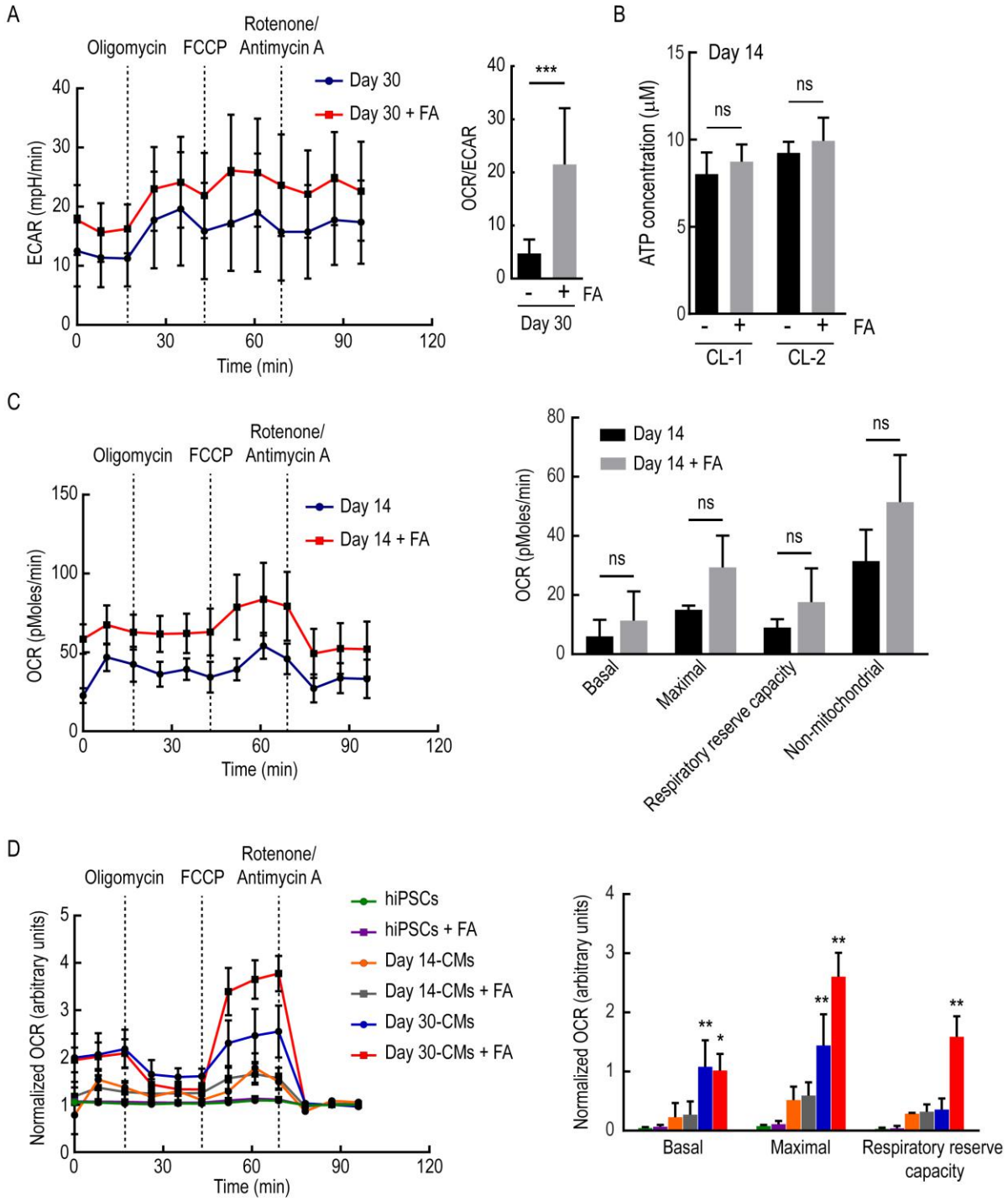

Supplementary figure 4: (A) Seahorse assay (left) showing extracellular acidification rates (ECAR) in CL-1 derived day 30-CMs pre- and post-FA supplementation with bar graphs (right) showing OCR to ECAR ratio. Bar graphs presented as mean ± SD (n=8 wells analyzed per group; nonparametric t-test). ***p<0.001 significantly different between comparison groups. (B) Bar graphs showing insignificant differences in ATP concentrations in CL-1 and CL-2 derived day 14-CMs pre- and post-FA supplementation. Bar graphs presented as mean ± SD (n=3 independent experiments; nonparametric t-test). Abbreviations: ns- not significant. (C) Seahorse assay (left) showing oxygen consumption rate (OCR) in CL-1 derived day 14-CMs pre- and post-

FA supplementation with bar graphs (right) showing insignificant differences in basal, maximal, non-mitochondrial OCR as well as respiratory reserve capacity. Bar graphs presented as mean ± SD (n=2 wells analyzed for day 14-CMs and n=5 wells analyzed for FA supplemented day 14-CMs; nonparametric t-test). Abbreviations: ns- not significant. (D) Overlaid seahorse assays (left) showing OCR in CL-1 hiPSCs and in CL-1 derived day 14- and day 30-CMs pre- and post-FA supplementation with bar graphs (right) showing basal and maximal OCR as well as respiratory reserve capacity. Bar graphs presented as mean ± SD (n=8 wells analyzed per group, except for day 14-CMs; n=2 and FA supplemented day 14-CMs; n=5; Kruskal-Wallis test) with data normalized to non-mitochondrial OCR. *$p<0.01$; **$p<0.001$ significantly different from glucose-maintained day 14-CMs not supplemented with FA.

Supplementary figure 5

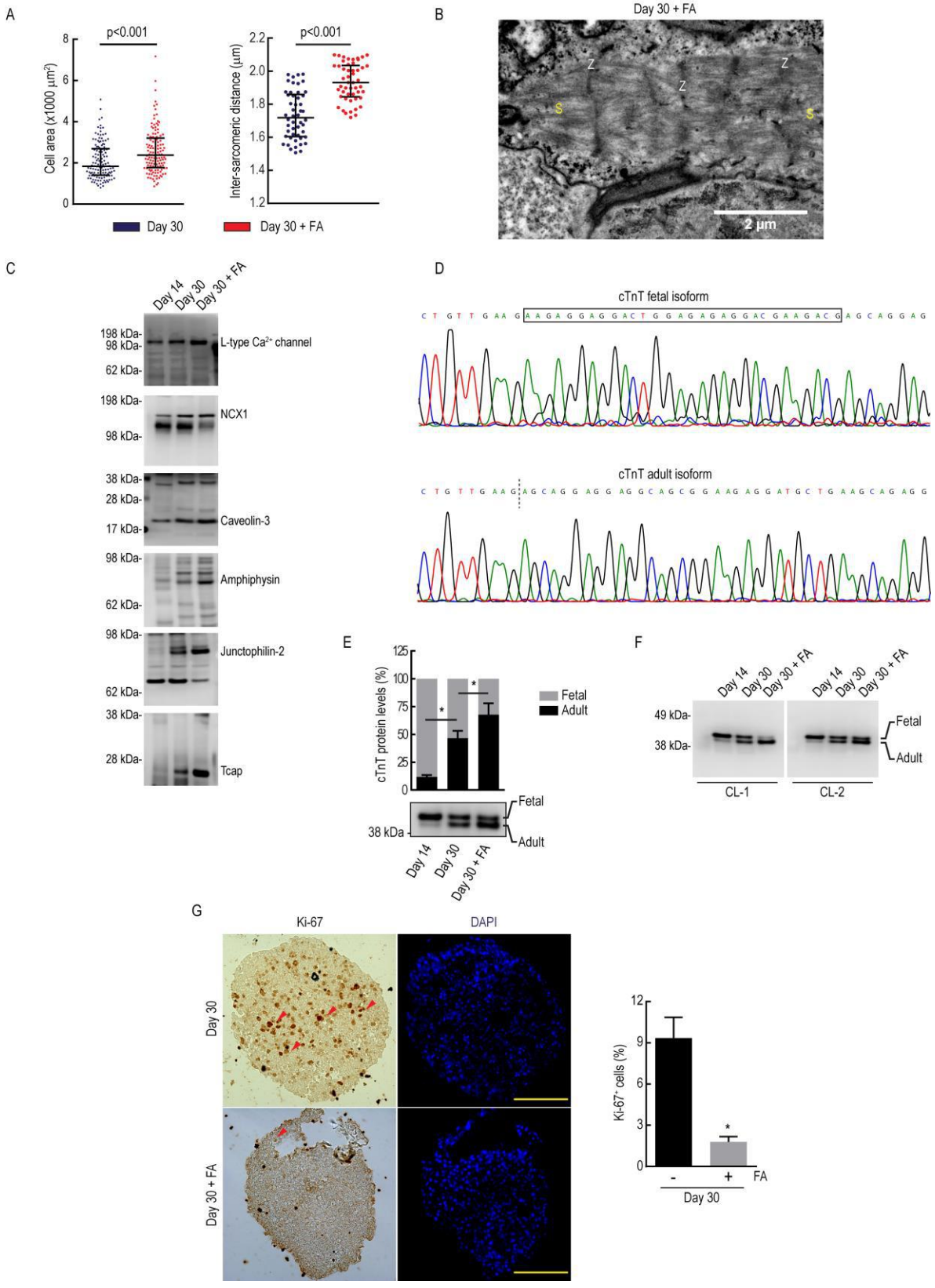

Supplementary figure 5: (A) Scatter dot plots (left) showing cell size of CL-2 derived day 30-CMs pre- and post-FA supplementation. Scatter dot plots presented as median with interquartile range (n=130 cells analyzed per group from n=3 independent experiments; parametric t-test). Scatter dot plots (right) showing inter-sarcomeric distance in CL-2 derived day 30-CMs pre- and post-FA supplementation. Scatter dot plots presented as median with interquartile range (n=50 cells analyzed per group from n=3 independent experiments; parametric t-test). (B) Transmission electron microscopy pictograph of CL-1 derived FA supplemented day 30-CMs showing highly developed sarcomeres containing regularly registered Z-discs. Abbreviations: S- sarcomeres; Z- Z-disc. (C) Uncropped Western blots showing expression levels of t-tubule associated proteins in CL-1 derived day 14-CMs as well as in day 30-CMs pre- and post-FA supplementation. (D) Sanger sequencing of the fetal and adult cardiac troponin T isoforms. Note the absence of a 30-bp fragment (boxed region) in the adult isoform. (E) Stacked graphs (top) showing percentage of fetal/adult cardiac troponin T isoforms expressed in CL-2 derived day 14-CMs as well as in day 30-CMs pre- and post-FA supplementation. Stacked graphs presented as mean ± SD (n=3 independent experiments; Kruskal-Wallis test). *$p<0.001$ significantly different between comparison groups. Western blots (bottom) showing discrimination of isoforms based on molecular weight. Note that FA supplemented day 30-CMs predominantly express the adult isoform. (F) Uncropped Western blots showing expression levels of cardiac troponin T isoforms in CL-1 and CL-2 derived day 14-CMs as well as in day 30-CMs pre- and post-FA supplementation. (G) Pictographs (left) of CL-1 derived day 30-CMs (clusters) pre- and post-FA supplementation stained against Ki-67 and counterstained with DAPI (blue). Note the drastic reduction in proliferation ($Ki\text{-}67^+$ cells; red arrowheads) post-FA supplementation. Scale bar: 100 µm. Bar graphs (right) showing percentage of proliferating cells in CL-1 derived day 30-CMs pre- and post-FA supplementation. Bar graphs presented as mean ± SD (n=3 clusters analyzed per group; nonparametric t-test). *$p<0.01$ significantly different from glucose-maintained day 30-CMs.

Supplementary table 1: List of antibodies used in the study

Protein	Molecular weight (kDa)	Host species	Manufacturer
NKX2-5 (F)		Rabbit	Cell Signaling Technology
cTnT (F)		Mouse	United States Biological
OPA1 (WB)	80-100	Mouse	Novus Biologicals
MFN1 (WB)	82	Mouse	Abcam
MFN2 (WB)	80	Mouse	Santa Cruz Biotechnology
FIS1 (WB)	17	Mouse	Santa Cruz Biotechnology
Phospho-DRP1 (Ser616) (WB)	78-82	Rabbit	Cell Signaling Technology
Phospho-DRP1 (Ser637) (WB)	78-82	Rabbit	Cell Signaling Technology
DRP1 (WB)	78-82	Rabbit	Cell Signaling Technology
GAPDH (WB)	37	Rabbit	Cell Signaling Technology
cTnT (WB)	40	Rabbit	Cell Signaling Technology
Phospho-PKA C (Thr197) (WB)	42	Rabbit	Cell Signaling Technology
PKA C-α (WB)	42	Rabbit	Cell Signaling Technology
COXIV (IF)	17	Rabbit	Cell Signaling Technology
α-actinin (IF)		Mouse	Sigma-Aldrich
MLC-2v (IF)		Rabbit	Synaptic Systems
L-type calcium channel (WB)	150	Mouse	Abcam
NCX1 (WB)	108	Rabbit	Abcam
Caveolin-3 (WB)	21	Rabbit	Abcam
Amphiphysin (WB)	76	Mouse	Abcam
Junctophilin-2 (WB)	74	Rabbit	Thermo Fisher Scientific
Tcap (WB)	19	Rabbit	Abcam
ITGA5 (WB)	150	Rabbit	Cell Signaling Technology
ITGA7 (WB)	130	Rabbit	Thermo Fisher Scientific
Integrin β1 (WB)	115, 135	Rabbit	Cell Signaling Technology
Integrin β1d (WB)	130	Mouse	Abcam
Ki-67 (IHC)		Mouse	Agilent Technologies
Abbreviations: WB- Western blot; IF- Immunofluorescence; F-Flow cytometry; IHC-Immunohistochemistry			

Supplementary table 2: List of primers used in the study

Gene	Forward primer	Reverse primer
OPA1	GCGGAAGACCTCAAGAAAGT	AGGCTGGACAAAAGACGTTGA
MFN1	GCCTCCTCTCCGCCTTTAAC	GCCATTATGCTAAGTCTCCGC
MFN2	AATCTGAGGCGACTGGTGAC	CTCCACCAGTCCTGACTTCAC
DNM1L	GGAGGCGCTAATTCCTGTCA	CTTTCCGCTGCTCTGCGTTC
FIS1	AGGCCTTAAAGTACGTCCGC	TGCCCACGAGTCCATCTTTC
TFAM	TGATTCACCGCAGGAAAAGC	ACGAGTTTCGTCCTCTTTAGCA
TFB2M	TCCACATTTGGAGTCCTTAGGAAA	GCCCTCGAGAAGACATAGCA
PARK2	CCCTGGGACTAGTGCAGAATTT	CCTGACGTCTGTGCACGTAA
BECN1	GGAAGGGTCTAAGACGTCCA	AATGGAGCTGTGAGTTCCTGG
MAP1LC3A	CCCTCAGACCGGCCTTTCAA	TGATCACCGGGATTTTGCTGG
PRKAA2	ACCAGGTGATCAGCACTCCA	TCTCTTCAACCCGTCCATGC
PPARGC1A	TGCATGAGTGTGTGCTCTGT	CAGCACACTCGATGTCACTC
PPARA	GCGAACGATTCGACTCAAGC	AACGAATCGCGTTGTGTGAC
ESRRA	GCATCCCAGGCTTCTCATCG	GACTAAGTCCTCAGCGAAGGC
NRF1	CAGCCGCTCTGAGAACTTCA	CGGTGTAAGTAGCCACATGGA
NFE2L2	CCAACTACTCCCAGGTTGCC	AGTGACTGAAACGTAGCCGAA
HK1	AGGACCGACCGTCCCC	ACTTGTCAATCTTTTTGACCTGG
PFKM	CTCAGAGAACAGCTGGGGAAG	TTCCCACGGTGTCTGGATCAT
PFKFB3	CAGCTGCCTGGACAAAACAT	CAGCTGCCTGGACAAAACAT
LDHA	AGCTGTTCCACTTAAGGCCC	TGGAACCAAAAGGAATCGGGA
ACACA	GATGCTCCTGGAACGTCGAA	TCCAAAAAGACCTAGCCCTCA
MLYCD	GGACGTCCGGGAAATGAATG	ACACGGTGAATGCCAGGTAA
CPT1B	GAGTGAACCCGAGCTGTGC	AGGTAGACGTGTTTCAGGGC
MYL2	TGGGCGAGTGAACGTGAAAA	AGGGTCCGCTCCCTTAAGTT
TNNT2	GACAGAGCGGAAAAGTGGGAA	CCTTCTCCCTCAGCTGATCTT
*TNNT2**	GAGGGAGAGCAGAGACCATGTCTG	AGCCTCCTTTGCTTCCTCTTCTTC
*Discriminates between fetal isoform 1 and adult isoform 3		

Supplementary table 3: List of enriched proteins (see Excel file)

Supplementary table 4: List of enriched Biological Processes (see Excel file)

Supplementary table 5: List of enriched Cellular Compartments (see Excel file)

Supplementary table 6: Inter-sarcomeric distance

CL-1 (µm)			CL-2 (µm)		
Cell #	**Day 30**	**Day 30 + FA**	**Cell #**	**Day 30**	**Day 30 + FA**
1	1.889	1.795	1	1.765	2.061
2	1.634	1.714	2	1.874	1.838
3	1.748	1.982	3	1.707	1.907
4	1.846	1.985	4	1.978	2.073
5	1.678	1.971	5	1.799	1.931
6	1.860	1.811	6	1.871	1.820
7	1.687	2.099	7	1.759	2.093
8	1.520	1.722	8	1.578	2.086
9	1.728	1.846	9	1.728	1.833
10	1.621	1.899	10	1.527	1.887
11	1.734	2.004	11	1.506	1.930
12	1.762	2.027	12	1.671	1.945
13	1.714	1.840	13	1.633	1.983
14	1.521	1.741	14	1.674	2.098
15	1.566	2.012	15	1.515	1.860
16	1.669	1.700	16	1.636	1.768
17	1.832	2.092	17	1.690	2.048
18	1.618	1.813	18	1.941	1.897
19	1.916	1.969	19	1.871	1.896
20	1.524	1.979	20	1.851	2.03
21	1.902	1.924	21	1.703	1.780
22	1.586	1.914	22	1.837	1.720
23	1.634	2.087	23	1.873	1.783
24	1.670	1.883	24	1.662	1.905
25	1.642	2.004	25	1.611	1.753
26	1.606	1.931	26	1.855	2.096
27	1.717	1.712	27	1.539	1.832
28	1.785	1.775	28	1.605	1.744
29	1.706	1.716	29	1.562	1.760
30	1.666	1.765	30	1.601	2.012
31	1.755	1.741	31	1.978	1.965
32	1.779	1.815	32	1.734	1.846
33	1.501	1.930	33	1.757	2.077
34	1.781	1.938	34	1.555	1.732
35	1.658	1.888	35	1.597	1.875
36	1.625	2.071	36	1.652	2.002
37	1.932	1.983	37	1.796	2.032
38	1.804	1.784	38	1.552	1.898
39	1.866	1.814	39	1.688	2.069
40	1.556	1.948	40	1.925	2.039
41	1.859	1.746	41	1.929	2.003
42	1.711	1.722	42	1.964	1.874
43	1.508	1.940	43	1.617	1.860
44	1.603	1.747	44	1.733	1.955
45	1.825	1.840	45	1.938	2.020

46	1.626	1.990	46	1.594	2.031
47	1.849	1.950	47	1.803	2.086
48	1.778	1.882	48	1.557	2.004
49	1.767	1.953	49	1.981	1.874
50	1.629	2.068	50	1.85	2.070

Supplementary table 7: List of ETC complex peptides identified by mass spectrometry

Complex	Day 14	Day 30
I	Ndufs1, Ndufs2* Ndufv1, Ndufv2, Ndufa9	Ndufs1, Ndufs2*, Ndufs7*, Ndufs8*, Ndufv1, Ndufv2, Ndufa2, Ndufa5, Ndufa8, Ndufa9, Ndufa10, Ndufab1, Ndufa12, Ndufa13, Ndufb1, Ndufb3, Ndufb4, Ndufb8, Ndufb9
II	SDHA, SDHB	SDHA, SDHB
III	ISP	ISP, COR1, QCR2, QCR7
IV	COX5A, COX5B,	COX2, COX4, COX5A, COX5B, COX6B, COX6C, COX7A
V	alpha, beta, gamma, delta, OSCP, b, d, f, g	alpha, beta, gamma, delta, OSCP, a, b, d, f, g
*encodes for the Q module		

References

[1] Mehta A, Ramachandra CJA, Singh P, Chitre A, Lua CH, Mura M, et al. Identification of a targeted and testable antiarrhythmic therapy for long-QT syndrome type 2 using a patient-specific cellular model. European heart journal. 2017.

[2] Mehta A, Verma V, Nandihalli M, Ramachandra CJ, Sequiera GL, Sudibyo Y, et al. A systemic evaluation of cardiac differentiation from mRNA reprogrammed human induced pluripotent stem cells. PloS one. 2014;9:e103485.

[3] Ramachandra CJ, Mehta A, Wong P, Shim W. ErbB4 Activated p38gamma MAPK Isoform Mediates Early Cardiogenesis Through NKx2.5 in Human Pluripotent Stem Cells. Stem cells. 2016;34:288-98.

[4] Mehta A, Ramachandra CJ, Sequiera GL, Sudibyo Y, Nandihalli M, Yong PJ, et al. Phasic modulation of Wnt signaling enhances cardiac differentiation in human pluripotent stem cells by recapitulating developmental ontogeny. Biochimica et biophysica acta. 2014;1843:2394-402.

[5] Mehta A, Ramachandra CJA, Chitre A, Singh P, Lua CH, Shim W. Acetylated Signal Transducer and Activator of Transcription 3 Functions as Molecular Adaptor Independent of Transcriptional Activity During Human Cardiogenesis. Stem cells. 2017;35:2129-37.

[6] Adav SS, Cheow ES, Ravindran A, Dutta B, Sze SK. Label free quantitative proteomic analysis of secretome by Thermobifida fusca on different lignocellulosic biomass. Journal of proteomics. 2012;75:3694-706.

[7] Metsalu T, Vilo J. ClustVis: a web tool for visualizing clustering of multivariate data using Principal Component Analysis and heatmap. Nucleic acids research. 2015;43:W566-70.

[8] Ramachandra CJ, Mehta A, Lua CH, Chitre A, Ja KP, Shim W. ErbB Receptor Tyrosine Kinase: A Molecular Switch Between Cardiac and Neuroectoderm Specification in Human Pluripotent Stem Cells. Stem cells. 2016;34:2461-70.

[9] Greensmith DJ. Ca analysis: an Excel based program for the analysis of intracellular calcium transients including multiple, simultaneous regression analysis. Computer methods and programs in biomedicine. 2014;113:241-50.

Supplementary table 3: List of enriched proteins

Down-regulated		Up-regulated	
Uniprot Accession	**Protein**	**Uniprot Accession**	**Protein**
A1A693	RNA-binding protein 15 (One-twenty two prote	A0PJH8	ZNHIT2 protein (Fragment)
A0AVT1	Ubiquitin-like modifier-activating enzyme 6 (Ub	A1L172	Acyl-CoA thioesterase 1
A2A2D8	Sal-like protein 4 (Zinc finger protein 797) (Zinc	A2A2Y4	FERM domain-containing protein 3 (Band 4.1-l
A2IDD0	Nucleoside diphosphate kinase, mitochondrial	A2RRG0	RNA-binding protein with multiple splicing 2
A4QPB0	IQ motif containing GTPase activating protein 1	A4D7U5	Cyclic AMP-dependent transcription factor ATF
A5D904	RPS9 protein (Fragment)	A4FUJ8	MKL1 proteinMKL1 proteinMKL1 protein
A6ND99	Deleted.	A4UJ43	Glutathione S-transferase (EC 2.5.1.18)
A6NDA1	HAUS augmin-like complex subunit 7	A5YM48	MYBPC3 proteinMYBPC3 protein
A6NDU8	UPF0600 protein C5orf51	**A5Z217**	Mutant desminMutant desminMutant desmin
A6NJH9	Eukaryotic translation initiation factor 1A, Y-chr	**A6NDT1**	Deleted.
A7E2E7	TBC1 domain family member 13	A6NM69	Non-specific lipid-transfer protein (NSL-TP) (EC
A8K067	cDNA FLJ75536, highly similar to Homo sapien	A6NN50	Obscurin-like protein 1Obscurin-like protein 1
A8K0J3	cDNA FLJ76732, highly similar to Homo sapien	A6NN60	Quinone oxidoreductase (EC 1.6.5.5) (NADPH
A8K3T5	cDNA FLJ78278, highly similar to Homo sapien	A6NP52	PRA1 family proteinPRA1 family protein
A8K4G7	cDNA FLJ78528, highly similar to Homo sapien	A6ZGJ0	ATP synthase subunit a (Fragment)
A8K4W5	cDNA FLJ76813, highly similar to Homo sapien	A6ZKI3	Retrotransposon Gag-like protein 8B (Mammal
A8K564	cDNA FLJ76716, highly similar to Homo sapien	A7E2D8	Calcium-transporting ATPase (EC 3.6.3.8)
A8K5S1	cDNA FLJ78650, highly similar to Homo sapien	A7E2Y1	Myosin-7B (Antigen MLAA-21) (Myosin cardiac
A8K6N3	cDNA FLJ76886, highly similar to Homo sapien	A7MD96	SYNPO protein (Fragment)
A8K7D9	Importin subunit alpha	**A8K103**	cDNA FLJ75454, highly similar to Homo sapien
A8K7W3	cDNA FLJ75780, highly similar to Homo sapien	**A8K132**	cDNA FLJ75476, highly similar to Homo sapien
A8K8N7	Phosphoribosylformylglycinamidine synthase (	A8K1J3	cDNA FLJ78534, highly similar to Homo sapien
A8K9G6	cDNA FLJ75133, highly similar to Homo sapien	**A8K3K1**	cDNA FLJ78096, highly similar to Homo sapien
A8K9K8	rRNA adenine N(6)-methyltransferase (EC 2.1	**A8K4A1**	cDNA FLJ76790cDNA FLJ76790
A8K9V9	cDNA FLJ76064	**A8K4I8**	cDNA FLJ78131, highly similar to Homo sapien
A8KA19	cDNA FLJ75831, highly similar to Homo sapien	**A8K5D5**	cDNA FLJ76832, highly similar to Homo sapien
A8MU44	Protein Hook homolog 1 (h-hook1) (hHK1)	**A8K5W7**	cDNA FLJ75180, highly similar to Homo sapien
B1AHB1	DNA helicase (EC 3.6.4.12)	**A8K6P5**	cDNA FLJ76887, highly similar to Homo sapien
B1AJP6	Deleted.	A8K6Q8	cDNA FLJ75881, highly similar to Homo sapien
B1AJY5	26S proteasome non-ATPase regulatory subun	A8K766	Electron transfer flavoprotein subunit beta (Bet

B1AMX9	Deleted.	**A8K787**	cDNA FLJ75273, highly similar to Homo sapien
B1APM4	Sterol O-acyltransferase 1 (Fragment)	**A8K7Z9**	cDNA FLJ78530, highly similar to Homo sapien
B1APY4	Receptor tyrosine kinase-like orphan receptor 1	A8K8B9	cDNA FLJ77368, highly similar to Homo sapien
B1ARP7	Deleted.	**A8K941**	cDNA FLJ77618cDNA FLJ77618
B2C310	Glutathione S-transferase pi 1 (Fragment)	A8K968	Band 4.1-like protein 3 (cDNA FLJ77757)
B2R548	Prefoldin subunit 4	**A8K9T8**	cDNA FLJ76106, highly similar to Homo sapien
B2R5M8	Isocitrate dehydrogenase [NADP] (EC 1.1.1.42	**A8K9U1**	cDNA FLJ76468, highly similar to Homo sapien
B2R5U7	cDNA, FLJ92633, highly similar to Homo sapie	**A8KA83**	cDNA FLJ78586, highly similar to Homo sapien
B2R5V9	cDNA, FLJ92652, highly similar to Homo sapie	**A8KAK5**	cDNA FLJ77399, highly similar to Homo sapien
B2R6A3	Na(+)/H(+) exchange regulatory cofactor NHE-	A8MX12	Myomesin-1Myomesin-1Myomesin-1
B2R951	cDNA, FLJ94214, highly similar to Homo sapie	A8MXZ9	Myosin-binding protein C, cardiac-type
B2R9I9	cDNA, FLJ94417, highly similar to Homo sapie	B0LUG2	ALDH2 (Fragment)ALDH2 (Fragment)
B2R9V7	Superoxide dismutase [Cu-Zn] (EC 1.15.1.1)	B0QY72	Malonyl-CoA-acyl carrier protein transacylase,
B2RA03	cDNA, FLJ94640, highly similar to Homo sapie	B0QYF8	Myoglobin (Fragment)Myoglobin (Fragment)
B2RA34	cDNA, FLJ94678, highly similar to Homo sapie	B0QYH4	Seizure 6-like proteinSeizure 6-like protein
B2RA72	cDNA, FLJ94734, Homo sapiens CHMP1.5 pro	**B0QYL3**	Deleted.
B2RAZ3	Interferon regulatory factor 3 (IRF-3)	B1AK13	3-hydroxymethyl-3-methylglutaryl-Coenzyme A
B2RBI2	cDNA, FLJ95525, highly similar to Homo sapie	B1APG4	cAMP-dependent protein kinase catalytic subu
B2RC50	cDNA, FLJ95853, highly similar to Homo sapie	B2MVI0	MHC class I antigenMHC class I antigen
B2RD14	Ubiquitin carboxyl-terminal hydrolase (EC 3.4.1	**B2R577**	Protein S100 (S100 calcium-binding protein)
B2RDG1	Fatty acyl-CoA reductase (EC 1.2.1.84)	**B2R5M9**	cDNA, FLJ92537, highly similar to Homo sapie
B2RDJ6	Probable cytosolic iron-sulfur protein assembly	**B2R5W3**	Poly [ADP-ribose] polymerase (PARP) (EC 2.4
B2RDV2	cDNA, FLJ96778, highly similar to Homo sapie	**B2R6H3**	Kinesin-like proteinKinesin-like protein
B2RDX5	cDNA, FLJ96812, highly similar to Homo sapie	**B2R6J2**	cDNA, FLJ92973, highly similar to Homo sapie
B2RDY9	Adenylyl cyclase-associated protein	**B2R6K4**	cDNA, FLJ92996, highly similar to Homo sapie
B2RDZ9	cDNA, FLJ96850	**B2R6S9**	cDNA, FLJ93097, highly similar to Homo sapie
B3KM50	cDNA FLJ10310 fis, clone NT2RM2000322, hi	**B2R6U8**	cDNA, FLJ93125, highly similar to Homo sapie
B3KM63	cDNA FLJ10380 fis, clone NT2RM2002030, hi	**B2R713**	cDNA, FLJ93224cDNA, FLJ93224
B3KM65	cDNA FLJ10383 fis, clone NT2RM2002100, hi	B2R894	Mitochondrial ribosomal protein L38, isoform C
B3KMD3	cDNA FLJ10729 fis, clone NT2RP3001260, hig	**B2R8Y4**	cDNA, FLJ94117, highly similar to Homo sapie
B3KMI3	Spastic paraplegia 20, spartin (Troyer syndrom	**B2R923**	cDNA, FLJ94174cDNA, FLJ94174
B3KMV5	cDNA FLJ12728 fis, clone NT2RP2000040, hig	**B2R9J4**	cDNA, FLJ94423, highly similar to Homo sapie
B3KN28	Phosphoacetylglucosamine mutase (PAGM) (E	B2RAH5	cDNA, FLJ94919, highly similar to Homo sapie

B3KNA1	cDNA FLJ14021 fis, clone HEMBA1002513, hi	B2RAQ8	cDNA, FLJ95058, highly similar to Homo sapie
B3KNP4	cDNA FLJ30087 fis, clone BNGH41000003, hi	**B2RB06**	cDNA, FLJ95242, highly similar to Homo sapie
B3KNV9	cDNA FLJ30554 fis, clone BRAWH2003693	**B2RB23**	cDNA, FLJ95265, highly similar to Homo sapie
B3KP09	tRNA (cytosine(34)-C(5))-methyltransferase (E	**B2RBX8**	cDNA, FLJ95758, highly similar to Homo sapie
B3KPC1	Protein pelota homolog (EC 3.1.-.-)	**B2RCL4**	cDNA, FLJ96143, highly similar to Homo sapie
B3KPQ5	cDNA FLJ32057 fis, clone NTONG2001642, hi	B2RCS5	Alpha-actinin-2 (Alpha-actinin skeletal muscle i
B3KQ33	cDNA FLJ32715 fis, clone TESTI2000784, hig	B2RCZ7	Ethylmalonic encephalopathy 1, isoform CRA_
B3KQ95	Squalene synthase (SQS) (SS) (EC 2.5.1.21) (	**B2RDE0**	cDNA, FLJ96567, highly similar to Homo sapie
B3KRC6	cDNA FLJ34004 fis, clone FCBBF1000232, hig	**B2RDE8**	cDNA, FLJ96580, highly similar to Homo sapie
B3KRN5	cDNA FLJ34626 fis, clone KIDNE2015433, hig	**B2RDK3**	Oxysterol-binding protein
B3KRR4	cDNA FLJ34750 fis, clone MESAN2009580, hi	**B2RDW0**	cDNA, FLJ96792, highly similar to Homo sapie
B3KRY3	cDNA FLJ35079 fis, clone PLACE6005283, hig	B2RMN7	Spectrin beta chainSpectrin beta chain
B3KS71	cDNA FLJ35671 fis, clone SPLEN2018180, hig	**B3KM58**	cDNA FLJ10358 fis, clone NT2RM2001238, hi
B3KSC2	cDNA FLJ35979 fis, clone TESTI2013545, hig	**B3KME6**	cDNA FLJ10802 fis, clone NT2RP4000817, hig
B3KSC8	cDNA FLJ36009 fis, clone TESTI2015675, hig	**B3KMS6**	cDNA FLJ12486 fis, clone NT2RM2000566, hi
B3KSG0	cDNA FLJ36142 fis, clone TESTI2025006, hig	**B3KMV8**	cDNA FLJ12766 fis, clone NT2RP2001520, hig
B3KSG9	Transmembrane 9 superfamily member	**B3KN05**	cDNA FLJ13129 fis, clone NT2RP3002969, hig
B3KSH0	cDNA FLJ36190 fis, clone TESTI2027271, hig	**B3KN49**	cDNA FLJ13562 fis, clone PLACE1008080, hig
B3KT00	cDNA FLJ37368 fis, clone BRAMY2024530, hi	**B3KNL8**	cDNA FLJ14908 fis, clone PLACE1005953, hig
B3KTM6	Ribosomal protein L5, isoform CRA_b (cDNA F	**B3KP72**	cDNA FLJ31284 fis, clone KIDNE2006880, hig
B3KUS7	Cdc42 effector protein 4 (Binder of Rho GTPas	B3KP89	cDNA FLJ31446 fis, clone NT2NE2000909, hig
B3KV02	cDNA FLJ41015 fis, clone UTERU2018712, hi	**B3KPZ7**	cDNA FLJ32517 fis, clone SMINT1000117, hig
B3KV49	cDNA FLJ16128 fis, clone BRACE2038269, m	**B3KR50**	cDNA FLJ33691 fis, clone BRAWH2002976, h
B3KV82	cDNA FLJ16243 fis, clone HCHON2000323, h	**B3KRW2**	cDNA FLJ34977 fis, clone NTONG2005822, hi
B3KW33	Oxysterol-binding protein	**B3KSC7**	cDNA FLJ36001 fis, clone TESTI2015213, hig
B3KW56	Eukaryotic translation initiation factor 3 subunit	B3KSI3	Branched-chain-amino-acid aminotransferase
B3KX20	cDNA FLJ44510 fis, clone UTERU3001652, hi	**B3KSZ4**	cDNA FLJ37346 fis, clone BRAMY2021310, hi
B3KY79	cDNA FLJ46620 fis, clone TLUNG2000654, hig	**B3KTN4**	Citrate synthaseCitrate synthase
B3KY97	cDNA FLJ16235 fis, clone FEBRA2028516	B3KTR0	Syntrophin, alpha 1 (Dystrophin-associated pro
B4DDF1	Nucleolar and spindle-associated protein 1 (Nu	**B3KU53**	cDNA FLJ39204 fis, clone OCBBF2005476, hi
B4DDF4	Calponin	**B3KUR3**	cDNA FLJ40459 fis, clone TESTI2041800, hig
B4DDG7	cDNA FLJ57898, highly similar to Adaptor-rela	**B3KUZ8**	Aspartate aminotransferase (EC 2.6.1.1)
B4DDS3	Cleft lip and palate transmembrane protein 1	**B3KV77**	cDNA FLJ16222 fis, clone CTONG3002947, hi

B4DE50	cDNA FLJ59582, highly similar to Ras-related	**B3KVA7**	cDNA FLJ16309 fis, clone SKMUS2007816, hi
B4DEK4	Sorting nexin-2 (Transformation-related gene 9	**B3KVN0**	cDNA FLJ16785 fis, clone NT2RI2015342, hig
B4DF77	cDNA FLJ58767, highly similar to Phosphofuri	**B3KW26**	cDNA FLJ41971 fis, clone SKMUS2007568, hi
B4DG55	cDNA FLJ53905, highly similar to Phosphatidy	**B3KWN2**	cDNA FLJ43415 fis, clone OCBBF2025527, hi
B4DG60	cDNA FLJ59620, highly similar to Homo sapier	**B3KXZ9**	cDNA FLJ46477 fis, clone THYMU3025118, hi
B4DGH0	cDNA FLJ60107, highly similar to DNA replicat	B3KY43	cDNA FLJ46798 fis, clone TRACH3031660, hi
B4DH17	cDNA FLJ59298, highly similar to Eukaryotic tr	B4DDI0	cDNA FLJ55951, highly similar to Homo sapier
B4DHC6	Amino acid transporter	B4DE36	Glucose-6-phosphate isomerase (EC 5.3.1.9)
B4DHX4	Rab GDP dissociation inhibitor	B4DE85	Phosphatidylserine synthase 1 (PSS-1) (PtdSe
B4DJ54	Soluble calcium-activated nucleotidase 1 (SCA	B4DEQ0	cDNA FLJ59482, highly similar to Electron tran
B4DJK0	Serine/arginine-rich-splicing factor 5 (cDNA FL	B4DEZ3	NADH dehydrogenase [ubiquinone] 1 alpha su
B4DLA3	cDNA FLJ58509, highly similar to Cullin-1	B4DF78	cDNA FLJ50462, highly similar to Disks large h
B4DLK7	cDNA FLJ54722, highly similar to Sulfatase-mo	**B4DF97**	cDNA FLJ59673, highly similar to Homo sapier
B4DLT1	cDNA FLJ59716, highly similar to Vacuolar pro	**B4DFL1**	Dihydrolipoyl dehydrogenase (EC 1.8.1.4)
B4DM04	cDNA FLJ53394, highly similar to Zinc finger p	**B4DG62**	cDNA FLJ56506, highly similar to Hexokinase-
B4DM74	60S ribosomal protein L18a	**B4DG82**	cDNA FLJ61094, highly similar to Rap guanine
B4DMG5	cDNA FLJ59256, highly similar to A-Raf proto-	**B4DGK8**	cDNA FLJ57723, moderately similar to Protein
B4DMJ6	cDNA FLJ50996, highly similar to 60S ribosom	**B4DGP4**	cDNA FLJ53288, moderately similar to LIM dor
B4DMQ7	Tumor protein p53 inducible protein 3, isoform	**B4DGV8**	cDNA FLJ54286, highly similar to Mus musculu
B4DMX4	cDNA FLJ57154, highly similar to Alpha-fetopr	B4DH21	cDNA FLJ58505, highly similar to Cyclin-T2
B4DN25	UDP-glucose 6-dehydrogenase (UDP-Glc dehy	**B4DH45**	cDNA FLJ53322, highly similar to Homo sapier
B4DN45	S-adenosylmethionine synthase isoform type-2	**B4DHJ9**	cDNA FLJ61262, highly similar to Ubiquitin-pro
B4DPU2	cDNA FLJ57136, highly similar to RNA U smal	**B4DHP4**	cDNA FLJ59688, highly similar to Cob(I)yrinic a
B4DQJ8	6-phosphogluconate dehydrogenase, decarbox	**B4DHX0**	cDNA FLJ51555, highly similar to Squalene mo
B4DQM6	cDNA FLJ55563, highly similar to Homo sapier	**B4DI57**	cDNA FLJ54111, highly similar to Serotransfer
B4DQV4	Sorting nexin-4	B4DIT7	cDNA FLJ58187, highly similar to Protein-gluta
B4DQW8	Ankyrin repeat and SAM domain-containing pro	**B4DIV2**	cDNA FLJ60575, highly similar to Ubiquinone b
B4DR55	Pyridoxal-dependent decarboxylase domain-co	B4DIW9	Serine/threonine-protein phosphatase 6 regula
B4DRA5	cDNA FLJ61346, highly similar to Protein trans	B4DJ71	Phosphate transporterPhosphate transporter
B4DRB3	cDNA FLJ52431, highly similar to Retinoblasto	B4DJ81	cDNA FLJ60586, highly similar to NADH-ubiqu
B4DRC7	cDNA FLJ57829	B4DJB4	Isocitrate dehydrogenase [NAD] subunit, mitoc
B4DRF1	cDNA FLJ55355, highly similar to N-acetylsero	**B4DJC2**	cDNA FLJ51665, highly similar to Homo sapier
B4DRU9	cDNA FLJ57179, highly similar to Homo sapier	B4DJE7	cDNA FLJ52595, highly similar to Medium-cha

B4DS49	cDNA FLJ60845, highly similar to Telomere-as	**B4DJF7**	cDNA FLJ56915cDNA FLJ56915
B4DSA4	Ferrochelatase (EC 4.99.1.1)	**B4DJK9**	PerilipinPerilipinPerilipinPerilipinPerilipin
B4DSL6	cDNA FLJ57190, highly similar to Actin-binding	**B4DJX1**	Acetyltransferase component of pyruvate dehy
B4DTC0	cDNA FLJ53096, highly similar to Collagen alp	**B4DKD0**	DNA topoisomerase 2 (EC 5.99.1.3) (Fragmen
B4DU16	cDNA FLJ54550, highly similar to Homo sapier	B4DL14	ATP synthase subunit gamma
B4DUV1	Fibulin-1	**B4DL49**	cDNA FLJ58073, moderately similar to Cathep
B4DUX5	Methionine aminopeptidase 2 (MAP 2) (MetAP	**B4DLW4**	cDNA FLJ60300, highly similar to Homo sapier
B4DV74	cDNA FLJ53855, highly similar to Kanadaptin	**B4DMU7**	cDNA FLJ59351, highly similar to Striatin-4
B4DVQ7	cDNA FLJ57616, highly similar to WD repeat p	**B4DN54**	cDNA FLJ55111, highly similar to Sorting and a
B4DYK6	cDNA FLJ56887, highly similar to Homo sapier	B4DNN2	DnaJ (Hsp40) homolog, subfamily B, member
B4DZI8	Coatomer subunit beta' (Beta'-coat protein) (Be	**B4DP10**	Secretory carrier-associated membrane protein
B4E086	cDNA FLJ51584, highly similar to Homo sapier	**B4DQ79**	Tyrosine-protein kinase (EC 2.7.10.2)
B4E0K5	Mitogen-activated protein kinase (EC 2.7.11.24	B4DQA3	cDNA FLJ58603, highly similar to Actin-binding
B4E0V0	Pyridoxine-5'-phosphate oxidase (EC 1.4.3.5) (	**B4DQI0**	cDNA FLJ59385cDNA FLJ59385
B4E128	Schlafen family member 5 (cDNA FLJ52101)	B4DQS6	Endoplasmic reticulum export factor CTAGE5 (
B4E138	cDNA FLJ50940, highly similar to PHD finger p	**B4DQT8**	cDNA FLJ61158, highly similar to ADP-ribosyla
B4E1E2	Hepatocyte growth factor-regulated tyrosine ki	**B4DQY2**	MICOS complex subunit MIC60 (Mitofilin)
B4E1H8	cDNA FLJ58222, highly similar to Golgi reasse	**B4DRG2**	cDNA FLJ55357, highly similar to Calmegin
B4E1K5	cDNA FLJ51181, highly similar to 7-dehydroch	B4DRN8	Palmitoyltransferase (EC 2.3.1.225)
B4E1L0	Adenylosuccinate synthetase isozyme 2 (AMP	**B4DRV5**	cDNA FLJ60840, highly similar to Nucleoporin
B4E1V0	cDNA FLJ54839, highly similar to Lactotransfe	**B4DRW6**	Alpha-1,4 glucan phosphorylase (EC 2.4.1.1)
B4E245	cDNA FLJ61538, highly similar to Switch-asso	**B4DS60**	cDNA FLJ58420, highly similar to Cytohesin-2
B4E2Z3	cDNA FLJ54090, highly similar to 4F2 cell-surf	**B4DSE2**	cDNA FLJ57277, highly similar to Tripeptidyl-p
B5BU16	Mitogen-activated protein kinase kinase 6	**B4DSH1**	cDNA FLJ51295, highly similar to Cell division
B7WP74	Pre-mRNA-splicing factor CWC22 homolog (F	**B4DSX6**	cDNA FLJ57427, highly similar to Glycogenin-1
B7Z265	Kinesin-like protein KIF22 (Kinesin-like DNA-bi	**B4DSZ1**	cDNA FLJ54877, highly similar to Syntaxin-12
B7Z291	Myotubularin-related protein 9	**B4DT77**	AnnexinAnnexinAnnexinAnnexinAnnexin
B7Z2G6	cDNA FLJ55617, highly similar to Dedicator of	B4DTB9	cDNA FLJ50666, weakly similar to Long-chain-
B7Z382	Cytosolic purine 5'-nucleotidase (EC 3.1.3.5) (	**B4DTC8**	cDNA FLJ57432, highly similar to Endoglin
B7Z3K0	cDNA FLJ51645, highly similar to Serine/threo	**B4DUC9**	cDNA FLJ53756, highly similar to SPRY doma
B7Z424	cDNA FLJ52513, highly similar to Lysosomal th	B4DUH1	cDNA FLJ51323, highly similar to Short-chain s
B7Z4K6	Deoxyribonuclease-2-alpha (EC 3.1.22.1) (Acid	B4DUP5	cDNA FLJ60165, highly similar to Translation i
B7Z4W0	cDNA FLJ51911, highly similar to Transcription	**B4DV94**	cDNA FLJ58285, highly similar to Homo sapier

B7Z4W4	cDNA FLJ50817, highly similar to UV excision	**B4DVE1**	cDNA FLJ53478, highly similar to Galectin-3-b
B7Z6L5	cDNA FLJ50681, highly similar to Testin	**B4DVG5**	cDNA FLJ53214, highly similar to Tubulointers
B7Z6M1	Plastin-3 (T-plastin)	**B4DVQ2**	cDNA FLJ60909, highly similar to Proline-rich p
B7Z6T9	cDNA FLJ50237, highly similar to Homo sapier	**B4DVZ4**	cDNA FLJ57870, highly similar to Thiosulfate s
B7Z6Y2	cDNA FLJ54942, highly similar to Homo sapier	B4DWI8	cDNA FLJ57805, highly similar to Homo sapier
B7ZKW8	CapZ-interacting protein	**B4DWV5**	GrpE protein homologGrpE protein homolog
B7ZL00	Protein transport protein Sec31A (ABP125) (A	**B4DWV9**	cDNA FLJ53108, highly similar to Guanine nuc
B7ZLC9	GEMIN5 protein	**B4DXF5**	cDNA FLJ51370, highly similar to Kelch-like pr
B8ZZQ6	Prothymosin alpha	**B4DY59**	cDNA FLJ56267, highly similar to Transducin b
B9DI73	Deleted.	B4DYB4	Nucleoporin NUP35 (35 kDa nucleoporin) (Mito
B9EG90	Topoisomerase (DNA) I	**B4DZ08**	Aconitate hydratase, mitochondrial (Aconitase)
C6GKU9	Mediator of RNA polymerase II transcription su	B4DZ88	Kinectin (CG-1 antigen) (Kinesin receptor)
C7DJS2	Glutathione S-transferase pi (Fragment)	**B4DZZ0**	PRA1 family proteinPRA1 family protein
C7DUW4	Mitogen activated protein kinase kinase 3	B4E0J8	Presequence protease, mitochondrial (hPreP)
C9IYN9	SET and MYND domain-containing protein 5 (F	**B4E0N9**	Glutamate dehydrogenase
C9J0A5	E3 ubiquitin-protein ligase BRE1A (Fragment)	B4E1F6	Beta-glucuronidase (EC 3.2.1.31) (Beta-G1)
C9J0J7	Profilin	**B4E1Q7**	cDNA FLJ57294, highly similar to Lipoamide a
C9J2I0	Arf-GAP domain and FG repeat-containing pro	**B4E1S3**	cDNA FLJ57860, highly similar to Transmembr
C9J4K0	Ashwin	**B4E290**	cDNA FLJ50039, highly similar to Homo sapier
C9J5G4	Follistatin-related protein 1 (Fragment)	**B4E2J2**	cDNA FLJ51755, highly similar to Glutathione S
C9J6P7	Nuclear valosin-containing protein-like (Fragme	B4E2K4	Aspartyl/asparaginyl beta-hydroxylase (EC 1.1
C9J813	Caldesmon (Fragment)	**B4E2V5**	cDNA FLJ52062, highly similar to Erythrocyte b
C9J931	GTP-binding protein Rheb	B4E2W0	Trifunctional enzyme subunit beta, mitochondri
C9J9P7	RNA-binding protein 5 (Fragment)	B4E324	cDNA FLJ60397, highly similar to Lysosomal p
C9JCN0	Deleted.	**B4E380**	Histone H3Histone H3Histone H3Histone H3
C9JGL2	Ubiquitin-like modifier-activating enzyme ATG7	B4E3K9	Superoxide dismutase [Mn], mitochondrial (EC
C9JIK8	Cysteine protease (EC 3.4.22.-) (Fragment)	**B4E3T9**	cDNA FLJ51473, highly similar to Junctophilin-
C9JJ34	Ran-specific GTPase-activating protein (Fragm	B5MDC5	cDNA FLJ52780, highly similar to Tissue alpha
C9JMA2	Mannan-binding lectin serine protease 1 (Frag	**B7Z1U1**	cDNA FLJ60457, highly similar to NADH-ubiqu
C9JMY1	Insulin-like growth factor-binding protein 2	B7Z2M8	cDNA FLJ54654, highly similar to Heat shock 7
C9JNR5	Insulin (Fragment)	B7Z2T3	Intraflagellar transport protein 56 (cDNA FLJ60
C9JNU9	Ubiquitin carboxyl-terminal hydrolase 4	**B7Z2Z1**	cDNA FLJ59523, highly similar to Scaffold atta
C9JQV0	Uncharacterized protein C7orf50 (Fragment)	B7Z358	39S ribosomal protein L50, mitochondrial (L50

C9JSL4	Prolyl 3-hydroxylase 2 (Fragment)	**B7Z438**	cDNA FLJ56352, highly similar to Succinyl-CoA
C9JTS3	Angio-associated migratory cell protein (Fragm	**B7Z4A1**	cDNA FLJ50798, weakly similar to Ubiquinol-cy
C9K058	Peptidyl-prolyl cis-trans isomerase (PPIase) (E	**B7Z4V2**	cDNA FLJ51907, highly similar to Stress-70 pr
D3DQT4	Tripartite motif-containing 3, isoform CRA_f (F	**B7Z4Z4**	cDNA FLJ51918, highly similar to Peroxisomal
D3DSU3	Kinesin family member 13B, isoform CRA_a	**B7Z553**	cDNA FLJ51266, highly similar to Vitronectin
D3DVH3	Inositol polyphosphate-4-phosphatase, type I,	**B7Z587**	cDNA FLJ51273, highly similar to Transmembr
D3VVD5	Ataxin 3 variant e	B7Z5C0	cDNA FLJ52352, highly similar to DnaJ homolo
D6RAW0	Ubiquitin-conjugating enzyme E2 D3 (Fragmen	**B7Z5P5**	cDNA FLJ51283, moderately similar to Obscur
D6RCQ0	Eukaryotic translation elongation factor 1 epsil	B7Z6B8	2,4-dienoyl-CoA reductase, mitochondrial (EC
D6REB4	Polyadenylate-binding protein-interacting prote	B7Z6X8	cDNA FLJ54740, highly similar to 5'-AMP-activ
D6REM9	Protein RUFY3 (Fragment)	B7Z792	cDNA FLJ53932, highly similar to NADH-ubiqu
D6REY2	Colorectal mutant cancer protein	**B7Z7N1**	cDNA FLJ50915, highly similar to NADH dehyd
D6RFF0	La-related protein 7 (Fragment)	B7Z7P0	cDNA FLJ51394, highly similar to Ubiquitin con
D6RGZ6	Versican core protein (Fragment)	**B7Z8A2**	cDNA FLJ51671, highly similar to Prenylcystein
D9N155	Adenosylhomocysteinase 3 (AdoHcyase 3) (E(	**B7Z8W3**	cDNA FLJ53272, highly similar to Homo sapien
E5RGH2	CCR4-NOT transcription complex subunit 7 (F	**B7Z918**	cDNA FLJ61074, highly similar to Echinoderm
E5RI99	60S ribosomal protein L30 (Fragment)	**B7Z922**	Phosphomannomutase (EC 5.4.2.8)
E5RIA1	Glycerol-3-phosphate acyltransferase 4 (Fragm	**B7Z992**	cDNA FLJ53698, highly similar to Gelsolin
E5RIF2	Brefeldin A-inhibited guanine nucleotide-excha	**B7Z9S8**	Sodium/potassium-transporting ATPase subun
E5RJ68	AP-3 complex subunit beta-1 (Adaptor protein	B7ZKQ9	SCARB1 protein (Scavenger receptor class B
E7ENU9	Macrophage-capping protein (Fragment)	B7ZLX0	Integrin alpha-V (Vitronectin receptor) (Vitrone
E7ES08	High mobility group protein B3 (Fragment)	B7ZM32	LPCAT4 protein (Fragment)
E7ET85	Exostosin-like 3	B7ZMA3	Uncharacterized protein (Fragment)
E7EWK3	ATP-dependent RNA helicase DHX36 (Fragme	B7ZMJ3	ADAMTSL4 proteinADAMTSL4 protein
E7EX53	Ribosomal protein L15 (Fragment)	B8QFA1	Plakophilin-2Plakophilin-2Plakophilin-2
E7EX73	Eukaryotic translation initiation factor 4 gamma	B8ZZJ1	Hyccin (Down-regulated by CTNNB1 protein A
E9PE77	Fibronectin (FN) (Cold-insoluble globulin) (CIG	B9EGN3	SYNJ1 proteinSYNJ1 proteinSYNJ1 protein
E9PGF9	Protein O-GlcNAcase (OGA) (EC 3.2.1.169) (B	B9TX64	Mediator complex subunit MED24 variant MED
E9PGW7	Mediator of RNA polymerase II transcription su	B9VP19	60 kDa chaperonin (Fragment)
E9PI88	GDP-mannose 4,6 dehydratase (EC 4.2.1.47)	**C4PGM0**	Specificity protien 1Specificity protien 1
E9PIR7	Thioredoxin reductase 1, cytoplasmic	C9J8H9	ATP synthase subunit f, mitochondrial
E9PKG1	Protein arginine N-methyltransferase 1	C9JAZ1	Metaxin-2 (Fragment)Metaxin-2 (Fragment)
E9PKJ0	Protein wntless homolog (Fragment)	C9JBZ4	HAUS augmin-like complex subunit 8 (HEC1/N

E9PLH9	GDP-L-fucose synthase (Fragment)	C9JE27	E3 ubiquitin-protein ligase rififylin (Fragment)
E9PN76	RING finger protein 214	C9JFR7	Cytochrome c (Fragment)
E9PPD9	Band 4.1-like protein 2 (Generally expressed p	C9JG87	39S ribosomal protein L39, mitochondrial (Frag
E9PPY7	Arfaptin-2	C9JHG2	Raftlin (Fragment)Raftlin (Fragment)
E9PQA1	Chromosome 11 open reading frame 58	C9JJX6	Armadillo repeat protein deleted in velo-cardio-
E9PS97	Alpha-parvin (Fragment)	C9JKQ2	NADH dehydrogenase [ubiquinone] 1 beta sub
F2Z2I2	6-phosphofructo-2-kinase/fructose-2,6-bisphos	C9JPE1	Mitochondrial carnitine/acylcarnitine carrier pro
F2Z3M0	tRNA-splicing endonuclease subunit Sen15	C9JPM9	Leucine-rich repeat transmembrane neuronal p
F2ZC06	Thyroid hormone receptor interacting protein 6	C9JQD0	Quinone oxidoreductase-like protein 1 (Fragme
F5GXW0	Adenosine deaminase	C9JRJ8	Sequestosome-1 (Fragment)
F5H3W1	Deleted.	C9JUN5	Coiled-coil domain-containing protein 12 (Frag
F5H459	AP complex subunit sigma	C9JV68	Zinc transporter 3 (Fragment)
F5H5M9	Deleted.	C9JWC3	Sorbin and SH3 domain-containing protein 2 (F
F5H6B2	Cell migration-inducing hyaluronidase 2	D3DNL3	G elongation factor, mitochondrial 1, isoform C
F5H6N3	Clathrin light chain A	D3DQH5	Coiled-coil domain containing 69, isoform CRA
F5H7N9	Deleted.	D3DTC2	Acyltransferase like 2, isoform CRA_a
F5H7R9	Parathymosin (Fragment)	D3DTY9	Tripartite motif-containing 25, isoform CRA_a
F5H8M2	Deleted.	D3DUJ0	AFG3 ATPase family gene 3-like 2 (Yeast), iso
F8VQR7	Cysteine and glycine-rich protein 2	D3DVK8	Calcium/calmodulin-dependent protein kinase
F8VUA6	60S ribosomal protein L18 (Fragment)	D3DVL7	Transforming growth factor beta regulator 4, is
F8VV52	CCR4-NOT transcription complex subunit 2 (F	D3DVQ1	Leucine zipper-EF-hand containing transmemb
F8VVL1	Density-regulated protein	D3DXF2	Abhydrolase domain containing 11, isoform CF
F8VW92	Deleted.	D5KJA2	Dehydrogenase/reductase (SDR family) memb
F8W1D1	Melanocyte protein PMEL (Fragment)	D6R8Z7	TSC22 domain family protein 3 (Fragment)
F8W808	N-alpha-acetyltransferase 10	D6R938	Calcium/calmodulin-dependent protein kinase
F8W8F5	Calpain-3	D6R9X8	Integrin alpha-3Integrin alpha-3
F8W9Q2	Deleted.	D6RA82	AnnexinAnnexinAnnexinAnnexinAnnexin
F8WC16	Glycerol-3-phosphate dehydrogenase 1-like pr	D6RB01	Soluble lamin-associated protein of 75 kDa
F8WDT8	Probable ATP-dependent RNA helicase DDX5	D6REZ6	RNA-binding protein 47 (Fragment)
F8WEA3	Myotubularin-related protein 14	D6RGV8	[Pyruvate dehydrogenase (acetyl-transferring)]
F8WFC6	Large subunit GTPase 1 homolog	D6W5F9	Anthrax toxin receptor 1, isoform CRA_a
G3V1D1	Ferritin	E5KRP6	Spastin (EC 3.6.4.3)Spastin (EC 3.6.4.3)
G3V1J5	Exosome complex exonuclease RRP44 (KIAA1	E5RFH6	Bifunctional epoxide hydrolase 2

G3V2B8	C-1-tetrahydrofolate synthase, cytoplasmic (C1	E5RHG9	Cytochrome b-c1 complex subunit 7
G3V5F0	Pinin	E5RHW4	Erlin-2 (Fragment)Erlin-2 (Fragment)
G3V5H8	Protein NDRG2 (Fragment)	E5RK64	Vesicle-associated membrane protein-associat
G5E9A6	Ubiquitin carboxyl-terminal hydrolase 11 (Ubiq	E5RK99	Collagen triple helix repeat-containing protein 1
G5E9P9	Rap1 GTPase-GDP dissociation stimulator 1 (	E7EMM4	Acid ceramidaseAcid ceramidase
G5E9R3	60S ribosomal protein L37a (Ribosomal protei	E7ENH5	Copine-1Copine-1Copine-1Copine-1Copine-1
G8JLA2	Myosin light polypeptide 6	E7EPW2	28S ribosomal protein S25, mitochondrial
H0UI99	Zinc finger, CCCH-type with G patch domain, i	E7ER77	Endoplasmic reticulum metallopeptidase 1
H0Y4R1	Inosine-5'-monophosphate dehydrogenase 2 (	E7EUY3	Propionyl-CoA carboxylase beta chain, mitoch
H0Y8F2	Transforming acidic coiled-coil-containing prot	E7EUY5	Single-stranded DNA-binding protein, mitochor
H0Y9D6	Beta-1,4-galactosyltransferase 7 (Fragment)	E7EV99	Alpha-adducinAlpha-adducinAlpha-adducin
H0Y9L4	Histone-lysine N-methyltransferase NSD2 (Fra	E7EVA0	Microtubule-associated protein
H0YA55	Serum albumin (Fragment)	E9PAV3	Nascent polypeptide-associated complex subu
H0YAH0	Protocadherin-7 (Fragment)	E9PAW4	Sorbin and SH3 domain-containing protein 2 (A
H0YCJ2	Phosphoinositide phospholipase C (EC 3.1.4.1	E9PB14	Pyruvate dehydrogenase protein X component
H0YCM7	Engulfment and cell motility protein 2 (Fragmer	E9PDN5	DystrophinDystrophinDystrophinDystrophin
H0YDP9	Receptor-type tyrosine-protein phosphatase ka	E9PE17	28S ribosomal protein S17, mitochondrial (Frag
H0YDZ4	Phosphatidylinositol 3,4,5-trisphosphate-deper	E9PGZ2	Leucine-rich repeat flightless-interacting protei
H0YEJ7	Rho GTPase-activating protein 42 (Fragment)	E9PH29	Thioredoxin-dependent peroxide reductase, mi
H0YEN5	40S ribosomal protein S2 (Fragment)	E9PHN7	Glutathione S-transferase Mu 2
H0YF20	Seipin (Fragment)	E9PJ02	FXYD domain-containing ion transport regulato
H0YHD0	Breast cancer metastasis-suppressor 1-like pro	E9PK85	Ras-related protein R-Ras2 (Fragment)
H0YHZ5	GPN-loop GTPase 3 (Fragment)	E9PKC0	Pleckstrin homology domain-containing family
H0YJ34	Fermitin family homolog 2 (Fragment)	E9PKH6	NADH dehydrogenase [ubiquinone] iron-sulfur
H0YJ50	Serine/threonine-protein kinase VRK1 (Fragme	E9PKV2	39S ribosomal protein L17, mitochondrial (Frag
H0YLR1	Deleted.	E9PKZ0	60S ribosomal protein L8 (Fragment)
H0YN21	DDB1- and CUL4-associated factor 11 (Fragm	**E9PLH7**	Deleted.
H3BMT0	Jupiter microtubule-associated homolog 2 (Fra	E9PML0	Cytochrome P450 4B1Cytochrome P450 4B1
H3BP35	Diphosphomevalonate decarboxylase (Fragme	E9PNW4	CD59 glycoproteinCD59 glycoprotein
H3BR57	Deleted.	E9PQ61	Zinc finger CCCH domain-containing protein 1
H3BT22	Origin recognition complex subunit 6	E9PQD8	Glutamine amidotransferase-like class 1 doma
H3BU49	ADP-ribosylation factor-like protein 2-binding p	E9PQP1	NADH dehydrogenase [ubiquinone] flavoprotei
H3BUM8	Ubiquitin domain-containing protein UBFD1	E9PR44	Alpha-crystallin B chain (Fragment)

H3BV23	Ubiquitin-like protein 7 (Fragment)	E9PRW1	Mitochondrial fission regulator 1-like (Fragmen
H7BXV5	Collagen alpha-1(XVIII) chain (Fragment)	F2Z3L7	Protein NipSnap homolog 3B
H7BZP2	Phosducin-like protein 3 (Fragment)	F5GXJ9	CD166 antigenCD166 antigenCD166 antigen
H7BZQ3	OTU domain-containing protein 5 (Fragment)	F5GXX5	Dolichyl-diphosphooligosaccharide--protein gly
H7C0E5	Zinc finger protein ZPR1 (Fragment)	F5H2L4	Acyl-coenzyme A thioesterase 13 (Acyl-CoA th
H7C466	Zinc finger CCCH domain-containing protein 1	**F5H2Q7**	Deleted.
I3L2C7	Gem-associated protein 4	**F5H2X3**	Deleted.
I3L3C4	Ribosomal L1 domain-containing protein 1 (Fra	F5H6N1	Protein mago nashi homolog 2
I3L425	Pigment epithelium-derived factor (Fragment)	**F5H7V7**	Deleted.
I3L441	Deleted.	**F5H801**	Deleted.
I3L521	Uncharacterized protein (Fragment)	F6PQP6	Epsin-2 (Fragment)Epsin-2 (Fragment)
I6L9C8	Zinc finger protein 428	F6V6Z1	Mitochondrial amidoxime reducing component
I7GPQ7	cDNA FLJ75793	F8VQD9	Autophagy-related protein 101 (Fragment)
J3K000	PEPD protein	**F8VWQ7**	Deleted.
J3KN76	Deleted.	F8W1A4	Adenylate kinase 2, mitochondrial (AK 2) (EC 2
J3KQ96	Treacle protein (Fragment)	F8W6G5	Aprataxin (Fragment)Aprataxin (Fragment)
J3KRA9	Serine/threonine-protein kinase SMG1 (Fragm	F8W8T1	Interferon-induced GTP-binding protein Mx1
J3QKY9	Conserved oligomeric Golgi complex subunit 1	**F8W8T3**	Deleted.
J3QL04	Tether-containing UBX domain for GLUT4 (Fra	F8W9E5	Septin-5 (Fragment)Septin-5 (Fragment)
J9ZVQ3	Apolipoprotein E (Fragment)	F8WAS3	NADH dehydrogenase [ubiquinone] 1 alpha su
K4DI93	Cullin 4B, isoform CRA_e (Cullin-4B)	F8WC54	Disintegrin and metalloproteinase domain-cont
K7EJB8	Protein phosphatase 1 regulatory subunit 14A	F8WCC8	Arylsulfatase A (ASA) (EC 3.1.6.8) (Cerebrosid
K7ELF3	Transcription factor E2-alpha (Fragment)	**G0TQY6**	Lutheran blood groupLutheran blood group
K7ELT5	Deleted.	G3V1V1	Zinc finger CCHC-type and RNA binding motif
K7EN63	BTB/POZ domain-containing protein KCTD15 (	**G3V288**	Deleted.
K7ENA8	Eukaryotic translation initiation factor 3 subunit	G3V473	Zinc finger CCCH domain-containing protein 14
K7EPL2	SUMO-activating enzyme subunit 2 (Fragment	G8IFA7	p90p90p90p90p90p90p90p90p90p90p90p90
K7EPP7	DnaJ homolog subfamily C member 7	H0UI04	Epilepsy, progressive myoclonus type 2A, Lafo
K7EPR4	AP-1 complex subunit mu-2 (Fragment)	H0UI53	HD domain containing 2, isoform CRA_a
K7EQ43	Ubiquitin-like protein 5	H0Y360	AMP deaminase 2 (Fragment)
K7EQX2	Kelch-like ECH-associated protein 1 (Fragmen	H0Y4R5	Transmembrane protein 201 (Fragment)
K7ERU8	Deleted.	H0Y962	Carbonyl reductase family member 4 (Fragmer
O00154	Cytosolic acyl coenzyme A thioester hydrolase	H0YBF7	Arf-GAP with SH3 domain, ANK repeat and PH

O00299	Chloride intracellular channel protein 1 (Chlorid
O00410	Importin-5 (Imp5) (Importin subunit beta-3) (Ka
O00625	Pirin (EC 1.13.11.24) (Probable quercetin 2,3-d
O14646	Chromodomain-helicase-DNA-binding protein 1
O14933	Ubiquitin/ISG15-conjugating enzyme E2 L6 (E(
O15294	UDP-N-acetylglucosamine--peptide N-acetylglu
O15357	Phosphatidylinositol 3,4,5-trisphosphate 5-phos
O15391	Transcription factor YY2 (Yin and yang 2) (YY-
O15397	Importin-8 (Imp8) (Ran-binding protein 8) (Ran
O43175	D-3-phosphoglycerate dehydrogenase (3-PGD
O43747	AP-1 complex subunit gamma-1 (Adaptor prote
O60493	Sorting nexin-3 (Protein SDP3)
O75113	NEDD4-binding protein 1 (N4BP1)
O75348	V-type proton ATPase subunit G 1 (V-ATPase
O95433	Activator of 90 kDa heat shock protein ATPase
O95758	Polypyrimidine tract-binding protein 3 (Regulat
O95801	Tetratricopeptide repeat protein 4 (TPR repeat
O95864	Fatty acid desaturase 2 (EC 1.14.19.3) (Acyl-C
O95865	N(G),N(G)-dimethylarginine dimethylaminohyd
O95999	B-cell lymphoma/leukemia 10 (B-cell CLL/lymp
P00491	Purine nucleoside phosphorylase (PNP) (EC 2
P02533	Keratin, type I cytoskeletal 14 (Cytokeratin-14)
P02792	Ferritin light chain (Ferritin L subunit)
P04259	Keratin, type II cytoskeletal 6B (Cytokeratin-6B
P05787	Keratin, type II cytoskeletal 8 (Cytokeratin-8) (
P07311	Acylphosphatase-1 (EC 3.6.1.7) (Acylphospha
P07339	Cathepsin D (EC 3.4.23.5) [Cleaved into: Cath
P07737	Profilin-1 (Epididymis tissue protein Li 184a) (P
P08123	Collagen alpha-2(I) chain (Alpha-2 type I collag
P08238	Heat shock protein HSP 90-beta (HSP 90) (He
P08727	Keratin, type I cytoskeletal 19 (Cytokeratin-19)
P09211	Glutathione S-transferase P (EC 2.5.1.18) (GS
P09496	Clathrin light chain A (Lca)
H0YC27	Regulator of microtubule dynamics protein 1 (P
H0YCB4	Transcription factor p65 (Fragment)
H0YCD3	Myocardial zonula adherens protein (Fragment
H0YDV6	DENN domain-containing protein 5A (Fragmen
H0YFP3	Protoporphyrinogen oxidase (Fragment)
H0YGC7	Acyl-CoA synthetase family member 3, mitoch
H0YGL9	Deleted.
H0YH31	2-oxoisovalerate dehydrogenase subunit alpha
H0YIM9	CHURC1-FNTB readthrough (Fragment)
H0YIV5	LETM1 domain-containing protein 1 (Fragment
H0YK61	ER membrane protein complex subunit 4
H0YM70	Proteasome activator complex subunit 2
H0YNE3	Proteasome activator complex subunit 1 (11S r
H0YNN4	Complex I intermediate-associated protein 30,
H3BM67	Nucleolar protein 3 (Fragment)
H3BP88	Deleted.
H3BPM9	Hepatoma-derived growth factor-related protei
H3BPX2	ObscurinObscurinObscurinObscurinObscurin
H3BQW8	Hydroxyacylglutathione hydrolase, mitochondri
H3BR50	Deleted.
H3BS73	Methyltransferase-like 26
H3BSG1	Protein zwilch homolog (Fragment)
H3BU69	Tyrosine-protein kinase CSK (Fragment)
H3BUR9	CDP-diacylglycerol--inositol 3-phosphatidyltran
H7BXK9	ATP-binding cassette sub-family B member 6,
H7BXL1	Transmembrane protein 41A
H7BYV1	Interferon-induced transmembrane protein 2 (P
H7BYW5	cAMP-dependent protein kinase type I-beta reg
H7BZE4	Myosin regulatory light chain 2, atrial isoform (F
H7C0Q5	Uncharacterized protein C7orf26 (Fragment)
H7C0R7	NADH-cytochrome b5 reductase 1 (Fragment)
H7C0X5	Probable serine carboxypeptidase CPVL (Frag
H7C126	3-hydroxyisobutyryl-CoA hydrolase, mitochond

P10915	Hyaluronan and proteoglycan link protein 1 (Ca	**H7C1R3**	Deleted.
P11172	Uridine 5'-monophosphate synthase (UMP syn	H7C1U8	MICOS complex subunit (Fragment)
P12004	Proliferating cell nuclear antigen (PCNA) (Cycl	H7C213	Translation initiation factor IF-2, mitochondrial
P12277	Creatine kinase B-type (EC 2.7.3.2) (Brain crea	H7C2W1	D-beta-hydroxybutyrate dehydrogenase, mitoc
P13611	Versican core protein (Chondroitin sulfate prot	**H7C455**	Deleted.
P13639	Elongation factor 2 (EF-2)	H7C4C5	Microtubule-associated protein (Fragment)
P14649	Myosin light chain 6B (Myosin light chain 1 slov	**H7C5L1**	Deleted.
P14735	Insulin-degrading enzyme (EC 3.4.24.56) (Abe	H9E7F7	Cytochrome c oxidase subunit 2 (Fragment)
P15144	Aminopeptidase N (AP-N) (hAPN) (EC 3.4.11.2	I3L0T6	rRNA methyltransferase 3, mitochondrial
P15531	Nucleoside diphosphate kinase A (NDK A) (ND	I3L1P8	Mitochondrial 2-oxoglutarate/malate carrier pro
P17812	CTP synthase 1 (EC 6.3.4.2) (CTP synthetase	I3L282	Zinc finger CCCH domain-containing protein 7A
P18077	60S ribosomal protein L35a (Cell growth-inhibit	**I3L3B4**	Uncharacterized protein (Fragment)
P18124	60S ribosomal protein L7 (Large ribosomal sub	I3L3J9	Ketimine reductase mu-crystallin (Fragment)
P19012	Keratin, type I cytoskeletal 15 (Cytokeratin-15)	I3L505	Acyl carrier protein (Fragment)
P19105	Myosin regulatory light chain 12A (Epididymis s	I6L894	Ankyrin-2Ankyrin-2Ankyrin-2Ankyrin-2
P19174	1-phosphatidylinositol 4,5-bisphosphate phosp	**J3KNX9**	Deleted.
P19623	Spermidine synthase (SPDSY) (EC 2.5.1.16) (	J3KSI8	28S ribosomal protein S7, mitochondrial (Fragr
P22234	Multifunctional protein ADE2 [Includes: Phosph	J3KSY6	5'(3')-deoxyribonucleotidase, cytosolic type
P22314	Ubiquitin-like modifier-activating enzyme 1 (EC	J3QKK8	Prostamide/prostaglandin F synthase (Fragme
P22392	Nucleoside diphosphate kinase B (NDK B) (ND	J3QL14	V-type proton ATPase subunit d 1 (Fragment)
P23610	Factor VIII intron 22 protein (CpG island protei	J3QL15	Deleted.
P24821	Tenascin (TN) (Cytotactin) (GMEM) (GP 150-2	J3QL56	Protein SCO1 homolog, mitochondrial
P24941	Cyclin-dependent kinase 2 (EC 2.7.11.22) (Cel	J3QLV6	CoroninCoroninCoroninCoroninCoronin
P25391	Laminin subunit alpha-1 (Laminin A chain) (Lar	J3QLW7	60S ribosome subunit biogenesis protein NIP7
P30041	Peroxiredoxin-6 (EC 1.11.1.15) (1-Cys peroxire	J3QQY2	Calcium load-activated calcium channel (Trans
P30414	NK-tumor recognition protein (NK-TR protein) (	J3QTB2	MICOS complex subunit
P31949	Protein S100-A11 (Calgizzarin) (Metastatic lym	K7EJP6	CDP-diacylglycerol--glycerol-3-phosphate 3-ph
P32320	Cytidine deaminase (EC 3.5.4.5) (Cytidine ami	K7EKI4	39S ribosomal protein L4, mitochondrial
P35251	Replication factor C subunit 1 (Activator 1 140	K7ELD9	Synaptogyrin-2Synaptogyrin-2Synaptogyrin-2
P35268	60S ribosomal protein L22 (EBER-associated p	K7EMM9	Contactin-associated protein 1
P35269	General transcription factor IIF subunit 1 (Gene	K7EMR7	ReticulonReticulonReticulonReticulon
P35579	Myosin-9 (Cellular myosin heavy chain, type A)	**K7EN55**	Deleted.
P35749	Myosin-11 (Myosin heavy chain 11) (Myosin he	K7ENF5	Mitochondrial import inner membrane transloca

P37802	Transgelin-2 (Epididymis tissue protein Li 7e) (	K7ENL3	Signal transducer and activator of transcription
P40222	Alpha-taxilin	K7EP04	Heat shock protein beta-6
P41208	Centrin-2 (Caltractin isoform 1)	K7EP90	RNA-binding protein 42
P41250	Glycine--tRNA ligase (EC 3.6.1.17) (EC 6.1.1.1	K7EPS4	Matrix-remodeling-associated protein 7
P42574	Caspase-3 (CASP-3) (EC 3.4.22.56) (Apopain)	K7EQX8	Matrix-remodeling-associated protein 7
P46087	Probable 28S rRNA (cytosine(4447)-C(5))-met	K7ERH7	Dystrobrevin alpha (Fragment)
P46821	Microtubule-associated protein 1B (MAP-1B) [(	K7ES30	Zinc finger protein 180Zinc finger protein 180
P49006	MARCKS-related protein (MARCKS-like protei	K7ESE6	Glucose-6-phosphatase 3 (Fragment)
P49327	Fatty acid synthase (EC 2.3.1.85) [Includes: [A	K7WVJ5	Cytochrome c oxidase subunit 2 (Fragment)
P50395	Rab GDP dissociation inhibitor beta (Rab GDI	L0R8E5	Alternative protein SF1Alternative protein SF1
P50453	Serpin B9 (Cytoplasmic antiproteinase 3) (CAP	O00151	PDZ and LIM domain protein 1 (C-terminal LIM
P50897	Palmitoyl-protein thioesterase 1 (PPT-1) (EC 3	O00186	Syntaxin-binding protein 3 (Platelet Sec1 prote
P52735	Guanine nucleotide exchange factor VAV2 (VA	O14880	Microsomal glutathione S-transferase 3 (Micros
P53396	ATP-citrate synthase (EC 2.3.3.8) (ATP-citrate	O15020	Spectrin beta chain, non-erythrocytic 2 (Beta-II
P53621	Coatomer subunit alpha (Alpha-coat protein) (A	O15031	Plexin-B2 (MM1)Plexin-B2 (MM1)
P54687	Branched-chain-amino-acid aminotransferase,	O15173	Membrane-associated progesterone receptor c
P54709	Sodium/potassium-transporting ATPase subun	O15230	Laminin subunit alpha-5 (Laminin-10 subunit a
P55010	Eukaryotic translation initiation factor 5 (eIF-5)	O15427	Monocarboxylate transporter 4 (MCT 4) (Solute
P55058	Phospholipid transfer protein (Lipid transfer pro	O43678	NADH dehydrogenase [ubiquinone] 1 alpha su
P55060	Exportin-2 (Exp2) (Cellular apoptosis susceptib	O43823	A-kinase anchor protein 8 (AKAP-8) (A-kinase
P61619	Protein transport protein Sec61 subunit alpha i	O43837	Isocitrate dehydrogenase [NAD] subunit beta,
P61956	Small ubiquitin-related modifier 2 (SUMO-2) (H	O60566	Mitotic checkpoint serine/threonine-protein kina
P62269	40S ribosomal protein S18 (Ke-3) (Ke3) (Small	O60613	Selenoprotein F (15 kDa selenoprotein)
P62277	40S ribosomal protein S13 (Small ribosomal su	O60884	DnaJ homolog subfamily A member 2 (Cell cyc
P62280	40S ribosomal protein S11 (Small ribosomal su	O75063	Glycosaminoglycan xylosylkinase (EC 2.7.1.-)
P62633	Cellular nucleic acid-binding protein (CNBP) (Z	O75157	TSC22 domain family protein 2 (TSC22-related
P63167	Dynein light chain 1, cytoplasmic (8 kDa dynein	O75323	Protein NipSnap homolog 2 (NipSnap2) (Gliob
P67809	Nuclease-sensitive element-binding protein 1 (	O75367	Core histone macro-H2A.1 (Histone macroH2A
P68104	Elongation factor 1-alpha 1 (EF-1-alpha-1) (Elo	O75396	Vesicle-trafficking protein SEC22b (ER-Golgi S
P78318	Immunoglobulin-binding protein 1 (B-cell signa	O75438	NADH dehydrogenase [ubiquinone] 1 beta sub
P78330	Phosphoserine phosphatase (PSP) (PSPase) (	O75792	Ribonuclease H2 subunit A (RNase H2 subunit
P98179	RNA-binding protein 3 (RNA-binding motif prot	O75923	Dysferlin (Dystrophy-associated fer-1-like prote
Q00534	Cyclin-dependent kinase 6 (EC 2.7.11.22) (Cel	O75947	ATP synthase subunit d, mitochondrial (ATPas

Q01469	Fatty acid-binding protein 5 (Epidermal-type fa
Q01650	Large neutral amino acids transporter small su
Q01970	1-phosphatidylinositol 4,5-bisphosphate phosp
Q01995	Transgelin (22 kDa actin-binding protein) (Prot
Q02790	Peptidyl-prolyl cis-trans isomerase FKBP4 (PP
Q02952	A-kinase anchor protein 12 (AKAP-12) (A-kina
Q05639	Elongation factor 1-alpha 2 (EF-1-alpha-2) (Eu
Q05BW9	PAPSS1 protein (Fragment)
Q06203	Amidophosphoribosyltransferase (ATase) (EC
Q06210	Glutamine--fructose-6-phosphate aminotransfe
Q07812	Apoptosis regulator BAX (Bcl-2-like protein 4)
Q08945	FACT complex subunit SSRP1 (Chromatin-spe
Q0VDF9	Heat shock 70 kDa protein 14 (HSP70-like pro
Q12765	Secernin-1
Q13126	S-methyl-5'-thioadenosine phosphorylase (EC
Q13404	Ubiquitin-conjugating enzyme E2 variant 1 (UE
Q13509	Tubulin beta-3 chain (Tubulin beta-4 chain) (Tu
Q13885	Tubulin beta-2A chain (Tubulin beta class IIa)
Q13951	Core-binding factor subunit beta (CBF-beta) (F
Q14019	Coactosin-like protein
Q14257	Reticulocalbin-2 (Calcium-binding protein ERC
Q14669	E3 ubiquitin-protein ligase TRIP12 (EC 2.3.2.2
Q14766	Latent-transforming growth factor beta-binding
Q14847	LIM and SH3 domain protein 1 (LASP-1) (Meta
Q14997	Proteasome activator complex subunit 4 (Prote
Q149P0	Golgi-specific brefeldin A-resistance guanine n
Q15031	Probable leucine--tRNA ligase, mitochondrial (
Q15181	Inorganic pyrophosphatase (EC 3.6.1.1) (Pyro
Q15417	Calponin-3 (Calponin, acidic isoform)
Q15738	Sterol-4-alpha-carboxylate 3-dehydrogenase, c
Q15758	Neutral amino acid transporter B(0) (ATB(0)) (I
Q15785	Mitochondrial import receptor subunit TOM34 (
Q15819	Ubiquitin-conjugating enzyme E2 variant 2 (DD
O75955	Flotillin-1Flotillin-1Flotillin-1Flotillin-1Flotillin-1
O75964	ATP synthase subunit g, mitochondrial (ATPas
O76041	Nebulette (Actin-binding Z-disk protein)
O94826	Mitochondrial import receptor subunit TOM70 (
O95168	NADH dehydrogenase [ubiquinone] 1 beta sub
O95210	Starch-binding domain-containing protein 1 (G
O95425	Supervillin (Archvillin) (p205/p250)
O95479	GDH/6PGL endoplasmic bifunctional protein [I
O95817	BAG family molecular chaperone regulator 3 (B
O95831	Apoptosis-inducing factor 1, mitochondrial (EC
O95881	Thioredoxin domain-containing protein 12 (EC
O95936	Eomesodermin homolog (T-box brain protein 2
P00387	NADH-cytochrome b5 reductase 3 (B5R) (Cyto
P00558	Phosphoglycerate kinase 1 (EC 2.7.2.3) (Cell r
P00568	Adenylate kinase isoenzyme 1 (AK 1) (EC 2.7.
P02461	Collagen alpha-1(III) chain
P02545	Prelamin-A/C [Cleaved into: Lamin-A/C (70 kD
P04792	Heat shock protein beta-1 (HspB1) (28 kDa he
P05141	ADP/ATP translocase 2 (ADP,ATP carrier prot
P05413	Fatty acid-binding protein, heart (Fatty acid-bin
P06576	ATP synthase subunit beta, mitochondrial (EC
P06732	Creatine kinase M-type (EC 2.7.3.2) (Creatine
P06899	Histone H2B type 1-J (Histone H2B.1) (Histone
P07205	Phosphoglycerate kinase 2 (EC 2.7.2.3) (Phos
P07237	Protein disulfide-isomerase (PDI) (EC 5.3.4.1)
P07355	Annexin A2 (Annexin II) (Annexin-2) (Calpactin
P07954	Fumarate hydratase, mitochondrial (Fumarase
P08133	Annexin A6 (67 kDa calelectrin) (Annexin VI) (A
P08590	Myosin light chain 3 (Cardiac myosin light chai
P08754	Guanine nucleotide-binding protein G(k) subun
P09497	Clathrin light chain B (Lcb)
P09525	Annexin A4 (35-beta calcimedin) (Annexin IV)
P09543	2',3'-cyclic-nucleotide 3'-phosphodiesterase (C

Q16555	Dihydropyrimidinase-related protein 2 (DRP-2)	P09669	Cytochrome c oxidase subunit 6C (Cytochrom
Q16643	Drebrin (Developmentally-regulated brain prote	P09884	DNA polymerase alpha catalytic subunit (EC 2
Q16647	Prostacyclin synthase (EC 5.3.99.4) (Prostagla	P0CG38	POTE ankyrin domain family member I
Q16658	Fascin (55 kDa actin-bundling protein) (Singed	P10301	Ras-related protein R-Ras (p23)
Q16864	V-type proton ATPase subunit F (V-ATPase su	P10606	Cytochrome c oxidase subunit 5B, mitochondri
Q1W6G4	LUC7-like (S. cerevisiae), isoform CRA_g (Put	P11177	Pyruvate dehydrogenase E1 component subur
Q2M1P5	Kinesin-like protein KIF7	P11216	Glycogen phosphorylase, brain form (EC 2.4.1
Q2NKW8	Adenosylhomocysteinase (EC 3.3.1.1) (Fragm	P11233	Ras-related protein Ral-A
Q2NL82	Pre-rRNA-processing protein TSR1 homolog	P12236	ADP/ATP translocase 3 (ADP,ATP carrier prot
Q2Q1W2	E3 ubiquitin-protein ligase TRIM71 (EC 2.3.2.2	P12532	Creatine kinase U-type, mitochondrial (EC 2.7.
Q2Q9B7	Glucose-6-phosphate 1-dehydrogenase (EC 1	P12829	Myosin light chain 4 (Myosin light chain 1, emb
Q32P41	tRNA (guanine(37)-N1)-methyltransferase (EC	P12883	Myosin-7 (Myosin heavy chain 7) (Myosin heav
Q3SY17	Solute carrier family 25 member 52 (Mitochond	P13073	Cytochrome c oxidase subunit 4 isoform 1, mit
Q3SYF1	Sorting nexin 12, isoform CRA_a (cDNA, FLJ9	P13533	Myosin-6 (Myosin heavy chain 6) (Myosin heav
Q49AJ9	RPL3 protein (Ribosomal protein L3, isoform C	P13591	Neural cell adhesion molecule 1 (N-CAM-1) (N
Q4LE33	TNC variant protein (Fragment)	P13804	Electron transfer flavoprotein subunit alpha, mi
Q4R9M7	Kinesin family member 1Bbeta isoform IV	P13984	General transcription factor IIF subunit 2 (EC 3
Q4ZG32	Uncharacterized protein EPB41L5 (Fragment)	P14406	Cytochrome c oxidase subunit 7A2, mitochond
Q53FE8	cDNA FLJ36526 fis, clone TRACH2003347, hi	P14543	Nidogen-1 (NID-1) (Entactin)
Q53SW3	Uncharacterized protein DPYSL5 (Fragment)	P14854	Cytochrome c oxidase subunit 6B1 (Cytochrom
Q53SY7	Uncharacterized protein CAD (Fragment)	P14923	Junction plakoglobin (Catenin gamma) (Desmo
Q53XA7	Fumarylacetoacetase (FAA) (EC 3.7.1.2) (Beta	P15924	Desmoplakin (DP) (250/210 kDa paraneoplasti
Q59F54	Solute carrier family 2 (Facilitated glucose tran	P16401	Histone H1.5 (Histone H1a) (Histone H1b) (His
Q59FI2	Protein tyrosine phosphatase, receptor type, F	P16615	Sarcoplasmic/endoplasmic reticulum calcium A
Q59FW9	Developmentally regulated GTP binding protei	P17174	Aspartate aminotransferase, cytoplasmic (cAsp
Q59GT1	Conserved helix-loop-helix ubiquitous kinase v	P17900	Ganglioside GM2 activator (Cerebroside sulfat
Q59H55	Protein tyrosine phosphatase, non-receptor typ	P17948	Vascular endothelial growth factor receptor 1 (
Q5H909	Melanoma-associated antigen D2	P20674	Cytochrome c oxidase subunit 5A, mitochondri
Q5H964	HECT, UBA and WWE domain containing 1 (F	P20700	Lamin-B1Lamin-B1Lamin-B1Lamin-B1
Q5H9L2	Transcription elongation factor A protein-like 5	P21796	Voltage-dependent anion-selective channel pro
Q5IJ48	Protein crumbs homolog 2 (Crumbs-like protei	P22695	Cytochrome b-c1 complex subunit 2, mitochon
Q5JP05	cGMP-dependent protein kinase 1 (cGK 1) (cG	P23284	Peptidyl-prolyl cis-trans isomerase B (PPIase E
Q5JPE4	Vacuolar protein sorting-associated protein 29	P23327	Sarcoplasmic reticulum histidine-rich calcium-b

Q5JR04	Mov10, Moloney leukemia virus 10, homolog (	P23743	Diacylglycerol kinase alpha (DAG kinase alpha
Q5JR91	Kinesin-like protein KIF2C (Fragment)	P23786	Carnitine O-palmitoyltransferase 2, mitochondr
Q5JV98	Serine/threonine-protein kinase 24 (Fragment)	P24752	Acetyl-CoA acetyltransferase, mitochondrial (E
Q5KU26	Collectin-12 (Collectin placenta protein 1) (CL-	P25705	ATP synthase subunit alpha, mitochondrial (AT
Q5R363	Deleted.	P26440	Isovaleryl-CoA dehydrogenase, mitochondrial (
Q5R370	Calcyclin-binding protein (CacyBP) (hCacyBP)	P26447	Protein S100-A4 (Calvasculin) (Metastasin) (P
Q5SY16	Polynucleotide 5'-hydroxyl-kinase NOL9 (EC 2	P26678	Cardiac phospholamban (PLB)
Q5T0D3	Deleted.	P26885	Peptidyl-prolyl cis-trans isomerase FKBP2 (PP
Q5T123	SH3 domain-binding glutamic acid-rich-like pro	P27144	Adenylate kinase 4, mitochondrial (AK 4) (EC 2
Q5T280	Putative methyltransferase C9orf114 (EC 2.1.1	P27658	Collagen alpha-1(VIII) chain (Endothelial collag
Q5T450	Deleted.	P28289	Tropomodulin-1 (Erythrocyte tropomodulin) (E-
Q5T7C4	High mobility group protein B1	P29966	Myristoylated alanine-rich C-kinase substrate (
Q5T8C6	Cell division cycle protein 16 homolog	P30038	Delta-1-pyrroline-5-carboxylate dehydrogenase
Q5TDH0	Protein DDI1 homolog 2 (EC 3.4.23.-)	P30044	Peroxiredoxin-5, mitochondrial (EC 1.11.1.15)
Q5TE63	BCL2-like 1 isoform 2 (BCL2-like 1, isoform CR	P30046	D-dopachrome decarboxylase (EC 4.1.1.84) (D
Q5U071	High-mobility group box 2	P30049	ATP synthase subunit delta, mitochondrial (AT
Q5UGI6	Serine/cysteine proteinase inhibitor clade G me	P30084	Enoyl-CoA hydratase, mitochondrial (EC 4.2.1.
Q5VV42	Threonylcarbamoyladenosine tRNA methylthio	P31040	Succinate dehydrogenase [ubiquinone] flavopr
Q5VXV2	Protein SET (HLA-DR-associated protein II) (In	P31930	Cytochrome b-c1 complex subunit 1, mitochon
Q64EX5	6-phosphofructo-2-kinase/fructose-2,6-bisphos	P31937	3-hydroxyisobutyrate dehydrogenase, mitocho
Q68CX6	Uncharacterized protein DKFZp686O13149	P32418	Sodium/calcium exchanger 1 (Na(+)/Ca(2+)-ex
Q68DE0	Uncharacterized protein DKFZp781D2217	P33897	ATP-binding cassette sub-family D member 1 (
Q68DM5	Uracil-DNA glycosylase	P35232	ProhibitinProhibitinProhibitinProhibitin
Q6AI38	Uncharacterized protein DKFZp762F247 (Frag	P35270	Sepiapterin reductase (SPR) (EC 1.1.1.153)
Q6FI81	Anamorsin (Cytokine-induced apoptosis inhibit	P35527	Keratin, type I cytoskeletal 9 (Cytokeratin-9) (C
Q6IBS0	Twinfilin-2 (A6-related protein) (hA6RP) (Prote	P35556	Fibrillin-2 [Cleaved into: Fibrillin-2 C-terminal p
Q6IQ49	Replication stress response regulator SDE2	P36551	Oxygen-dependent coproporphyrinogen-III oxi
Q6LAN8	Collagen type I alpha 1 (Fragment)	P36776	Lon protease homolog, mitochondrial (EC 3.4.2
Q6LER7	Alpha-galactosidase A (EC 3.2.1.22) (Alpha-D-	P36957	Dihydrolipoyllysine-residue succinyltransferase
Q6MZM7	Uncharacterized protein DKFZp686O12165 (F	P40925	Malate dehydrogenase, cytoplasmic (EC 1.1.1.
Q6N0A7	Uncharacterized protein DKFZp686H05229 (Fr	P40939	Trifunctional enzyme subunit alpha, mitochond
Q6NUR1	Non-SMC condensin I complex, subunit G	P42785	Lysosomal Pro-X carboxypeptidase (EC 3.4.16
Q6NVV1	Putative 60S ribosomal protein L13a protein R	P43155	Carnitine O-acetyltransferase (Carnitine acetyl

Q6PCE3	Glucose 1,6-bisphosphate synthase (EC 2.7.1.
Q6XZF7	Dynamin-binding protein (Scaffold protein Tuba
Q6ZMD1	cDNA FLJ23994 fis, clone HRC11286
Q6ZTK5	Transmembrane 9 superfamily member
Q6ZUX7	LHFPL tetraspan subfamily member 2 protein (
Q6ZVX7	F-box only protein 50 (NCC receptor protein 1
Q75MG1	Basic leucine zipper and W2 domain-containin
Q7KZY0	Matrix metalloproteinase 15 (Membrane-insert
Q7L190	Developmental pluripotency-associated protein
Q7L576	Cytoplasmic FMR1-interacting protein 1 (Speci
Q7L9L4	MOB kinase activator 1B (Mob1 homolog 1A) (
Q7Z459	Ski oncoprotein (Fragment)
Q7Z478	ATP-dependent RNA helicase DHX29 (EC 3.6
Q7Z4W5	RNA helicase
Q7Z6Z7	E3 ubiquitin-protein ligase HUWE1 (EC 2.3.2.2
Q7Z7M0	Multiple epidermal growth factor-like domains p
Q86TU7	Histone-lysine N-methyltransferase setd3 (EC
Q86TV2	Legumain (EC 3.4.22.34) (Asparaginyl endope
Q86V21	Acetoacetyl-CoA synthetase (EC 6.2.1.16) (Ac
Q8IV08	Phospholipase D3 (PLD 3) (EC 3.1.4.4) (Choli
Q8IXH7	Negative elongation factor C/D (NELF-C/D) (T
Q8IYS2	Uncharacterized protein KIAA2013
Q8N236	cDNA FLJ34968 fis, clone NTONG2004844, hi
Q8N2F1	cDNA PSEC0206 fis, clone HEMBA1002913, v
Q8N3C0	Activating signal cointegrator 1 complex subun
Q8N6S3	Similar to ribonucleotide reductase protein r2 c
Q8N995	3-hydroxy-3-methylglutaryl coenzyme A syntha
Q8N9H8	Exonuclease mut-7 homolog (EC 3.1.-.-) (Exor
Q8NBJ4	Golgi membrane protein 1 (Golgi membrane pr
Q8NDU9	Uncharacterized protein ORC5L (Fragment)
Q8NFI3	Cytosolic endo-beta-N-acetylglucosaminidase
Q8NFW1	Collagen alpha-1(XXII) chain
Q8TAA9	Vang-like protein 1 (Loop-tail protein 2 homolo

P43897	Elongation factor Ts, mitochondrial (EF-Ts) (E
P45880	Voltage-dependent anion-selective channel pro
P47985	Cytochrome b-c1 complex subunit Rieske, mito
P48047	ATP synthase subunit O, mitochondrial (Oligor
P48723	Heat shock 70 kDa protein 13 (Microsomal stre
P48735	Isocitrate dehydrogenase [NADP], mitochondri
P49411	Elongation factor Tu, mitochondrial (EF-Tu) (P
P49748	Very long-chain specific acyl-CoA dehydrogena
P49755	Transmembrane emp24 domain-containing pro
P50225	Sulfotransferase 1A1 (ST1A1) (EC 2.8.2.1) (Ar
P50402	EmerinEmerinEmerinEmerinEmerinEmerin
P50440	Glycine amidinotransferase, mitochondrial (EC
P50461	Cysteine and glycine-rich protein 3 (Cardiac LI
P51153	Ras-related protein Rab-13 (Cell growth-inhibit
P51688	N-sulphoglucosamine sulphohydrolase (EC 3.1
P52943	Cysteine-rich protein 2 (CRP-2) (Protein ESP1
P54577	Tyrosine--tRNA ligase, cytoplasmic (EC 6.1.1.1
P54725	UV excision repair protein RAD23 homolog A (
P55001	Microfibrillar-associated protein 2 (MFAP-2) (M
P55145	Mesencephalic astrocyte-derived neurotrophic
P55268	Laminin subunit beta-2 (Laminin B1s chain) (La
P55327	Tumor protein D52 (Protein N8)
P55769	NHP2-like protein 1 (High mobility group-like n
P57105	Synaptojanin-2-binding protein (Mitochondrial o
P60174	Triosephosphate isomerase (TIM) (EC 5.3.1.1)
P61224	Ras-related protein Rap-1b (GTP-binding prote
P61604	10 kDa heat shock protein, mitochondrial (Hsp
P61966	AP-1 complex subunit sigma-1A (Adaptor prote
P62341	Thioredoxin reductase-like selenoprotein T (Se
P62805	Histone H4Histone H4Histone H4Histone H4
P62820	Ras-related protein Rab-1A (YPT1-related prot
P62879	Guanine nucleotide-binding protein G(I)/G(S)/G
P62979	Ubiquitin-40S ribosomal protein S27a (Ubiquiti

Q8TEF1	FLJ00246 protein (Fragment)
Q8WUN4	FAM40A protein (Fragment)
Q8WVY7	Ubiquitin-like domain-containing CTD phospha
Q8WWH5	Probable tRNA pseudouridine synthase 1 (EC
Q8WWI5	Choline transporter-like protein 1 (CDw92) (So
Q8WX92	Negative elongation factor B (NELF-B) (Cofact
Q8WX93	Palladin (SIH002) (Sarcoma antigen NY-SAR-
Q8WXD5	Gem-associated protein 6 (Gemin-6) (SIP2)
Q8WYK3	Thymidylate synthase (TS) (TSase) (EC 2.1.1.
Q92598	Heat shock protein 105 kDa (Antigen NY-CO-2
Q92673	Sortilin-related receptor (Low-density lipoprotei
Q92974	Rho guanine nucleotide exchange factor 2 (Gu
Q969E2	Secretory carrier-associated membrane protei
Q96BN8	Ubiquitin thioesterase otulin (EC 3.4.19.12) (D
Q96C90	Protein phosphatase 1 regulatory subunit 14B
Q96E14	RecQ-mediated genome instability protein 2 (h
Q96EK5	KIF1-binding protein
Q96EK6	Glucosamine 6-phosphate N-acetyltransferase
Q96ER3	Protein SAAL1 (Synoviocyte proliferation-asso
Q96HX0	TUBB2C protein (Fragment)
Q96HY6	DDRGK domain-containing protein 1 (Dashurin
Q96IB4	DIP2B protein (Fragment)
Q96IR1	RPS4X protein (Fragment)
Q96KB5	Lymphokine-activated killer T-cell-originated pr
Q96L67	Nardilysin
Q96NZ8	WAP, Kazal, immunoglobulin, Kunitz and NTR
Q96P48	Arf-GAP with Rho-GAP domain, ANK repeat a
Q96RE7	Nucleus accumbens-associated protein 1 (NA
Q96RS6	NudC domain-containing protein 1 (Chronic my
Q96RW7	Hemicentin-1 (Fibulin-6) (FIBL-6)
Q96T88	E3 ubiquitin-protein ligase UHRF1 (EC 2.3.2.2
Q99536	Synaptic vesicle membrane protein VAT-1 hom
Q99598	Translin-associated protein X (Translin-associa
P63092	Guanine nucleotide-binding protein G(s) subun
P63096	Guanine nucleotide-binding protein G(i) subuni
P63316	Troponin C, slow skeletal and cardiac muscles
P68133	Actin, alpha skeletal muscle (Alpha-actin-1) [C
P78540	Arginase-2, mitochondrial (EC 3.5.3.1) (Argina
P80404	4-aminobutyrate aminotransferase, mitochondr
P83111	Serine beta-lactamase-like protein LACTB, mit
P84090	Enhancer of rudimentary homolog
Q01082	Spectrin beta chain, non-erythrocytic 1 (Beta-II
Q01449	Myosin regulatory light chain 2, atrial isoform (
Q01813	ATP-dependent 6-phosphofructokinase, platele
Q03252	Lamin-B2Lamin-B2Lamin-B2Lamin-B2
Q04446	1,4-alpha-glucan-branching enzyme (EC 2.4.1.
Q04941	Proteolipid protein 2 (Differentiation-dependent
Q05BS8	SFRS2IP protein (Fragment)
Q05BX6	RABEP1 protein (Fragment)
Q05DA4	p4HA2 proteinp4HA2 proteinp4HA2 protein
Q05DK5	ADD2 protein (Fragment)
Q05DQ7	ACTR10 protein (Fragment)
Q08722	Leukocyte surface antigen CD47 (Antigenic su
Q09666	Neuroblast differentiation-associated protein A
Q0QEY7	Succinate dehydrogenase [ubiquinone] iron-su
Q0QF37	Malate dehydrogenase (EC 1.1.1.37) (Fragme
Q10589	Bone marrow stromal antigen 2 (BST-2) (HM1.
Q12846	Syntaxin-4 (Renal carcinoma antigen NY-REN-
Q12955	Ankyrin-3 (ANK-3) (Ankyrin-G)
Q12988	Heat shock protein beta-3 (HspB3) (Heat shoc
Q13011	Delta(3,5)-Delta(2,4)-dienoyl-CoA isomerase, r
Q13162	Peroxiredoxin-4 (EC 1.11.1.15) (Antioxidant en
Q13222	GATA-4 protein (Fragment)
Q13405	39S ribosomal protein L49, mitochondrial (L49
Q13423	NAD(P) transhydrogenase, mitochondrial (EC
Q13425	Beta-2-syntrophin (59 kDa dystrophin-associat

Q99856	AT-rich interactive domain-containing protein 3	Q13707	ACTA2 protein (Fragment)
Q9BPW0	Serine/threonine-protein phosphatase (EC 3.1.	Q13813	Spectrin alpha chain, non-erythrocytic 1 (Alpha
Q9BQ70	Transcription factor 25 (TCF-25) (Nuclear loca	Q13825	Methylglutaconyl-CoA hydratase, mitochondria
Q9BQI0	Allograft inflammatory factor 1-like (Ionized cal	Q14108	Lysosome membrane protein 2 (85 kDa lysoso
Q9BR76	Coronin-1B (Coronin-2)	Q14126	Desmoglein-2 (Cadherin family member 5) (HD
Q9BRA2	Thioredoxin domain-containing protein 17 (14 k	Q14151	Scaffold attachment factor B2 (SAF-B2)
Q9BRP4	Proteasomal ATPase-associated factor 1 (Prot	Q14195	Dihydropyrimidinase-related protein 3 (DRP-3)
Q9BTE3	Mini-chromosome maintenance complex-bindi	Q14677	Clathrin interactor 1 (Clathrin-interacting protei
Q9BTQ7	Similar to ribosomal protein L23 (Fragment)	Q14980	Nuclear mitotic apparatus protein 1 (Nuclear m
Q9BUD9	AAK1 protein	Q15120	[Pyruvate dehydrogenase (acetyl-transferring)]
Q9BV57	1,2-dihydroxy-3-keto-5-methylthiopentene diox	Q15149	Plectin (PCN) (PLTN) (Hemidesmosomal prote
Q9BVA1	Tubulin beta-2B chain	Q15172	Serine/threonine-protein phosphatase 2A 56 k
Q9BVG4	Protein PBDC1 (Polysaccharide biosynthesis d	Q15836	Vesicle-associated membrane protein 3 (VAMP
Q9BXX0	EMILIN-2 (Elastin microfibril interface-located p	Q16082	Heat shock protein beta-2 (HspB2) (DMPK-bin
Q9C056	Homeobox protein Nkx-6.2 (Homeobox protein	Q16270	Insulin-like growth factor-binding protein 7 (IBP
Q9C0C4	Semaphorin-4C	Q16441	PROS1 protein (Fragment)
Q9GZP4	PITH domain-containing protein 1	Q1KMD3	Heterogeneous nuclear ribonucleoprotein U-lik
Q9GZV0	cDNA FLJ12454 fis, clone NT2RM1000555, hi	Q1RLN5	ARHGAP12 protein (Rho GTPase-activating pr
Q9H3K6	BolA-like protein 2	Q1WWL2	PTGFRN protein (Fragment)
Q9H3N1	Thioredoxin-related transmembrane protein 1 (	**Q2F839**	Heat shock 70 kDa protein 9B (Fragment)
Q9H3P7	Golgi resident protein GCP60 (Acyl-CoA-bindi	Q2NLC8	GSTK1 protein (Fragment)
Q9H4A4	Aminopeptidase B (AP-B) (EC 3.4.11.6) (Argin	Q2NLD4	PURA protein (Fragment)
Q9H617	Transmembrane protein 164 (cDNA: FLJ22679	**Q2QD09**	Triosephosphate isomerase (EC 5.3.1.1) (Frag
Q9H678	cDNA: FLJ22530 fis, clone HRC12866	Q2VPB7	AP-5 complex subunit beta-1 (Adaptor-related
Q9H6T3	RNA polymerase II-associated protein 3	Q2YDB7	Peptidyl-prolyl cis-trans isomerase F, mitochon
Q9H7E2	Tudor domain-containing protein 3	Q3ZCW5	Succinate-CoA ligase subunit beta (EC 6.2.1.-)
Q9H7Z6	Histone acetyltransferase KAT8 (EC 2.3.1.48)	**Q3ZTS6**	Sarcomeric muscle protein (Fragment)
Q9H993	Protein-glutamate O-methyltransferase (EC 2.1	Q49A62	AMT proteinAMT proteinAMT protein
Q9H9Z2	Protein lin-28 homolog A (Lin-28A) (Zinc finger	Q4KMP7	TBC1 domain family member 10B (Rab27A-GA
Q9HBR0	Putative sodium-coupled neutral amino acid tra	Q502X2	Diablo homolog (Drosophila) (HCG1782202, is
Q9HC35	Echinoderm microtubule-associated protein-lik	**Q53EX3**	Glypican 1 variant (Fragment)
Q9HCK8	Chromodomain-helicase-DNA-binding protein 8	**Q53G62**	Mitochondrial ribosomal protein S28 variant (Fr
Q9NR09	Baculoviral IAP repeat-containing protein 6 (EC	**Q53G79**	Carnitine O-palmitoyltransferase II, mitochondr

Q9NR12	PDZ and LIM domain protein 7 (LIM mineraliza
Q9NR30	Nucleolar RNA helicase 2 (EC 3.6.4.13) (DEAD
Q9NR46	Endophilin-B2 (SH3 domain-containing GRB2-
Q9NRG7	Epimerase family protein SDR39U1 (EC 1.1.1.
Q9NUW4	BRIX (Brix domain containing 2, isoform CRA_
Q9NWS0	PIH1 domain-containing protein 1 (Nucleolar p
Q9NWY4	Histone PARylation factor 1
Q9NXN4	Ganglioside-induced differentiation-associated
Q9NZL4	Hsp70-binding protein 1 (HspBP1) (Heat shock
Q9P0C1	HSPC260 (Fragment)
Q9UBH6	Xenotropic and polytropic retrovirus receptor 1
Q9UES0	SNARE protein Ykt6 (Fragment)
Q9UHD1	Cysteine and histidine-rich domain-containing p
Q9UHV9	Prefoldin subunit 2
Q9UID3	Vacuolar protein sorting-associated protein 51
Q9UJJ2	Zinc finger protein 280C (Fragment)
Q9UJY4	ADP-ribosylation factor-binding protein GGA2 (
Q9ULT8	E3 ubiquitin-protein ligase HECTD1 (EC 2.3.2.
Q9UPT8	Zinc finger CCCH domain-containing protein 4
Q9UQD4	SH3-containing Grb-2-like 1 protein
Q9Y250	Leucine zipper putative tumor suppressor 1 (F
Q9Y266	Nuclear migration protein nudC (Nuclear distrib
Q9Y570	Protein phosphatase methylesterase 1 (PME-1
Q9Y5A7	NEDD8 ultimate buster 1 (Negative regulator o
Q9Y5B9	FACT complex subunit SPT16 (Chromatin-spe
Q9Y5V3	Melanoma-associated antigen D1 (MAGE tumo
Q9Y617	Phosphoserine aminotransferase (EC 2.6.1.52
Q9Y678	Coatomer subunit gamma-1 (Gamma-1-coat p
Q9Y6K1	DNA (cytosine-5)-methyltransferase 3A (Dnmt3
Q9Y6Y0	Influenza virus NS1A-binding protein (NS1-BP)

Q53GC8	Peroxisomal D3,D2-enoyl-CoA isomerase isofo
Q53GE3	Pyruvate dehydrogenase E1 component subur
Q53SW4	Uncharacterized protein NDUFA10 (Fragment)
Q53T40	Uncharacterized protein FHL2 (Fragment)
Q562R1	Beta-actin-like protein 2 (Kappa-actin)
Q58F18	LHX1 protein (Fragment)
Q59EK1	Adducin 3 isoform a variant (Fragment)
Q59F48	Deoxyribonuclease I-like 3 variant (Fragment)
Q59G16	SWI/SNF-related matrix-associated actin-depe
Q59GC9	Syntaxin binding protein 1 variant (Fragment)
Q59GG0	Sulfotransferase (EC 2.8.2.-) (Fragment)
Q59H37	Laminin alpha 2 subunit variant (Fragment)
Q5HYD9	Uncharacterized protein DKFZp686M0619 (Fra
Q5HYI5	Uncharacterized protein DKFZp313C1541
Q5JTV8	Torsin-1A-interacting protein 1 (Lamin-associa
Q5JW53	Kinetochore-associated protein DSN1 homolog
Q5K4L6	Long-chain fatty acid transport protein 3 (FATP
Q5QNZ2	ATP synthase peripheral stalk-membrane subu
Q5QTQ6	MSTP010 (cDNA FLJ11394 fis, clone HEMBA1
Q5RI15	Cytochrome c oxidase assembly protein COX2
Q5RLJ0	CLECLECLECLECLECLECLECLECLECLE
Q5SRE5	Nucleoporin NUP188 homolog (hNup188)
Q5STN0	Deleted.
Q5T171	Pygopus homolog 2 (Drosophila), isoform CRA
Q5T200	Zinc finger CCCH domain-containing protein 1
Q5T5E9	Threonine--tRNA ligase, mitochondrial
Q5T7A4	Deleted.
Q5T7F1	Neuropilin-1 (Vascular endothelial cell growth f
Q5T858	Deleted.
Q5TCI8	Prelamin-A/CPrelamin-A/CPrelamin-A/C
Q5TEC6	Histone H3Histone H3Histone H3Histone H3
Q5TFQ8	Signal-regulatory protein beta-1 isoform 3 (SIR
Q5U5X0	Complex III assembly factor LYRM7 (LYR moti

Q5VT52	Regulation of nuclear pre-mRNA domain-conta
Q5W0J6	Enoyl-CoA hydratase domain-containing protei
Q5W145	NADH dehydrogenase [ubiquinone] 1 beta sub
Q5W9G0	KIAA0638 splice variant 2 (Fragment)
Q5XKP0	MICOS complex subunit MIC13 (Protein P117)
Q5XWD3	Leucine-rich repeat protein LRIG1
Q63Z41	Uncharacterized protein DKFZp686M0146 (Fra
Q63ZY3	KN motif and ankyrin repeat domain-containing
Q68D64	Uncharacterized protein DKFZp686E23276 (Fr
Q68DW4	MICOS complex subunit
Q6AHX3	Uncharacterized protein DKFZp761N1221 (Fra
Q6BDS2	UHRF1-binding protein 1 (ICBP90-binding prot
Q6DD87	Zinc finger protein 787 (TTF-I-interacting pepti
Q6DEN2	DPYSL3 proteinDPYSL3 protein
Q6IAA8	Ragulator complex protein LAMTOR1 (Late en
Q6IAN0	Dehydrogenase/reductase SDR family membe
Q6ICA4	DJ402G11.5 proteinDJ402G11.5 protein
Q6ICS0	Annexin (Fragment)Annexin (Fragment)
Q6IQ22	Ras-related protein Rab-12
Q6JSD7	Aquaporin 1 splice variant 3 (Fragment)
Q6LBM3	Fibroblast growth factor 1 (Acidic fibroblast gro
Q6LEE2	4a-carbinolamine dehydratase (Fragment)
Q6NVU6	Inactive Ufm1-specific protease 1 (UfSP1)
Q6P4A8	Phospholipase B-like 1 (EC 3.1.1.-) (LAMA-like
Q6P587	Acylpyruvase FAHD1, mitochondrial (EC 3.7.1.
Q6PJM8	RRP1B protein (Fragment)
Q6R327	Rapamycin-insensitive companion of mTOR (A
Q6RW13	Type-1 angiotensin II receptor-associated prote
Q6ZP26	cDNA FLJ26672 fis, clone MPG03403, highly s
Q6ZU43	cDNA FLJ44007 fis, clone TESTI4023762
Q6ZWP6	Isobutyryl-CoA dehydrogenase, mitochondrial (
Q702N8	Xin actin-binding repeat-containing protein 1 (C
Q75N88	Fibrillin 1Fibrillin 1Fibrillin 1Fibrillin 1Fibrillin 1

Q7KZE5	Pre-B-cell leukemia transcription factor 2
Q7Z3D6	D-glutamate cyclase, mitochondrial (EC 4.2.1.4
Q7Z417	Nuclear fragile X mental retardation-interacting
Q7Z434	Mitochondrial antiviral-signaling protein (MAVS
Q7Z4Y4	GTP:AMP phosphotransferase AK3, mitochond
Q7Z503	Succinate--CoA ligase [ADP-forming] subunit b
Q7Z554	Troponin T cardiac isoform (Troponin T type 2
Q7Z7K6	Centromere protein V (CENP-V) (Nuclear prote
Q86SE4	L1 cell adhesion molecule (Fragment)
Q86SX6	Glutaredoxin-related protein 5, mitochondrial (M
Q86TG7	Retrotransposon-derived protein PEG10 (Emb
Q86U28	Iron-sulfur cluster assembly 2 homolog, mitoch
Q86UE4	Protein LYRIC (3D3/LYRIC) (Astrocyte elevate
Q86UK7	E3 ubiquitin-protein ligase ZNF598 (EC 2.3.2.2
Q86UP4	Interferon alpha 2bInterferon alpha 2b
Q86UX3	Multidrug resistance-associated protein 5 (ATP
Q86V59	Paraneoplastic antigen-like protein 8A (PNMA-
Q86XN0	MRPL43 protein (Fragment)
Q86XV3	DIP2C protein (Fragment)
Q8IUG5	Unconventional myosin-XVIIIb
Q8IV81	SFRS8 protein (Fragment)
Q8IVF2	Protein AHNAK2Protein AHNAK2
Q8IXM3	39S ribosomal protein L41, mitochondrial (L41
Q8IY95	Transmembrane protein 192
Q8IYB3	Serine/arginine repetitive matrix protein 1 (SR-
Q8IZ52	Chondroitin sulfate synthase 2 (EC 2.4.1.175)
Q8N129	Protein canopy homolog 4
Q8N142	Adenylosuccinate synthetase isozyme 1 (AMPS
Q8N4V1	Membrane magnesium transporter 1 (ER mem
Q8N6F2	MRPS27 protein (cDNA FLJ46849 fis, clone UT
Q8N926	cDNA FLJ38501 fis, clone HCHON1000176, m
Q8NBX0	Saccharopine dehydrogenase-like oxidoreduct
Q8NCW8	3-oxoacyl-CoA thiolase (Fragment)

Q8NDT2	Putative RNA-binding protein 15B (One-twenty
Q8NE79	Blood vessel epicardial substance (hBVES) (P
Q8NEI6	ZNF644 protein (Fragment)
Q8TAF3	WD repeat-containing protein 48 (USP1-assoc
Q8TAS0	ATP synthase subunit gamma (Fragment)
Q8TB52	F-box only protein 30F-box only protein 30
Q8TBT6	Uncharacterized protein (Fragment)
Q8TEA7	TBC domain-containing protein kinase-like pro
Q8WU76	Sec1 family domain-containing protein 2 (Synta
Q8WW12	PEST proteolytic signal-containing nuclear pro
Q8WYJ5	Protein kinase C inhibitor-2
Q8WZ42	Titin (EC 2.7.11.1) (Connectin) (Rhabdomyosa
Q92506	Estradiol 17-beta-dehydrogenase 8 (EC 1.1.1.(
Q92871	Phosphomannomutase 1 (PMM 1) (EC 5.4.2.8
Q92878	DNA repair protein RAD50 (hRAD50) (EC 3.6.-
Q93000	CHL1 protein (Fragment)
Q93100	Phosphorylase b kinase regulatory subunit bet
Q969H8	Myeloid-derived growth factor (MYDGF) (Interl
Q96AB3	Isochorismatase domain-containing protein 2
Q96BS4	FBL protein (Fragment)
Q96C23	Aldose 1-epimerase (EC 5.1.3.3) (Galactose m
Q96CN7	Isochorismatase domain-containing protein 1
Q96CP5	PMPCB protein (Fragment)
Q96D15	Reticulocalbin-3 (EF-hand calcium-binding pro
Q96D53	Atypical kinase COQ8B, mitochondrial (EC 2.7
Q96DC0	DCI protein (Dodecenoyl-Coenzyme A delta is
Q96EH3	Mitochondrial assembly of ribosomal large sub
Q96G15	TEAD3 protein (Fragment)
Q96G95	[3-methyl-2-oxobutanoate dehydrogenase [lipo
Q96GX3	KIAA0118 protein (Fragment)
Q96HD1	Cysteine-rich with EGF-like domain protein 1
Q96HE7	ERO1-like protein alpha (ERO1-L) (ERO1-L-al
Q96HS1	Serine/threonine-protein phosphatase PGAM5

Q96IX5	Up-regulated during skeletal muscle growth pr
Q96KR6	Protein FAM210B, mitochondrial
Q96LW7	Caspase recruitment domain-containing protei
Q96ME4	cDNA FLJ32471 fis, clone SKNMC2000322, hi
Q96NH6	Uveal autoantigen with coiled-coil domains and
Q96PK6	RNA-binding protein 14 (Paraspeckle protein 2
Q96PM9	Zinc finger protein 385A (Hematopoietic zinc fi
Q96QR8	Transcriptional activator protein Pur-beta (Puri
Q96S55	ATPase WRNIP1 (EC 3.6.1.3) (Werner helicas
Q96S66	Chloride channel CLIC-like protein 1 (Mid-1-rel
Q96SL4	Glutathione peroxidase 7 (GPx-7) (GSHPx-7) (
Q99470	Stromal cell-derived factor 2 (SDF-2)
Q99735	Microsomal glutathione S-transferase 2 (Micros
Q99766	ATP synthase subunit s, mitochondrial (ATP sy
Q9BQ69	O-acetyl-ADP-ribose deacetylase MACROD1 (
Q9BQ95	Evolutionarily conserved signaling intermediate
Q9BQE5	Apolipoprotein L2 (Apolipoprotein L-II) (ApoL-II
Q9BQS8	FYVE and coiled-coil domain-containing protei
Q9BRG1	Vacuolar protein-sorting-associated protein 25
Q9BRJ2	39S ribosomal protein L45, mitochondrial (L45
Q9BRX8	Redox-regulatory protein FAM213A (Peroxired
Q9BTI6	FLOT2 proteinFLOT2 proteinFLOT2 protein
Q9BTT5	Similar to NADH dehydrogenase (Ubiquinone)
Q9BTY2	Plasma alpha-L-fucosidase (EC 3.2.1.51) (Alph
Q9BU61	NADH dehydrogenase [ubiquinone] 1 alpha su
Q9BUB1	cAMP-dependent protein kinase type II-alpha r
Q9BUH6	Protein PAXX (Paralog of XRCC4 and XLF) (X
Q9BVJ8	HEXA protein (Fragment)
Q9BX40	Protein LSM14 homolog B (Protein FAM61B) (
Q9BXW7	Haloacid dehalogenase-like hydrolase domain-
Q9H0U4	Ras-related protein Rab-1B
Q9H2X5	Sulfhydryl oxidase (EC 1.8.3.2)
Q9H330	Transmembrane protein 245 (Protein CG-2)

Q9H3H9	Transcription elongation factor A protein-like 2
Q9H6N6	Putative uncharacterized protein MYH16 (Myos
Q9H7H0	Methyltransferase-like protein 17, mitochondria
Q9H9B4	Sideroflexin-1 (Tricarboxylate carrier protein) (
Q9HAT2	Sialate O-acetylesterase (EC 3.1.1.53) (H-Lse)
Q9HBH5	Retinol dehydrogenase 14 (EC 1.1.1.-) (Alcoho
Q9HBL7	Plasminogen receptor (KT) (Plg-R(KT))
Q9HCC0	Methylcrotonoyl-CoA carboxylase beta chain, r
Q9HCJ3	Ribonucleoprotein PTB-binding 2 (Protein rave
Q9NPC6	Myozenin-2 (Calsarcin-1) (FATZ-related protei
Q9NQC3	Reticulon-4 (Foocen) (Neurite outgrowth inhibit
Q9NQH7	Xaa-Pro aminopeptidase 3 (X-Pro aminopeptio
Q9NVI7	ATPase family AAA domain-containing protein
Q9NWE6	cDNA FLJ10079 fis, clone HEMBA1001896, w
Q9NWH9	SAFB-like transcription modulator (Modulator o
Q9NWQ9	Uncharacterized protein C14orf119
Q9NWU5	39S ribosomal protein L22, mitochondrial (L22
Q9NWV7	cDNA FLJ20572 fis, clone REC01048
Q9NX40	OCIA domain-containing protein 1 (Ovarian ca
Q9NXG6	Transmembrane prolyl 4-hydroxylase (P4H-TM
Q9NXJ5	Pyroglutamyl-peptidase 1 (EC 3.4.19.3) (5-oxo
Q9NXV2	BTB/POZ domain-containing protein KCTD5
Q9NZ08	Endoplasmic reticulum aminopeptidase 1 (EC
Q9NZ23	Drug-sensitive protein 1 (Gastric-associated di
Q9NZ45	CDGSH iron-sulfur domain-containing protein 1
Q9NZM4	BRD4-interacting chromatin-remodeling compl
Q9P0M6	Core histone macro-H2A.2 (Histone macroH2A
Q9P2K3	REST corepressor 3REST corepressor 3
Q9UBQ7	Glyoxylate reductase/hydroxypyruvate reducta
Q9UBY9	Heat shock protein beta-7 (HspB7) (Cardiovas
Q9UEH5	24-kDa subunit of complex I (EC 1.6.5.3) (Frag
Q9UF24	Uncharacterized protein DKFZp586K0821 (Fra
Q9UFM8	Neuroplastin (Fragment)

		Q9UFN0	Protein NipSnap homolog 3A (NipSnap3A) (Pr
		Q9UHL4	Dipeptidyl peptidase 2 (EC 3.4.14.2) (Dipeptidy
		Q9UI09	NADH dehydrogenase [ubiquinone] 1 alpha su
		Q9UJC5	SH3 domain-binding glutamic acid-rich-like pro
		Q9UJY1	Heat shock protein beta-8 (HspB8) (Alpha-crys
		Q9UK59	Lariat debranching enzyme (EC 3.1.-.-)
		Q9UMS6	Synaptopodin-2 (Genethonin-2) (Myopodin)
		Q9UPE4	Mitochondrial import inner membrane transloca
		Q9UQM7	Calcium/calmodulin-dependent protein kinase
		Q9Y277	Voltage-dependent anion-selective channel pro
		Q9Y2H5	Pleckstrin homology domain-containing family
		Q9Y305	Acyl-coenzyme A thioesterase 9, mitochondria
		Q9Y3B4	Splicing factor 3B subunit 6 (Pre-mRNA branch
		Q9Y3C6	Peptidyl-prolyl cis-trans isomerase-like 1 (PPIa
		Q9Y4D8	Probable E3 ubiquitin-protein ligase HECTD4 (
		Q9Y512	Sorting and assembly machinery component 5
		Q9Y547	Intraflagellar transport protein 25 homolog (He
		Q9Y5B2	Junction adhesion molecule
		Q9Y623	Myosin-4 (Myosin heavy chain 2b) (MyHC-2b)
		Q9Y655	Myelin gene expression factor 2
		Q9Y666	Solute carrier family 12 member 7 (Electroneut
		Q9Y6C2	EMILIN-1 (Elastin microfibril interface-located p

Bold font represents unmapped proteins

Supplementary table 4: List of enriched Biological Processes

Down-regulated				Up-regulated			
Term	**Count**	**%**	**P-Value**	**Term**	**Count**	**%**	**P-Value**
cell-cell adhesion	43	8.6	2.00E-19	mitochondrial respiratory chain complex I assembly	19	3	2.50E-12
translational initiation	21	4.2	2.10E-09	mitochondrial ATP synthesis coupled proton transport	12	1.9	2.10E-11
rRNA processing	24	4.8	5.30E-08	metabolic process	28	4.5	2.70E-11
SRP-dependent cotranslational protein targeting to membrane	16	3.2	6.50E-08	mitochondrial electron transport, NADH to ubiquinone	16	2.5	5.70E-11
nuclear-transcribed mRNA catabolic process, nonsense-mediated decay	17	3.4	2.80E-07	ATP biosynthetic process	13	2.1	8.30E-11

viral transcription	15	3	3.70E-06	tricarboxylic acid cycle	13	2.1	8.30E-11
purine ribonucleoside monophosphate biosynthetic process	6	1.2	2.00E-05	fatty acid beta-oxidation	14	2.2	1.80E-09
mitotic nuclear division	19	3.8	2.90E-04	branched-chain amino acid catabolic process	10	1.6	4.70E-09
cellular response to epidermal growth factor stimulus	7	1.4	3.00E-04	muscle filament sliding	12	1.9	4.10E-08
translation	19	3.8	3.70E-04	regulation of cardiac muscle contraction by regulation of the release of sequestered calcium ion	9	1.4	1.10E-07
intracellular protein transport	18	3.6	4.60E-04	regulation of the force of heart contraction	9	1.4	1.10E-07
nucleoside metabolic process	5	1	1.80E-03	muscle contraction	18	2.9	1.60E-07
global genome nucleotide-excision repair	6	1.2	2.00E-03	mitochondrial translational elongation	16	2.5	2.00E-07
glutamine metabolic process	5	1	2.20E-03	ATP synthesis coupled proton transport	9	1.4	4.20E-07
G1/S transition of mitotic cell cycle	10	2	2.60E-03	fatty acid beta-oxidation using acyl-CoA dehydrogenase	8	1.3	1.30E-06
purine nucleotide biosynthetic process	4	0.8	4.20E-03	oxidation-reduction process	44	7	4.20E-06
CTP biosynthetic process	4	0.8	4.20E-03	AMP metabolic process	5	0.8	7.00E-06
UTP biosynthetic process	4	0.8	4.20E-03	ATP metabolic process	9	1.4	1.00E-05
cholesterol biosynthetic process	6	1.2	4.30E-03	aerobic respiration	9	1.4	1.30E-05
cellular response to interleukin-4	5	1	4.40E-03	regulation of heart rate	9	1.4	1.30E-05
L-serine biosynthetic process	3	0.6	4.70E-03	cardiac muscle contraction	10	1.6	2.00E-05
antigen processing and presentation of exogenous peptide antigen via MHC class II	9	1.8	4.80E-03	cristae formation	6	1	3.20E-05
nucleobase-containing small molecule interconversion	5	1	5.20E-03	mitochondrial translational termination	13	2.1	4.00E-05
negative regulation of actin filament polymerization	4	0.8	5.40E-03	mitochondrial electron transport, cytochrome c to oxygen	7	1.1	4.40E-05
GTP biosynthetic process	4	0.8	5.40E-03	respiratory electron transport chain	7	1.1	4.40E-05
cell division	20	4	5.90E-03	oxidative phosphorylation	6	1	5.10E-05
actomyosin structure organization	5	1	6.90E-03	response to unfolded protein	9	1.4	8.40E-05

DNA damage response, signal transduction by p53 class mediator resulting in cell cycle arrest	7	1.4	8.40E-03	mitochondrial electron transport, ubiquinol to cytochrome c	6	1	1.10E-04
protein transport	21	4.2	1.00E-02	glyoxylate metabolic process	7	1.1	2.20E-04
'de novo' IMP biosynthetic process	3	0.6	1.10E-02	activation of protein kinase A activity	6	1	2.90E-04
pyrimidine nucleoside biosynthetic process	3	0.6	1.10E-02	response to hydrogen peroxide	9	1.4	3.40E-04
negative regulation of stress-activated MAPK cascade	3	0.6	1.10E-02	regulation of ryanodine-sensitive calcium-release channel activity	6	1	3.80E-04
negative regulation of fibroblast proliferation	5	1	1.10E-02	regulation of ventricular cardiac muscle cell action potential	5	0.8	3.90E-04
positive regulation of ATPase activity	5	1	1.10E-02	ADP biosynthetic process	4	0.6	4.00E-04
oxidation-reduction process	28	5.6	1.20E-02	leucine catabolic process	4	0.6	4.00E-04
actin cytoskeleton organization	10	2	1.20E-02	establishment of protein localization to plasma membrane	8	1.3	5.50E-04
cellular response to drug	7	1.4	1.40E-02	relaxation of cardiac muscle	5	0.8	5.70E-04
translational elongation	4	0.8	1.40E-02	renal water homeostasis	7	1.1	7.20E-04
positive regulation of neuron projection development	8	1.6	1.40E-02	gluconeogenesis	8	1.3	7.40E-04
DNA replication	11	2.2	1.40E-02	membrane raft assembly	4	0.6	7.70E-04
cell proliferation	19	3.8	1.80E-02	bundle of His cell-Purkinje myocyte adhesion involved in cell communication	4	0.6	7.70E-04
methylation	7	1.4	1.80E-02	striated muscle contraction	5	0.8	8.00E-04
microtubule-based process	5	1	1.90E-02	hydrogen ion transmembrane transport	9	1.4	1.20E-03
ribosome biogenesis	5	1	1.90E-02	GTP metabolic process	4	0.6	1.30E-03
lipid transport	7	1.4	2.10E-02	electron transport chain	4	0.6	1.30E-03
neural tube closure	7	1.4	2.30E-02	ER to Golgi vesicle-mediated transport	15	2.4	1.40E-03
nucleotide-excision repair, DNA duplex unwinding	4	0.8	2.40E-02	ventricular cardiac muscle tissue morphogenesis	6	1	1.50E-03
viral process	16	3.2	2.50E-02	cardiac muscle fiber development	4	0.6	2.00E-03
pyrimidine nucleotide metabolic process	3	0.6	2.60E-02	lipid homeostasis	7	1.1	2.10E-03
osteoblast differentiation	8	1.6	3.00E-02	response to reactive oxygen species	7	1.1	2.10E-03
response to ethanol	8	1.6	3.10E-02	glucose metabolic process	9	1.4	2.20E-03
purine nucleotide metabolic process	3	0.6	3.20E-02	cellular response to glucagon stimulus	7	1.1	2.40E-03

cytoplasmic translation	4	0.8	3.30E-02	cellular oxidant detoxification	9	1.4	2.90E-03
ribosomal large subunit biogenesis	4	0.8	3.30E-02	cell-cell adhesion	20	3.2	3.00E-03
lipid catabolic process	7	1.4	3.50E-02	carnitine shuttle	4	0.6	3.00E-03
cellular response to UV	5	1	3.60E-02	regulation of release of sequestered calcium ion into cytosol by sarcoplasmic reticulum	5	0.8	3.00E-03
positive regulation of proteasomal ubiquitin-dependent protein catabolic process	6	1.2	3.60E-02	negative regulation of peptidyl-cysteine S-nitrosylation	3	0.5	3.50E-03
glucose metabolic process	6	1.2	4.20E-02	extracellular matrix organization	16	2.5	3.60E-03
cytoskeleton organization	10	2	4.20E-02	succinate metabolic process	4	0.6	4.20E-03
regulation of mitochondrial membrane potential	4	0.8	4.50E-02	cell redox homeostasis	9	1.4	5.20E-03
cellular response to amino acid stimulus	5	1	4.50E-02	response to ischemia	6	1	5.30E-03
inositol phosphate metabolic process	5	1	4.50E-02	skin development	6	1	6.00E-03
endocytosis	9	1.8	4.60E-02	glutathione derivative biosynthetic process	5	0.8	6.40E-03
response to estradiol	7	1.4	4.60E-02	regulation of heart rate by cardiac conduction	6	1	6.80E-03
regulation of cell shape	9	1.8	4.80E-02	regulation of cellular response to growth factor stimulus	3	0.5	6.90E-03
immune system process	4	0.8	4.90E-02	valine catabolic process	3	0.5	6.90E-03
nuclear-transcribed mRNA poly(A) tail shortening	4	0.8	4.90E-02	adenine transport	3	0.5	6.90E-03
positive regulation of viral transcription	4	0.8	4.90E-02	regulation of acetyl-CoA biosynthetic process from pyruvate	4	0.6	7.20E-03
nucleotide-excision repair, preincision complex assembly	4	0.8	4.90E-02	translation	18	2.9	7.40E-03
cellular oxidant detoxification	6	1.2	5.00E-02	fatty acid biosynthetic process	7	1.1	9.00E-03
epithelial cell differentiation	6	1.2	5.00E-02	actin filament capping	4	0.6	9.20E-03
nucleobase-containing compound metabolic process	5	1	5.10E-02	substrate adhesion-dependent cell spreading	6	1	9.70E-03
hepatocyte apoptotic process	3	0.6	5.20E-02	generation of precursor metabolites and energy	7	1.1	9.80E-03
positive regulation of axon extension	4	0.8	5.30E-02	protein folding	14	2.2	1.00E-02
one-carbon metabolic process	4	0.8	5.30E-02	regulation of cardiac conduction	7	1.1	1.30E-02

response to testosterone	4	0.8	5.30E-02	response to hormone	6	1	1.50E-02
negative regulation of early endosome to late endosome transport	2	0.4	5.60E-02	regulation of cellular response to heat	8	1.3	1.50E-02
establishment of monopolar cell polarity	2	0.4	5.60E-02	regulation of cell communication by electrical coupling	3	0.5	1.60E-02
serine family amino acid biosynthetic process	2	0.4	5.60E-02	response to muscle stretch	4	0.6	1.70E-02
pentose-phosphate shunt, oxidative branch	2	0.4	5.60E-02	regulation of heart contraction	5	0.8	2.20E-02
nicotinamide riboside catabolic process	2	0.4	5.60E-02	regulation of cardiac muscle contraction by calcium ion signaling	3	0.5	2.30E-02
'de novo' GDP-L-fucose biosynthetic process	2	0.4	5.60E-02	transition between fast and slow fiber	3	0.5	2.30E-02
pentose biosynthetic process	2	0.4	5.60E-02	positive regulation of cation channel activity	3	0.5	2.30E-02
pyridoxine biosynthetic process	2	0.4	5.60E-02	paranodal junction assembly	3	0.5	2.30E-02
response to hydrogen peroxide	5	1	5.70E-02	establishment of protein localization to chromatin	3	0.5	2.30E-02
ruffle organization	3	0.6	5.90E-02	xenobiotic catabolic process	3	0.5	2.30E-02
purine-containing compound salvage	3	0.6	5.90E-02	NADH metabolic process	3	0.5	2.30E-02
nucleoside triphosphate biosynthetic process	3	0.6	5.90E-02	cytoskeleton organization	12	1.9	2.50E-02
lipid biosynthetic process	3	0.6	5.90E-02	response to heat	6	1	2.50E-02
positive regulation of translation	5	1	6.40E-02	proton transport	6	1	2.70E-02
positive regulation of cellular protein metabolic process	3	0.6	6.70E-02	regulation of sodium ion transmembrane transport	3	0.5	2.90E-02
apoptotic DNA fragmentation	3	0.6	6.70E-02	malate metabolic process	3	0.5	2.90E-02
vesicle-mediated transport	9	1.8	7.10E-02	response to methylmercury	3	0.5	2.90E-02
insulin receptor signaling pathway	6	1.2	7.20E-02	porphyrin-containing compound biosynthetic process	3	0.5	2.90E-02
protein folding	10	2	7.40E-02	negative regulation of cAMP-dependent protein kinase activity	3	0.5	2.90E-02
positive regulation of protein import into nucleus	3	0.6	7.50E-02	ketone body biosynthetic process	3	0.5	2.90E-02

negative regulation of inflammatory response	6	1.2	7.60E-02	cellular response to reactive oxygen species	4	0.6	3.10E-02
wound healing	6	1.2	7.90E-02	skeletal muscle tissue development	6	1	3.10E-02
cellular protein modification process	7	1.4	8.00E-02	reactive oxygen species metabolic process	5	0.8	3.20E-02
negative regulation of glial cell differentiation	2	0.4	8.30E-02	response to drug	18	2.9	3.60E-02
'de novo' UMP biosynthetic process	2	0.4	8.30E-02	vesicle-mediated transport	11	1.7	3.90E-02
S-adenosylhomocysteine catabolic process	2	0.4	8.30E-02	pyruvate metabolic process	4	0.6	3.90E-02
protein oligomerization	5	1	8.40E-02	carbohydrate metabolic process	12	1.9	4.10E-02
negative regulation of neuron apoptotic process	8	1.6	8.50E-02	negative regulation of extrinsic apoptotic signaling pathway	5	0.8	4.20E-02
retrograde vesicle-mediated transport, Golgi to ER	6	1.2	8.60E-02	regulation of cell migration	7	1.1	4.30E-02
nucleotide-excision repair, DNA incision, 5'-to lesion	4	0.8	8.80E-02	regulation of mitochondrial membrane permeability	3	0.5	4.50E-02
ER to Golgi vesicle-mediated transport	9	1.8	8.90E-02	chaperone mediated protein folding requiring cofactor	3	0.5	4.50E-02
nuclear import	3	0.6	9.20E-02	cell volume homeostasis	3	0.5	4.50E-02
nucleoside diphosphate phosphorylation	3	0.6	9.20E-02	positive regulation of potassium ion transport	3	0.5	4.50E-02
nucleotide-excision repair, DNA incision	4	0.8	9.40E-02	embryonic eye morphogenesis	3	0.5	4.50E-02
response to drug	14	2.8	9.80E-02	protein homooligomerization	12	1.9	4.50E-02
transcription elongation from RNA polymerase II promoter	6	1.2	1.00E-01	macroautophagy	7	1.1	4.80E-02
protein targeting	4	0.8	1.00E-01	phospholipid biosynthetic process	5	0.8	4.90E-02
Wnt signaling pathway, calcium modulating pathway	4	0.8	1.00E-01	mitochondrion organization	7	1.1	5.10E-02
response to reactive oxygen species	4	0.8	1.00E-01	cytoskeletal anchoring at plasma membrane	3	0.5	5.40E-02
				creatine metabolic process	3	0.5	5.40E-02
				long-chain fatty-acyl-CoA biosynthetic process	5	0.8	5.70E-02
				protein homotetramerization	6	1	5.70E-02
				phosphorylation	8	1.3	5.90E-02

				COPII vesicle coating	6	1	6.00E-02
				glycogen biosynthetic process	4	0.6	6.00E-02
				protein targeting to plasma membrane	4	0.6	6.00E-02
				canonical glycolysis	4	0.6	6.00E-02
				vesicle docking involved in exocytosis	4	0.6	6.00E-02
				positive regulation of catalytic activity	7	1.1	6.20E-02
				mitochondrial genome maintenance	3	0.5	6.30E-02
				cardiac myofibril assembly	3	0.5	6.30E-02
				oxaloacetate metabolic process	3	0.5	6.30E-02
				virion assembly	3	0.5	6.30E-02
				positive regulation of glycoprotein metabolic process	2	0.3	6.80E-02
				membrane assembly	2	0.3	6.80E-02
				protein localization to M-band	2	0.3	6.80E-02
				protein localization to membrane raft	2	0.3	6.80E-02
				dosage compensation	2	0.3	6.80E-02
				cardiac muscle cell action potential	2	0.3	6.80E-02
				cerebellar Purkinje cell layer morphogenesis	2	0.3	6.80E-02
				isoleucine catabolic process	2	0.3	6.80E-02
				brain development	12	1.9	6.80E-02
				glycosphingolipid metabolic process	5	0.8	7.00E-02
				osteoblast differentiation	8	1.3	7.00E-02
				cholesterol homeostasis	6	1	7.10E-02
				fatty acid beta-oxidation using acyl-CoA oxidase	3	0.5	7.30E-02
				myofibril assembly	3	0.5	7.30E-02
				cell communication by electrical coupling involved in cardiac conduction	3	0.5	7.30E-02
				negative regulation of apoptotic process	23	3.7	7.40E-02
				regulation of blood pressure	6	1	7.50E-02
				glycogen metabolic process	4	0.6	7.80E-02
				sarcomere organization	4	0.6	7.80E-02

				anion transport	3	0.5	8.30E-02
				positive regulation of receptor recycling	3	0.5	8.30E-02
				regulation of muscle contraction	3	0.5	8.30E-02
				negative regulation of oxidative stress-induced intrinsic apoptotic signaling pathway	3	0.5	8.30E-02
				response to oxidative stress	8	1.3	8.80E-02
				muscle organ development	7	1.1	8.90E-02
				positive regulation of ATPase activity	4	0.6	9.10E-02
				negative regulation of cysteine-type endopeptidase activity involved in apoptotic process	6	1	9.10E-02
				ventricular cardiac muscle cell action potential	3	0.5	9.40E-02
				energy homeostasis	3	0.5	9.40E-02
				cell adhesion mediated by integrin	3	0.5	9.40E-02
				cardiac muscle hypertrophy in response to stress	3	0.5	9.40E-02
				regulation of I-kappaB kinase/NF-kappaB signaling	3	0.5	9.40E-02
				exploration behavior	3	0.5	9.40E-02
				endoplasmic reticulum calcium ion homeostasis	3	0.5	9.40E-02
				epithelial cell differentiation	6	1	9.60E-02
				viral process	16	2.5	9.90E-02

Supplementary table 5: List of enriched Cellular Compartments

Down-regulated				Up-regulated			
Term	**Count**	**%**	**P-Value**	**Term**	**Count**	**%**	**P-Value**
cytosol	220	43.8	3.30E-44	mitochondrion	185	29.4	3.00E-66
cytoplasm	242	48.2	1.10E-23	mitochondrial inner membrane	99	15.7	1.10E-52
extracellular exosome	162	32.3	1.90E-23	mitochondrial matrix	76	12.1	2.80E-41
cell-cell adherens junction	45	9	2.70E-19	extracellular exosome	229	36.4	3.70E-41
membrane	111	22.1	2.00E-11	myelin sheath	33	5.2	5.10E-17
focal adhesion	37	7.4	8.80E-11	Z disc	29	4.6	1.70E-16
nucleoplasm	126	25.1	7.10E-10	membrane	133	21.1	1.40E-11
nucleolus	55	11	3.20E-09	mitochondrial proton-transporting ATP synthase complex	12	1.9	1.50E-11

nucleus	202	40.2	1.20E-08	mitochondrial respiratory chain complex I	16	2.5	3.80E-11
extracellular matrix	25	5	1.30E-06	sarcolemma	17	2.7	2.10E-08
ribosome	18	3.6	2.10E-06	focal adhesion	37	5.9	5.20E-08
ruffle	12	2.4	2.50E-05	mitochondrial nucleoid	12	1.9	2.10E-07
cytosolic large ribosomal subunit	10	2	7.40E-05	M band	9	1.4	5.00E-07
Golgi apparatus	43	8.6	1.10E-04	extracellular matrix	29	4.6	9.30E-07
protein complex	26	5.2	1.10E-04	intercalated disc	10	1.6	1.60E-05
actin cytoskeleton	17	3.4	2.40E-04	mitochondrial membrane	14	2.2	1.60E-05
lamellipodium	13	2.6	1.20E-03	costamere	7	1.1	2.70E-05
microtubule	19	3.8	1.70E-03	T-tubule	9	1.4	3.20E-05
Gemini of coiled bodies	4	0.8	2.60E-03	sarcomere	9	1.4	3.90E-05
stress fiber	7	1.4	3.00E-03	cAMP-dependent protein kinase complex	5	0.8	4.10E-05
cell periphery	6	1.2	3.50E-03	mitochondrial outer membrane	17	2.7	4.40E-05
growth cone	10	2	3.70E-03	A band	6	1	6.60E-05
SMN complex	4	0.8	4.30E-03	proton-transporting ATP synthase complex, catalytic core F(1)	4	0.6	1.50E-04
cytoskeleton	20	4	5.00E-03	mitochondrial large ribosomal subunit	9	1.4	1.80E-04
melanosome	9	1.8	5.40E-03	membrane raft	19	3	2.20E-04
actin filament	7	1.4	7.40E-03	cell-cell adherens junction	25	4	2.60E-04

clathrin adaptor complex	4	0.8	8.00E-03	cytosol	146	23.2	3.60E-04
cytosolic small ribosomal subunit	6	1.2	8.60E-03	melanosome	12	1.9	5.90E-04
collagen trimer	8	1.6	1.10E-02	endoplasmic reticulum	47	7.5	6.20E-04
COP9 signalosome	5	1	1.30E-02	mitochondrial respiratory chain complex III	5	0.8	7.20E-04
spindle	9	1.8	1.50E-02	peroxisome	12	1.9	7.60E-04
cell leading edge	5	1	1.90E-02	mitochondrial respiratory chain	5	0.8	9.80E-04
extrinsic component of membrane	7	1.4	2.20E-02	actin cytoskeleton	18	2.9	1.20E-03
intracellular ribonucleoprotein complex	9	1.8	2.90E-02	basal lamina	5	0.8	1.30E-03
small ribosomal subunit	4	0.8	3.40E-02	myosin complex	8	1.3	1.40E-03
myosin complex	5	1	4.30E-02	ribosome	15	2.4	1.50E-03
nuclear matrix	7	1.4	4.40E-02	muscle myosin complex	5	0.8	1.70E-03
cell	7	1.4	5.00E-02	lateral plasma membrane	8	1.3	1.90E-03
myelin sheath	9	1.8	5.00E-02	perinuclear region of cytoplasm	36	5.7	2.20E-03
intracellular ferritin complex	2	0.4	5.20E-02	endoplasmic reticulum membrane	46	7.3	2.50E-03
collagen type I trimer	2	0.4	5.20E-02	spectrin	4	0.6	2.70E-03
COPI vesicle coat	3	0.6	5.20E-02	mitochondrial intermembrane space	9	1.4	3.40E-03
vesicle	8	1.6	5.40E-02	lysosome	17	2.7	4.30E-03

nuclear body	4	0.8	5.60E-02	sarcoplasmic reticulum membrane	6	1	5.30E-03
Golgi stack	4	0.8	5.60E-02	endoplasmic reticulum lumen	15	2.4	5.60E-03
cytoplasmic mRNA processing body	6	1.2	5.60E-02	lysosomal membrane	19	3	5.60E-03
basement membrane	6	1.2	5.90E-02	lamin filament	3	0.5	6.50E-03
chromosome	7	1.4	6.10E-02	mitochondrial proton-transporting ATP synthase complex, coupling factor F(o)	4	0.6	6.70E-03
clathrin-coated vesicle	5	1	6.80E-02	lysosomal lumen	9	1.4	7.80E-03
trans-Golgi network membrane	6	1.2	6.90E-02	basolateral plasma membrane	14	2.2	8.10E-03
SMN-Sm protein complex	3	0.6	7.30E-02	mitochondrial envelope	4	0.6	8.50E-03
Bcl-2 family protein complex	2	0.4	7.70E-02	specific granule	4	0.6	8.50E-03
CBM complex	2	0.4	7.70E-02	ciliary base	5	0.8	1.20E-02
XPC complex	2	0.4	7.70E-02	myofibril	5	0.8	1.40E-02
neuronal cell body	14	2.8	7.70E-02	intracellular membrane-bounded organelle	30	4.8	1.40E-02
intermediate filament	7	1.4	8.00E-02	nuclear inner membrane	6	1	1.40E-02
cell-cell junction	9	1.8	8.80E-02	myosin filament	4	0.6	1.50E-02
Z disc	7	1.4	9.40E-02	myelin sheath adaxonal region	3	0.5	1.60E-02
				cell surface	29	4.6	1.70E-02
				filopodium membrane	4	0.6	1.80E-02
				peroxisomal matrix	6	1	1.90E-02
				dendritic spine	9	1.4	2.00E-02

				sarcoplasmic reticulum	5	0.8	2.70E-02
				spectrin-associated cytoskeleton	3	0.5	2.80E-02
				MICOS complex	3	0.5	2.80E-02
				pore complex	3	0.5	3.50E-02
				stress fiber	6	1	3.50E-02
				synaptic vesicle	8	1.3	3.60E-02
				neuromuscular junction	6	1	3.70E-02
				I band	4	0.6	4.10E-02
				endosome	14	2.2	4.20E-02
				nuclear envelope	11	1.7	4.30E-02
				microfibril	3	0.5	4.30E-02
				desmosome	4	0.6	4.60E-02
				cytoskeleton	20	3.2	4.70E-02
				nucleotide-activated protein kinase complex	3	0.5	5.10E-02
				striated muscle thin filament	3	0.5	5.10E-02
				paranode region of axon	3	0.5	6.00E-02
				cardiac myofibril	2	0.3	6.60E-02
				calcium ion-transporting ATPase complex	2	0.3	6.60E-02
				mitochondrial electron transfer flavoprotein complex	2	0.3	6.60E-02
				dense fibrillar component	2	0.3	6.60E-02

				mitochondrial respiratory chain complex IV	3	0.5	6.90E-02
				endoplasmic reticulum exit site	3	0.5	6.90E-02
				midbody	9	1.4	7.00E-02
				lipid particle	6	1	7.10E-02
				lamellipodium	10	1.6	9.20E-02
				striated muscle myosin thick filament	2	0.3	9.80E-02
				laminin-11 complex	2	0.3	9.80E-02
				proteasome activator complex	2	0.3	9.80E-02
				heterotrimeric G-protein complex	4	0.6	9.90E-02